



Fluvial transport and risk of mercury in a gold mining area

Francisco J. Picado Pavón

Fluvial transport and risk of mercury in a gold mining area

Francisco J. Picado Pavón

Akademisk avhandling, som för avläggande av filosofie doktorsexamen vid naturvetenskapliga fakulteten vid Lunds Universitet, kommer att offentligen försvaras i Blå Hallen, Ekologihuset, Sölvegatan 37, tisdag 30 september 2008, klockan 10.00.

Fakultetens opponent: Karen Hudson-Edwards, Senior lecturer, School of Earth Sciences, University of London, Birkbeck College, Malet St, London WC1E 7HX, England

Dissertation
Lund 2008

Organization LUND UNIVERSITY Department of Ecology Chemical Ecology and Ecotoxicology Ecology Building SE-22362, Lund, Sweden	Document name DOCTORAL DISSERTATION
	Date of issue September 3, 2008
Author(s) Francisco J. Picado Pavón	Sponsoring organization
Title and subtitle Fluvial transport and risk of mercury in a gold mining area	
Abstract <p>My thesis is part of an overall environmental program evaluating the environmental and human health stress in areas of Nicaragua affected by anthropogenic emission of metals and man-made organic substances. I examine the fluvial transport of mercury contextually associated with the extent of the contamination and the observed human and environmental stress in a gold mining area. Field measurements (Papers I, II, IV, and V), experimental assays (Paper III), and risk assessment (Paper VI) are used in the investigation on a basin scale. Even though the same processes and mechanisms apply for the accumulation and the movement of mercury in river and ground water systems, the local hydrogeological and climatic conditions together with the dynamic of mining activity make the fluvial transport and the accumulation of mercury site specific. Therefore, I consider that efforts to elucidate the transport and fate of mercury dependence on local environmental settings and its implication for humans are compulsory in assessing the impact of the poorly-controlled use of mercury in gold mining areas. Hence, to take actions for human and environmental protection.</p> <p>At the basin scale, flowing water is thought to export and dissipate the pollution. Hence, rivers and streams in gold mining areas are used for mercury-enriched waste disposal. Notwithstanding, levels of mercury of environmental concern are observed in water and river sediments. Since mercury in sediments is a threat to streams organisms and exposes riverine human populations through the consumption of mercury-contaminated fish, the accumulation of mercury in the sediment phase has been of particular importance from the perspective of human health. Therefore, it is of great importance to elucidate the processes involved in the fluvial transport and phase partitioning of mercury in a river, and the interaction with the groundwater system in such sensitive areas. Even though environmental levels of mercury in gold mining watersheds are low, a risk evaluation is also needed, because mercury bio-concentrates and bioaccumulates in exposed receptors. The results of my studies may also help to promote the environmental control and to contribute to the development of water quality criteria that can be used for regulatory purposes in gold mining areas of a developing country.</p> <p>The insights gained from the investigations carried out in the Sucio river basin call for an environmental and human health care and apply for an environmental monitoring. Together with other findings reported by other studies, the insights can be a core of useful information to implement alternatives in the abatement of the contamination in the river basin.</p>	
Key words Transport, Sedimentation, Sorption, Mercury, River, Groudwater, Risk, Gold Mining.	
Classification system and/or index terms (if any)	
Supplementary bibliographical information	Language English
ISSN and key title	ISBN 978-91-7105-280-3
Recipient's notes	Number of pages 132
	Price
	Security classification

Distribution by (name and address) Francisco J. Picado Pavón Department of Ecology Ecology Building SE-22362, Lund, Sweden
I, the undersigned, being the copyright owner of the abstract of the above-mentioned dissertation, hereby grant to all reference sources permission to publish and disseminate the abstract of the above-mentioned dissertation.

Signature _____

Date September 3, 2008

**Fluvial transport and risk of mercury
in a gold mining area**

Francisco J. Picado Pavón

Acknowledgments

The Swedish International Development Cooperation Agency (Sida/SAREC) supported these studies through an environmental research multidisciplinary program (PMIA). It is a cooperative project involving the National Autonomous University of Nicaragua (UNAN-Managua) and Lund University.

I thank Professor Göran Bengtsson, who guided me through several disciplines of the science without any conditions. I thank Göran's wife, Marita, who shared her time with the Nicaraguans.

The Centro para la Investigación en Recursos Acuáticos de Nicaragua (CIRA-UNAN) and Centro de Investigaciones Geocientíficas (CIGEO-UNAN) supported the field work by providing laboratory facilities and equipments, in particular the directors Salvador Montengro, Katherine Vammen and Dionisio Rodriguez, who is the coordinator of the PMIA. I want to thank people whom helped me to carried out my field work. They are: Oscar Cruz (el tigre), Miguel García (el capitan), Roger Chavarría, José Luis, Julio Guevara, Jader Guevara, Don Ramiro Duarte.

The Royal Physiographic Society in Lund-Sweden provided me with the computer.

Thank to the staffs from Ecology, and the PhDs from the Chemical Ecology and Ecotoxicology. I want to specially thank Olof Regnell for share his knowledge. He is one of mercury experts at Department of Ecology. I want also to thank Johannes Jaremo to be a good friend.

Some Nicaraguan students shared energy working on some of my investigations.

Thank to the staffs from Faculty of Medicine and from the Department of Engineering Geology, Lund University, in particular Kjell Anderson.

Christina Flores and her family have been my second family.

To my parents' death,

A MAL y GAMA,

to my lovely wife

A doctoral thesis at a university in Sweden is produced either as a monograph or as a collection of papers. In the latter case, the introductory part constitutes the formal thesis which summarizes the accompanying papers. These have either already been published or are manuscripts at various stages (in press, submitted or in ms).

© Francisco J. Picado Pavón
ISBN 978-91-7105-280-3.

Contents

Page

Introduction	8
Transport of mercury in streams and rivers	8
Mercury in groundwater	12
Gold mining activity and environmental mercury emission	13
A study case: Gold mining in the Sucio River basin (St Domingo district), Chontales-Nicaragua	14
Environmental and human mercury exposure in gold mining areas	16
Mercury toxicity	18
Perspectives	23
Conclusions	23
References	24

This thesis is based on the following papers, which are referred to by their Roman numerals.

- I. Picado, F. and Bengtsson, G. 2008. Temporal and spatial distribution of waterborne mercury in a gold miner's river. (*manuscript*)
- II. Bengtsson, G. and Picado, P. 2008. Sedimentation and resuspension of particle bound mercury in a polluted river. (*manuscript*)
- III. Bengtsson, G. and Picado, F. 2008. Mercury sorption to sediments: Dependence on grain size, dissolved organic carbon, and suspended bacteria. *Chemosphere (in press)*
- IV. Medoza, J. A., Ulriksen, P., Picado, F., and Dahlin, T. 2008. Aquifer interactions with a polluted mountain river of Nicaragua. *Hydrological processes (in press)*
- V. Enfield C., Bengtsson G., Picado., F., and Mendoza A. 2006. A methodology for bi-directional measurement of flux at the Groundwater- river water interface in turbulent and rocky streams. (*manuscript*)
- VI. Picado, F., Mendoza, A., Cuadra, S., Barmen, G., Jakobsson, K., and Bengtsson, G. 2008. Ecological, Groundwater, and Human Health Risk Assessment in a Mining Region of Nicaragua. (*manuscript*)

Paper III and IV are reprinted with permission from the publishers.

Fluvial transport and risk of mercury in a gold mining area

Introduction

Mercury reaches surface water when it is released in mill tailings of the gold recovery process and any of the other routes, such as atmospheric deposition and leaching by runoff from contaminated soils, because mercury on dust, particles, and droplets may precipitate by dry and wet deposition or may be washed from surface soils into surface water during rainfall. In rivers and streams, the fate and transport of the mercury are influenced by physical-chemical, and biological processes. Hence, the mercury concentrations vary spatially and temporally within the stream. Although predictive and descriptive models (solute transport equations) (Kimball et al., 1994; Runkel et al., 1996; Nazarov and Demidov, 2001) can be used to quantify this variation, most researchers describe the fluxes of mercury based in field observations.

At basin scale, rivers and streams of gold mining areas are used to export or dilute the mercury pollution by a downstream transportation of the mercury-enriched mill tailings. Nonetheless, high mercury concentrations in environmental samples, e.g. surface water, groundwater, soils, sediments, plants, etc., are always reported to have a negative impact on the ecology and human health in gold mining areas.

Transport of mercury in streams and rivers

The levels of mercury in recipient rivers and their fluvial dissipation depend on natural processes and the amount of

mercury released into the streambed (Telmer et al., 2006). The amount of mercury depends on the amount of mined ores in the mill tailings, because mercury largely concentrates in the ore particles (Lima et al., 2008), such that mercury concentrations higher than e.g. 200 $\mu\text{g/g}$ have been observed in mill tailings (Farid et al., 1991). Nevertheless, a phase partitioning of mercury takes place when mercury enters to rivers. In the water, mercury is present in both soluble and particulate forms (Hurley et al., 1995; Stordal et al., 1996; Balogh et al., 1997). Soluble mercury species are free ionic mercury and both inorganic and organic complexes (Wallschläger et al., 1998), but the prevailing mercury concentrations are associated with the particulate phase (Whyte and Kirchener, 2000; Maurice-Bourgoin et al., 2003), because suspended particles have been contaminated during the process of gold recovery. Hence, the mass of mercury in suspended sediments can be hundreds of times the mass mercury dissolved per litre of water in recipient rivers (Telmer et al., 2006). Partition coefficients ($\log K_d$) of mercury in rivers varies between 3 and 7 (Babiarz et al., 2001; Maurice-Bourgoin et al., 2003) and are influenced by rainstorm events that incorporate suspended matter in stream water, such that particulate mercury concentrations increase in the water phase (Balogh et al., 1997; Babiarz et al., 1998). Dissolved organic matter also contributes to the mobility of mercury in stream water and to the variation of dissolved mercury concentrations (Maurice-Bourgoin et al., 2003). The mercury concentrations vary along rivers (Leigh, 1997) and can gradually decrease over long distances (Paper I). The spatial and temporal changes of mercury concentrations follow the variations of suspended particulate matter concentrations (Nimick et al.,

2007), such that particulate matter has been suggested as a good predictor of mercury concentration in rivers (Balogh et al., 1997; Whyte and Kirchener, 2000; Telmer et al., 2006). Temporal patterns of both dissolved and particulate mercury concentrations are observed over relatively short distance and low flow conditions, such that the higher concentrations observed temporally, e.g. in a miner's river, reflect the mercury amalgamation events at the mining operation sites (Paper I). In contrast, the aqueous concentrations of mercury are more or less homogeneously distributed in the downstream direction far from mining sites (Paper I). Long transport of mercury allows scavenger mechanisms, such as adsorption, sedimentation (Ullrich et al., 2007), precipitation (Sjöblom et al., 2004), biological uptake, and mercury evasion (Maprani et al., 2005; Nimick et al., 2007), to scavenge mercury from the aqueous phase.

It is widely accepted that the retardation of the movement of contaminants in heterogeneous media is due to sorption mechanisms. In the sorption process, dissolved mercury species become associated with a solid surface (Runkel et al., 1996; Runkel and Kimball, 1999). Both the formation of chemical complexes and electrostatic attraction between mercury and sediment or soil particles (Paper III) are mechanisms involved in the sorption (Yin et al., 1996; Gissinger et al., 1999). Sorption takes place in both liquid (stream water) and solid (streambed) phases (Carrol et al., 2000), such that in the river water, dissolved mercury can interact with suspended particles, and sediments can remove dissolved mercury from the water column. In natural water, both inorganic (hydrated oxides of aluminium, iron and manganese, aluminosilicates) and organic

sorbents (particulate suspended matter, dissolved organic matter) are present and interact with ionic mercury species.

Sorption is also involved in the bioavailability and dispersion of mercury in rivers and streams. For instance, the dispersal of mercury in gold miner's rivers is particularly linked to the mercury adsorbed onto fine-grained river sediments. The fluvial spread of sediment-borne mercury generally results in an heterogeneous spatial distribution of mercury, such that a patchy spatial accumulation of mercury is observed in the streambed of rivers and streams (Callahan et al., 1994; Leigh, 1997). In sediments, primarily the organic matter on particles' surface adsorbs mercury because mercury has high affinity for organic molecules. Humic and fulvic acids, which are the major components of organic matter, are the principal sorbents of mercury and most of other metals (Lodenius et al., 1987; Johansson and Iverfeldt, 1994; Matthiessen, 1996; Wang et al., 1997; Schlüter, 2000). For instance, humic substances contain a large number of functional groups, such as carboxylic and phenolic that bind mercury, but also a smaller number of strong metal complexing groups such as amine, carbonyl, and sulfhydryl groups (Lodenius et al., 1987; Johansson and Iverfeldt, 1994; Matthiessen, 1996; Wang et al., 1997; Biester and Zimmer, 1998; Schlüter, 2000). It is thought that the mechanism for mercury binding to functional groups of organic matter is by formation of complexes via chemical bonds and cation exchange. The products of reactions between mercury ions and organic ligands can be bound in soil, sediments and organisms containing these then. Therefore, organic matter rich sediments have high mercury concentrations. In

addition, mercury concentrates in the finest particles because they have large surface areas, which have been almost entirely coated by organic matter. However, it has been suggested that large particles accumulate oxides coatings and associated metals due to their long resident time in rivers (Whitney, 1975; Tessier et al., 1982). Therefore, sandy particles, which are poorly coated with organic matter, also adsorb important amounts of mercury (Paper III) (Lima et al., 2008) and of other metals (Moore et al., 1989). Nevertheless, the mercury concentrations in sediments and soils negatively correlate with the particle size distribution (Paper III).

Organic contents in sediment samples are strongly correlated with the mercury concentrations, and because the organic content in suspended particles is high, a large amount of waterborne mercury becomes associated with the suspended phase in most fluvial systems (Paper I) (Maurice-Bourgoin et al., 2003; Telmer et al., 2006). The amount of mercury associated with suspended particulate matter depends on size and nature of molecules of suspended particulate matter, and its mineral composition (Quémerais et al., 1999). Nevertheless, even though the organic-mercury binding is the prevailing mechanism for mercury sorption to sediments, mercury can be also adsorbed on mineral surfaces via chemical reaction between a surface hydroxyl group on the mineral surface and hydroxylated mercury species (Paper III) (Sarkar et al., 1999; Walcarius et al., 1999; Sarkar et al., 2000) or via cation exchange, resulting from electrostatic interaction (Yin et al., 1997; Kraepiel et al., 1999) (Paper III). For instance, the suspended matter in miners' rivers, which is mostly composed by mineral particles poorly coated with organic matter, also are the major

transporter of mercury. Mineral surfaces are mostly represented by silica minerals, silicate clay minerals, iron, aluminum and manganese oxides, pyrite and quartz (Sarkar et al., 1999; Walcarius et al., 1999; Sarkar et al., 2000) and are effective sorbents of metal ions. In some fluvial system, the transport and accumulation of metals is attributed to suspended particulate matter due to its large surface area and oxide coatings (Salomão et al., 2001).

Normally, oxy-hydroxides of iron, manganese and aluminum are constituents of soil and sediment from tropical environments (Roulet et al., 1998; Roulet et al., 1998b; Hylander et al., 2000). These minerals are chemical reactive (Honeyman and H.Santschi, 1988) and can efficiently retain mercury (Forbes et al., 1974; Roulet et al., 1998; Roulet et al., 1998b; Hylander et al., 2000), such that the transport of particulate mercury in rivers and streams also depends on the occurrence of these sediment constituents. Sorbed mercury in some hydroxides such as goethite (Forbes et al., 1974) has also been modeled by surface complexation (Gissinger et al., 1999). The result show a maximum adsorption at pH around 7 (Gissinger et al., 1999). Mercury and other metals also precipitate with iron and manganese oxides in the river system, such that this scavenger mechanisms has been observed in zones of groundwater influx (Sjöblom et al., 2004; Coynel et al., 2007). In contrast, together with humic and fulvic acids (Maurice-Bourgoin et al., 2003), these minerals are components of colloidal particles (0.4 μm -10 kD) and enhances the transport of mercury in rivers, such that it has been suggested that the colloidal phase regulates the partitioning of mercury in rivers (Babiarz et al., 2001). In addition, natural organic matter can be in the

dissolved form, and dissolved organic matter plays an important role in the transport and fate of mercury in fluvial systems (Paper I) (Maurice-Bourgoin et al., 2003). For instance, dissolved organic matter contributes to the long-ranged transport of mercury. At low pH, mercury dissolves and associates with dissolved organic carbon, and dissolved mercury concentrations have been positively correlated with the concentration of dissolved organic matter in aquatic systems. The presence of carboxylic and phenolic groups gives the net negative charge of dissolved organic carbon; these negative charges are responsible to bind mercury.

Although the transport and fluxes of mercury are driven by the river discharge (Balogh et al., 1997), the large amount of particulate matter, commonly observed in gold miners' rivers, reduce the mobility of mercury in the stream due to settling of mercury associated with denser particles (Maurice-Bourgoin et al., 2003). Nonetheless, at high flow conditions, the resuspension of sediment particles (Mudroch and Clair, 1986; Hurley et al., 1998; Ullrich et al., 2007), which results from the action of flowing water forces, promotes the downstream spreading of mercury (Paper II). This transport mechanism becomes intensified by the rainstorm events (Hurley et al., 1998). During the process of sediment particles resuspension, coarser particles sink to the riverbed, thereby shifting the bulk of removed particles towards finer particles (Walling, 1983; Walling, 1988). This process can result in an enrichment of mercury in suspended sediments (Paper II) (Balogh et al., 1997).

Natural processes, such as the sedimentation (Paper II) and disturbances

and the mobilization of mercury-bound sediment particles during high flow events, have largely influenced the transport and fate of mercury in rivers systems (Telmer et al., 2006). The process of sedimentation is responsible for the storage of mercury in aquatic systems (Paper II). For instance, the sedimentation of the downstream-dispersed tailing material into the riverbed in some gold mining areas has resulted in the accumulation of large amounts of mercury. The concentrations of mercury in the sediments are higher than the reported probable effect concentration to freshwater organisms (CEQC/CCME, 1999). In sediments, mercury undergoes chemical and bacterial-mediated transformations, such that deposited mercury is transformed to methyl mercury. However, even though the concentration of methyl mercury in the sediments is about less than 1.5% of the total mercury content (Ullrich et al., 2001), aquatic organisms such as fish accumulate mercury at levels that represent a risk for human health.

Despite mercury concentration in river impacted by anthropogenic activities are of environmental concern, the concentrations can also decrease by dilution due to influx of connecting streams or groundwater recharge (Maurice-Bourgoin et al., 2003). Moreover, mercury can also be exchanged between river and groundwater such as other metals (Coynel et al., 2007). In the unsaturated zone, mercury is transported by leached flow rate interacting with the solid matrix (Schlüter and Gäth, 1997). Charge and grain size from the aquifer medium influence the adsorption capacity for many metals, because smaller particles have large surface area and coarser grains are coated with organic matter and with oxide and hydroxides of iron (Coston et al., 1995; Brown-Jr et al., 1999; Brown et al., 1999), which could enhance the

retention of mercury (Paper III). Solute transport processes involve the groundwater flow description and the solute-aquifer interaction, such as equilibrium reaction, adsorption and precipitation mechanism. Groundwater adds iron to rivers. and mercury, as other metals, can adsorb to or co-precipitate with iron-enriched particles (Sjöblom et al., 2004; Coynel et al., 2007). The temporal variation of the above processes in combination with the anthropogenic release of mercury results in a heterogeneous spatial distribution of mercury concentrations.

Mercury in groundwater

Groundwater reservoirs are the main water supply for humans in most cases. Notwithstanding, the quality of groundwater is sometimes at risk due to the interaction with contaminated surface water (Paper IV and V), because rivers and streams are parts of the groundwater flow system. Contaminated groundwater can also be a threat to the quality of surface water by bringing mercury to it (Krabbenhoft and Babiarz, 1992). Global background concentrations of mercury are very low, e.g. in the order of nanograms of total mercury per litre (Krabbenhoft and Babiarz, 1992), and these levels are several order of magnitude lower than in contaminated groundwater (Barringer et al., 2006). Adsorption, dilution, exchange reactions and precipitation (Krabbenhoft and Babiarz, 1992) seem to be the major physicochemical processes that can alter the metal concentrations during their transport in aquifer. Mathematical models predicting the transport and fate of reactive solutes, which move in both saturated and unsaturated zones, have been developed (Islam et al., 2001) and can be used to elucidate the movement of mercury and

other contaminants in aquifer media and in groundwater/surface water exchange situations (Krabbenhoft and Babiarz, 1992), but it would result in the use of simple differential equation for a steady state or in a differential equation for most complex scenarios (Winter, 1999). However, field observations on temporal groundwater and surface water level variations in down and upwelling areas in combination with the observed temporal variation of aqueous mercury concentrations have been carried out. This approach is useful to explore and for elucidating the transport of mercury during ground/surface water interactions (Paper IV and V). The use of natural tracer to study the groundwater and river water interaction is commonly used (Rodgers et al., 2004), but the hydrogeologic conditions (low groundwater flow, a fractured media, presence of stagnant water in the hyporheic zone, etc) are not optimal to track the tracer sometimes.

Although the principle that topographically elevated areas are groundwater recharged and rivers, streams and lakes in topographically low areas recharge aquifers is true for regional flow systems, it does not always apply at a local framework. Therefore, detailed observations are required (Paper IV and V) to assess the risk of contamination of groundwater resources in such situation. In this study (Paper IV and V), groundwater and river water levels, as well as temporal changes in water temperature in combination with mercury concentration and bacteria number determined in both surface and groundwater demonstrate the interaction of a mercury-contaminated river and shallow groundwater (Paper IV). It was found that hydrologic processes, such as seasonally low or high river water levels, can cause mercury to move from

one compartment to the other. In addition, groundwater flux measurements in down and upwelling sites along the river can be used either to assess the infiltration of mercury to the groundwater or the dilution of mercury concentrations in the river (Paper V).

Gold mining activity and environmental mercury emission

Mercury is considered as one of the worst sources of anthropogenic impact on the global environment (Wilken and Horvat, 1997; Boening, 2000), and gold mining is considered an economical activity in several regions around the world (Straaten, 2000; Lacerda, 2003). However, the poorly-controlled use of mercury in the processes of amalgamation and distillation results not only in a widespread environmental contamination (Lacerda, 2003; Telmer et al., 2006) but also in human mercury exposure. Metallic mercury (Hg^0) efficiently extracts gold and it is inexpensive, e.g. 1 kg of mercury cost as 1 g of gold. Therefore, mercury is still used in artisanal mining operations, but more than 1 kg of Hg is lost to the environment when 1 kg of gold is produced (Pfeiffer and Lacerda, 1988; Straaten, 2000; Lacerda, 2003). The environmental pollution takes place when mercury is emitted to the atmosphere and when mercury is discharged together with mined ores to surface water. Mining wastes contain large quantities of mercury-enriched solid material commonly composed by quartz particles (Lima et al., 2008). For instance in the past, from 1550 to almost three centuries after, the amount of mercury released to the environment globally by the process of mercury-gold amalgamation was 250,000 tons (Lacerda, 1997). In addition, more recently, the contribution of small-scale gold mining

activities to the annual global mercury emission is estimated to about 450 t (Lacerda, 2003). The atmospheric emission, which is generally higher than 50% of the total emission (Straaten, 2000; Lacerda, 2003), is affected by the local climatic conditions (Lacerda et al., 1999; Tsiros, 2001) and it occurs when amalgamated gold is smelted and mercury evaporates to the air as elemental mercury (Hg^0). Mercury in the air, which is one of the exposure sources to humans, is oxidized and it quickly ends up in soils and surface water due to local wet or dry deposition (Lodenius, 1998). For instance, the atmospheric local deposition rates of mercury in tropical conditions is several times higher than at a regional scale (Lacerda et al., 1999), such that higher anomalous mercury concentrations are observed in soils nearby gold processing sites. Once in soils and aquatic environments, the oxidized mercury (Hg^{2+}) is transformed under physical and chemical specific conditions to methyl mercury by bacterial activity. Methyl mercury is the most toxic chemical species of mercury and it accumulates in living organisms (Huckabee et al., 1979).

Although, mercury-bound ore particles settle down nearby gold processing areas, a large fraction that is associated with the finest particles in mining tailings travel long distances. However, the movement of mercury is retarded by a gradual sedimentation of the suspended particles (Telmer et al., 2006). Sediments, which act as sinks, become the major input of mercury in aquatic organisms. For instance, methyl mercury comprises more than 70% of the total mercury in fish (Huckabee et al., 1979; Akagi et al., 1994), and fish is the main pathway of mercury exposure to humans (Clarkson, 1992). The long distance transport of mercury is

driven by the river flow and mostly influenced by the waterborne particulate matter. High flows export mercury from polluted rivers, by either resuspension of contaminated sediment or dissolved associated with dissolved organic matter and other mercury carriers, to connecting watersheds.

The levels of mercury observed in water and bottom sediments of rivers of gold mining areas exceed 2.1 µg/l (EPA, 1995) and 0.49 µg/g (CEQC/CCME, 1999), which are the criteria maximum concentrations (CMC) (the highest concentration of total mercury to which aquatic life can be exposed for a short period of time without deleterious effects) and the concentration associated with probable effects on fresh water organisms, respectively.

In gold mining areas, shallow groundwater sources are also threatened by polluted river water when river infiltrates to groundwater and when mercury is mobilized from the polluted upper soil layers to the groundwater due to runoff infiltration. In addition to mercury exposure through drinking water, humans also accumulate mercury due to consumption of contaminated food (e.g. fish) and occupational exposure, such that the observed burden body concentrations are above the permissible exposure levels that have been established for human protection.

Environmental prevalent high concentrations of mercury in such areas of the world and in their human population must call the attention for environmental regulations.

A study case: Gold mining in the Sucio River (St Domingo district), Chontales-Nicaragua

Loss of mercury during gold recovery, which results in an environmental and human health stress, varies in gold mining areas. Much research concerning the effects of mercury on terrestrial and aquatic biota has demonstrated the potential risk that it represents (WHO, 1989b) because of its toxicity, accumulation and its tendency to become biomagnified in terrestrial and aquatic ecosystem, and also because of its properties, mobility, transformation in the environment, and presence in humans.

As in other developing countries, the major use of mercury in Nicaragua has been in gold mining for amalgamation with gold and other metals. Emission factors (Hg: Au ratios) larger than 1 can be due to an uncontrolled excessive use of mercury. For instance in Nicaragua, an emission of 40 t of mercury during 100 year has been reported from a basin area of 11 650 km² belonging to Mico and Sucio rivers from Chontales, a gold mining district (André et al., 1997), which gives 0.4 t per year. According to Lacerda (2003) the present-day annual emission is between 0.6 and 0.18 t in the same area.

In St Domingo as well as in other gold mining areas in Nicaragua, the gold recovery relies mainly on manual labor and the mining activity dates back more than 100 years. Miners manually extract gold from rich surface deposits, but also from primary gold quartz veins that require more sophisticated equipment. Although most of the households depend on agriculture and cattle grazing as the main source of income and sustenance, the gold mining activity is a means of livelihood for

the rest of the St Domingo inhabitants. The gold production in Nicaragua varies between 1 and 2 tons per year and the Nicaraguan miners represent 0.6% of the estimated total number of miners in Latin America (543,000 and 1,039,000) (Valenzuela and Fytas, 2002). Nowadays in St Domingo, the number of workers actively involved in the mining activities is more than 400 artisanal gold miners (workers who extract gold on manual basis). The miners use the mercury-gold amalgamation method because it is a simple process and it requires low investment. However, this practice is undertaken with a poor technical knowledge, without regulation and neglecting the human health and the environment care. During the mining activity, metallic mercury is lost to the atmosphere through evaporation when gold particles in crushed ores are amalgamated with mercury, and when amalgam is burned on bonfires in rough and open field conditions.

The gold mining activity is responsible for the discharge of sediment and associated mercury into Sucio river, and as in other gold mining areas (Malm, 1998; Tarras-Wahlberg et al., 2001; Limbong et al., 2003), it leads to the accumulation of mercury to acute levels in the environment.

Mining areas, e.g in Brazil, in Tanzania (Ikingura et al., 1997), in China (Lin et al., 1997), to mention some examples, carry similar small-scale amalgamation activities, each with a significant contribution to global mercury emissions. These gold mining areas have the same histories linked to gold mining activities as the St Domingo in Nicaragua. The amounts of mercury annually released from these gold mining areas into the environment, which range between 6 and

2000 tons (Lacerda and Marins, 1997; Lacerda and Salomos, 1998; Malm, 1998; Ikingura et al., 1997; Lin et al., 1997), are not generally comparable with each other, as they may depend on many factors, such as the mining activity itself, the gold production, technique, and the amounts of mercury used. For instance, the annual mercury emission from St Domingo is about 0.4, however, it is probably underestimated, as it assumes a working time of ten months per year and uses the monthly total mercury emission reported by André et al. (1997). Although the annual mercury emission in the Amazon in Brazil (~ 180 t/year) (Lacerda and Marins, 1997; Lacerda and Salomos, 1998; Malm, 1998) is much higher than in St Domingo, mercury occurs at similar concentrations in the environment of both areas. Concentration of total mercury ranges between 0.01 and 300 µg/l in water; between 0.02 and 150 µg/g in sediments; between 0.05 and 1100 µg/g in soils, and in fish the concentration are in the range of 0.03 and 4.0 µg/g. In humans the concentration of total mercury are between 3 and 1200 µg/l and between 0.7 and 180 µg/g in urine and hair respectively (Lacerda and Marins, 1997; Lacerda and Salomos, 1998; Malm, 1998; Ikingura et al., 1997; Lin et al., 1997).

The mercury concentrations in river water in the Amazon, Tanzania and the St Domingo are similar (André et al., 1997; WHO, 1990) and higher than mercury concentration in pristine environment (WHO, 1990) and the maximum permissible level of 1.0 µg l⁻¹ in drinking water (WHO, 1989b). This raises some concern about risks for aquatic life and people. Rivers from these gold mining areas should not be used for drinking water or for animals watering, since the levels of mercury in river water are above those

recommended for drinking water (Paper I and II).

Both water and sediment in rivers in the St Domingo gold mining area are sources of mercury to fish, and fish has been considered the main source of mercury to humans in those areas (Paper VI). For instance, in the Amazon region and other mercury contaminated areas, mercury concentration in fish has been monitored as an indicator of river and lakes contamination (Bidone et al., 1997).

Environmental and human mercury exposure in gold mining areas

People from gold mining environments are repeatedly exposed to inorganic mercury and methyl mercury (Akagi et al., 1995). Mercury enters into the human body through mercury-contaminated fish, direct inhalation, mercury-contaminated drinking water, and skin uptake. In the body, mercury undergoes the following processes: absorption, distribution, metabolism, and excretion.

Although mercury is released into surface water as a metallic liquid (Hg^0), it is oxidized and trapped in sediments as inorganic mercury. In the sediments, mercury is biotically transformed to organic mercury compounds (e.g., methyl mercury and mono-valent methyl mercury) by sulphate reducing bacteria (Compeau and Bartha, 1985; Gilmour and Henry, 1991). The transformation can take place at both anaerobic and aerobic conditions. Organic mercury is taken up from sediments by phytoplankton, which are eaten by invertebrates and small fish, which are eaten by large predatory fish. Other sources of mercury to fish, such as runoff water from mercury-contaminated soils,

have also been identified (Lindqvist, 1984).

Mercury bound to large organic matter molecules is thought to be too polar and it could not cross biological membranes. Nevertheless, mercury enters into fish mainly via their food and through the gills. Once mercury has crossed the gills, it is transported by blood to various tissues, mainly accumulating in the liver (Clarkson, 1994; CTEM et al., 2000). Although most of the environmental mercury to which fish is exposed is inorganic, high concentrations of methyl mercury are found in fish, because inorganic mercury is not retained and is relatively unavailable for fish assimilation (Lawson and Mason, 1998; Morel et al., 1998). Most mercury retained in fish is methyl mercury (Bidone et al., 1997), although it is slowly eliminated bound to sulphhydryl groups.

Human exposure to mercury through consumption of mercury-contaminated fish has been widely documented (Lindqvist, 1984; Akagi et al., 1995; Palheta and Taylor, 1995; Dolbec et al., 2002) and its accumulation in the human body has been associated with irreversible alterations of the nervous system. Inorganic and organic mercury is transported through aquatic food chains from sediment to humans. Concentrations of organic mercury in human samples, e.g. blood, scalp hair, are also indicators of human mercury exposure (Lindqvist, 1984; Akagi et al., 1995; Palheta and Taylor, 1995; Dolbec et al., 2002). For instance, concentrations higher than 0.02 mg/g in hair samples in women at the upper Madera River in Brazil are attributed to consumption of contaminated fish.

In humans, the gastrointestinal tract could absorb about 95% of methyl mercury in

ingested fish (Aberg et al., 1969). Once the gastrointestinal tract has absorbed organic mercury, mercury is transported through the body in the bloodstream until it accumulates in different target organs in the body. Methyl mercury is found mainly in red blood cells in a ratio to plasma methyl mercury of about 20:1. In blood, its half-life seems to be about 40 days (Smith et al., 1994). The transport of methyl mercury into the tissues is mediated by the formation of a methyl mercury cysteine complex (Aschner and Aschner, 1990). The complex is transported into the cells via neutral amino acid carrier proteins (Kerper et al., 1992). Most mercury in hair and blood from people exposed through fish consumption and living in gold mining areas seems to be methyl mercury (Lindqvist, 1984; Akagi et al., 1995; Palheta and Taylor, 1995; Dolbec et al., 2002), such that the ratio between total mercury and methyl mercury is almost 1. In the scalp hair, methyl mercury is incorporated in the hair follicles. A strong correlation has been found between the concentrations of total mercury in hair and blood (WHO, 1990; Akagi et al., 1995), which indicates that the concentration in hair can be an indicator of methyl mercury exposure in fish-eater populations (WHO, 1990).

Bioaccumulation of methyl mercury can be due to its stability in the body and due to re-absorption of methyl mercury secreted into the bile. There is no evidence for methylation in the body. In contrast, demethylation in the body is slow and involves hydroxyl radicals produced by cytochrome P-450 reductase (Suda and Hirayama, 1992). In the body, methyl mercury is converted to ionic mercury by microorganisms living in the intestines. About 90% of the absorbed dose of methyl mercury can be excreted as ionic mercury.

Efforts have been made to prevent consumption of fish contaminated with mercury. Simple models have been proposed to predict possible hazardous exposure to mercury by fish consumption (Paradis et al., 1997; Renzoni et al., 1998). For instance, from the levels of mercury in fish and the daily fish consumption, body human weight, and other parameters, the personal daily intake can be estimated (Paradis et al., 1997). However, models are parameter (fish species eaten, size of meal, number of daily meals, human susceptibility) sensitive, such that the output prediction is adjusted to a narrow set of conditions.

The tolerable daily intake of mercury (TDI) for a person is 0.47 μg of Hg per kg body weight according to WHO (1990). A personal daily intake above the TDI has been considered to be hazardous. This and other findings are good approaches to assess the risk associated with consumption of mercury-contaminated fish. However, they are based on several assumptions, such as steady-state condition, which can result in underestimated values. They do not include other mercury sources, and they still need to be improved in order to be more predictable.

Another important exposure source of mercury in humans is the release of metallic mercury (Hg^0) during burning Au-Hg amalgam, which is absorbed through the respiratory tract, the gastrointestinal tract, and the skin (Lipfert, 1997). Levels of mercury in blood, hair and urine samples are indicators of metallic mercury exposure (Akagi et al., 1995) with urine samples as more reliable indicators of long term exposure. In gold mining areas, humans inhale metallic mercury vapour, which is readily absorbed by red blood

cells in the lungs. In the blood, the adsorption is facilitated and enhanced by the lipid solubility of Hg° and its high vapor pressure, which allows it to cross the lipid-containing cell membranes and dissolve in blood lipids. The distribution of absorbed metallic mercury is limited by slow oxidation, which can be a defensive mechanism. Inside the red blood cells, it is oxidized to divalent mercury (Hg(II)) by hydrogen peroxide and catalase enzymes (Clarkson, 1994). Catalase is found in almost all tissues, so oxidation can occur throughout the body. Both metallic and ionic mercury species can reach the brain cells (Clarkson, 1994; Pamphlett and Waley, 1996a; Pamphlett and Waley, 1996b; Pamphlett and Waley, 1998). The latter crosses the blood-brain barrier more slowly than metallic mercury (Hursh et al., 1988; Clarkson, 1994). If the oxidation of metallic mercury takes place in the brain, ionic mercury can be retained in it and cause tremor, insomnia, depression, irritability, etc. Divalent mercury is soluble in water and can be easily excreted from the body via urine as sulfhydryl conjugates (Clarkson, 1994), but in plasma and erythrocytes, protein sulfhydryl groups can bind divalent mercury (Hall et al., 1994).

Exhalation can be another defence mechanism in humans. In the liver, divalent mercury is reduced to Hg° (Dunn et al., 1981) and transported to the lungs and then exhaled. Alternatively, Hg(II) can react with reduced glutathione (G) in the liver forming a mercury-glutathione complex (GS-Hg-SG) due to its strong tendency to bind to sulphur-containing functional groups. GS-Hg-SG is released into the bile and then carried to the intestines and excreted with the faeces (Ballaton and Clarkson, 1984; Ishihara, 2000). Elimination of mercury from the body after exposure to metallic mercury is

mostly via faeces. Metallic mercury vapour can also occur in sweat but in very small amounts.

The skin poorly absorbs metallic mercury. When 1 cm^2 of skin is exposed to 1.0 mg of mercury in 1 m^3 of surrounding air, it can absorb about 0.02 ng of mercury (Hursh et al., 1989). Mercury is mostly absorbed through the sebaceous gland cells or through follicular walls, because they are more permeable than the epidermal cell layers. Moist skin is a symptom for mercury dermal exposure. Metallic mercury penetrates the skin more readily than ionic species.

Mercury-contaminated drinking water is also a source of mercury to humans. Inorganic and organic mercury can be ingested from contaminated drinking water. Metallic mercury is unlikely to be ingested in this way, but if it is, sulphide in the body prevents its absorption by coating it. The gastrointestinal tract efficiently absorbs both inorganic and organic mercury. Inorganic mercury may be absorbed by electrostatic attraction of mercury by the brush border membrane followed by diffusion through it. (Endo et al., 1990; Foulkes and Bergman, 1993). More than 95% of the methyl mercury content in drinking water is taken up (Aberg et al., 1969).

Mercury toxicity

Low doses of mercury exposure have been associated to different health disorders in humans. For instance, disorders mainly in the nervous, motor, and renal systems, are consequences of consumption of mercury-contaminated food in humans, although, alterations in the cardiovascular, immune and reproductive system are also observed. Depending on its chemical form and the

dose, mercury is toxic to humans, animals and plants. Exposure to mercury affects the gastrointestinal tract, respiratory tract and kidney. At least 95% of ingested methyl mercury is taken up in the gastrointestinal tract (Inskip and Piotrowski, 1985), which is the main pathway of entry in humans. In the body, methyl mercury seems to have a half-life between 70 and 80 days (CTEM et al., 2000). The kidney is the target organ for inorganic species, but in extreme cases of mercury exposure, the brain may also be a target organ for elemental mercury. About 80% of the inhaled metallic mercury is readily absorbed into the body, where it can stay for one or two months (CTEM et al., 2000). An increase in urinary excretion of some proteins such as N-acetyl- β -glucosaminidase, β_2 -microglobulin and retinol-binding protein, may indicate kidney damage (Divine et al., 1999). During prolonged exposure to mercury vapour, humans suffer from irritability, tremor and erethism, memory disturbance (hallucinations and delirium), fatigue and confusion (Piikivi & Hanninen, 1989). No chronic effects on humans are expected after continuous inhalation of air with less than $0.3 \mu\text{g m}^{-3}$ metallic mercury (WHO, 1990). Inorganic mercury could be considered as a neurotoxin that causes sporadic motor neuron disease (Arvidson, 1992; Pamphlett and Waley, 1996a). It has been found in large amounts in cortical motor neurons and smaller amounts in some brain stem and cerebellar neurons (Pamphlett and Waley, 1996b; Pamphlett and Waley, 1998). It is suspected that in the inorganic form, mercury can bypass the blood-brain barrier (Aschner and Aschner, 1990; Arvidson, 1992) and damage neurons.

In the case of methylmercury exposure, the critical organ seems to be the brain, but the developing nervous system is more

sensitive. Adult and foetal brains are susceptible to methyl mercury, as shown by neurotoxic effects to methyl mercury exposure (WHO, 1990; Myers et al., 2000). Chronic exposure has resulted in neurological damage, paresthesia (a sensation of pricking, tingling, or creeping on the skin), ataxia (an inability to coordinate voluntary muscular movements that is symptomatic of some nervous disorders), sensory disturbance, tremors, impairment of hearing, blurred vision (Cavalleri and Gobba, 1995), speech difficulties, blindness, deafness and death (Harada, 1995; Myers et al., 2000). Some of these effects have been endpoints of neurotoxicity in children and women who have consumed large amounts of mercury-contaminated fish during pregnancy (Altmann et al., 1998; Cox et al., 1995; Grandjean et al., 1997; Myers et al., 2000; WHO, 1990).

Historical mercury poisonings serve to highlight the reasons why humans should be concerned about mercury toxicology. In the 50's, many people were poisoned by consumption of organic mercury contaminated fish in Minamata bay (Japan). The concentrations ranged from 6 to 36 mg of methyl mercury per kg of fish (Tamashiro et al., 1986), and in 1971-72, hundreds of people in Iraq died after ingesting bread containing a mean concentration of 9 mg kg^{-1} of organic mercury (Bakir et al., 1973; Marsh et al., 1987).

Methyl mercury penetrates the placental barrier and affects the developing foetuses (CTEM et al., 2000). It moves through the placenta as a methyl mercury-cysteine conjugate by the same transport system as methionine and phenylalanine (Kajiwara et al., 1996). Children with prenatal exposure to low levels of methyl mercury experience

mental retardation, cerebral palsy, blindness, deafness, increased blood pressure and decrease heart rate (Salonen et al., 1995; Sorensen et al., 1999). Heart disease has also been detected in adults. For instance, a studied fishermen population with a daily consumption of 0.03 kg of fish containing 95 μg of mercury had a risk of acute myocardial infarction (Salonen et al., 1995). No chronic effects on humans are expected after of daily consumption of food with less than 0.3 $\mu\text{g kg}^{-1}$ methylmercury (WHO, 1990).

The end points used in human toxicity assessment are mainly developmental neurotoxicity, overt neurological symptoms in adults, and impaired neurological development and delayed sequelae in children (Grandjean et al., 1997; Davidson et al., 1998). They have been evaluated for human populations that are heavily dependent on consumption of fish and marine-mammals. In the Seychelles islands, no prenatal effects were observed in populations with a mean mercury concentration of 6.8 $\mu\text{g g}^{-1}$ in maternal hair collected at birth (Davidson et al., 1998; Myers et al., 2000). Nevertheless, in a Faroe Island study, where children were exposed to similar levels as in the Seychelles population, memory, attention and language abnormalities were related with prenatal exposure (Grandjean et al., 1997).

Maternal hair and adult blood are biomarkers of methyl mercury exposure. About 90% of mercury in the hair appears as methyl mercury. The half-life in blood and hair is between 48 and 53 days (Sherlock et al., 1984; Cox et al., 1989). In a study on humans, a mean concentration of mercury of 0.2 $\mu\text{g g}^{-1}$ in adult blood was associated with 300 μg of mercury intake

per day for which a critical dose of 4.3 $\mu\text{g kg}^{-1}$ per day corresponds to a lowest-observed-adverse-effect level (LOAEL) (Friberg and Group, 1971). It means that a person of 70 kg body weight and a daily intake of more than 300 μg of mercury would exceed the LOAEL ($300/70 = 4.3$). However, susceptibility depends on factors such as age and health status, and an uncertainty factor of 10 has been proposed to be added to the critical dose. The uncertainty is illustrated by observations on prenatal exposure, in which maternal hair concentrations of organic mercury varied between 4 and 15 $\mu\text{g g}^{-1}$, corresponding to a daily intake of 0.3 to 1.3 $\mu\text{g kg}^{-1}$. The high value agreed with the no-observed-adverse-effect level (NOAEL), and the uncertainty factor varied from 3 to 10 (Grandjean et al., 1997; Davidson et al., 1998). Mercury has also been found in umbilical cord tissue. A mean of 0.24 ng g^{-1} d.w. was reported from 176 children born in Minamata between 1950 and 1975 (Akagi et al., 1998). Children with congenital Minamata disease had higher methyl mercury concentrations in the cord than other children from the same area (Abreu et al., 1998; Harada et al., 1999).

In gold mining areas, a significant exposure source of mercury is freshwater fish, which bio-accumulates methyl mercury from polluted environments (Friberg and Group, 1971; Bidone et al., 1997; Davidson et al., 1998). For instance, in some mining regions, fish have reached levels of total mercury from 130 $\mu\text{g kg}^{-1}$ in detritivore species to more than 500 $\mu\text{g kg}^{-1}$ in piscivore fish (Moreira, 1996). The level of daily exposure through consumption of contaminated fish for adult populations in these mining areas is 1.6 $\mu\text{g kg}^{-1}$, which is more than five times greater than the reference dose of 0.3 $\mu\text{g kg}^{-1} \text{ day}^{-1}$

(Bidone et al., 1997). Humans from gold mining areas, with less than $50 \mu\text{g g}^{-1}$ of total mercury in the hair, show reduced psychomotor performance (Lebel et al., 1996; Lebel et al., 1998; Dolbec et al., 2002). Another significant route of exposure in gold mining sites is the inhalation of mercury-contaminated air. Atmospheric mercury concentrations in gold mining areas in Brazil are up to 0.2 mg m^{-3} (Moreira, 1996), which can cause reduction of coordination ability and increase in tremor intensity (Netterstrom et al., 1996).

Freshwater organisms in gold miner's rivers are continuously exposed to mercury. Effects due to mercury exposures include diversity decline, death, and low growth. Chronic toxic effects include shortened life span, reproductive problems, and low fertility.

Organic mercury is more toxic to microorganisms than inorganic mercury species (WHO, 1989b) and adverse effects appear at exposure concentrations of $1 \mu\text{g}$ of methyl mercury per litre according to WHO (1989b). Effects on survival and growth are notorious when microorganisms are exposed to mercury. Single species cultures (such as unicellular green algae) suffer from reduced photosynthesis when the inorganic mercury concentration exceeds $20 \mu\text{g l}^{-1}$ (WHO, 1989b) but the reduction as well as inhibition of growth is dependant on pH, cell density, light intensity, temperature, and exposure time (WHO, 1989b). Diversity may decline as some mercury susceptible genera disappear from the community, while mercury-resistant genera persist (WHO, 1989b).

Ionic inorganic mercury and methyl mercury have high acute toxicity to aquatic organisms. For instance, 1 mg l^{-1} of

inorganic mercury is enough to decrease the chlorophyll content in some plants and reduce photosynthesis by 50% in others (WHO, 1989a; Boening, 2000).

For aquatic invertebrates, the toxicity data vary greatly depending on their different susceptibilities to different mercury species, developmental stage, the development of tolerance, and the chemical and physical properties of the medium where they live. Concentrations lower than $10 \mu\text{g l}^{-1}$ generally result in acute toxicity for the most sensitive developmental stage of many species of aquatic invertebrates (Boening, 2000). Organic species are 10-100 times more toxic than inorganic species.

Concentrations of mercury in fish tissues generally increase with increasing age of the fish, and males seem to have more mercury than females of equal age (WHO, 1989b). Fish accumulate mercury via their food and via passive uptake from water through the gills (Ribeiro et al., 1996). Physiological and biochemical effects (respiratory rate reduction, lack of movement, reduction of food consumption, reduction in blood hemoglobin content, reduced body weight and protein content, etc.) have been reported in fish exposed to mercury. The 96-h LC_{50} vary from 0.03 to 0.40 mg l^{-1} for freshwater species and is higher for marine fish (WHO, 1989a; Boening, 2000).

After a general consideration of the exposure source of mercury and its consequence in humans and aquatic organisms given by the scientific studies, which apply for gold mining areas, a risk evaluation was felt needed to protect the environment and humans living in a gold mining watershed (Paper VI). Bases for risk assessment are the levels of mercury

observed in groundwater, sediments and river water. Mercury has been spread by stream water resulting in a heterogeneous distribution of mercury in the local environment. Paper VI presents an integrative approach for risk assessment to provide a common understanding of the risk associated to pollution by mercury on a basin scale. Groundwater, not commonly included in ecological risk assessment, benthic organisms and fish as ecological endpoint species, and human health treated by consumption of contaminated fish, were considered potential receptors of the pollution.

This thesis addresses fluvial transport of mercury in a river on a temporal and spatial scale of high resolution, highlights the relevance of organic matter and bacteria in predicting the retention of mercury, proposes a methodology to measure the water fluxes in the groundwater/river water interface, suggests sediment resuspension as an important process involved in the fluvial transport of mercury, and suggests an approach to integrate the risk for different endpoints on a basin scale in gold mining areas.

Months and years, and kilometres are the scale units commonly adopted to elucidate the transport of mercury in rivers. Those scales apply to most situations, but the transport of mercury in small gold miners' rivers needs a smaller scale to be elucidated, because the concentrations of mercury vary hourly in a day due to daily episodic releases of mercury and to rapid changes in the concentration of waterborne suspended ore particles. In addition, suspended particles settle down and resuspend over short distances. Therefore, observations of high resolution are proposed to elucidate the transport of

mercury in such river conditions. The process of sedimentation retards the movement of mercury, since most released mercury is sorbed on sediment particles. Because the extent of sorption depends on characteristics of the surface of particles, an analysis of the influence of natural sediment-particle coaters, such as organic matter and bacteria, on a microcosm scale sheds light on the description and prediction of the retention of mercury in fluvial systems.

In contrast to sedimentation, little attention has been given to the mercury-sediment particles resuspension, probably because the movement of mercury by this mechanism is extremely small compared with that in the water phase. Nevertheless, this process becomes relevant in gold miners' rivers because most mercury is concentrated in suspended ore particles and because a longitudinal variation of the particulate mercury concentration is observed due to resuspension. In addition, ground water influx can contribute to the resuspension of particulate mercury in the streams; therefore a methodology is proposed to measure the discharge of groundwater into rivers. The methodology measures the river water infiltration, which can be useful in assessing the impact of the mercury contaminated river on the groundwater quality.

Risk assessment is a difficult task. It is even more difficult when a comparison of risk between several endpoints of different nature is needed. Nevertheless, efforts on risk comparison have to be made because e.g. in gold mining areas, the released mercury ends up in different receptors. The approach presented in this thesis could be used for other scenarios.

Perspectives

Although gold mining activity is an attractive surrogate alternative of sustenance, sometimes thought of as an additional source of income, for people in small gold mining areas, it has resulted in an environmental quality and human health decline due to the uncontrolled or poor-controlled use of mercury. I would say “mercury obscures gold mining areas, as much as gold bright them”.

The uncontrolled or poor-controlled use of mercury in the artisanal gold processing is the main factor of the environmental emission. The use of an inefficient technique for gold recovery, the lack of knowledge about mercury toxicity, and the avoidance of local environmental regulation, also contribute to the emissions. These statements can be the starting point to: i) implement clean alternatives, ii) develop educational campaigns, and iii) improve environmental regulations.

The academic community and environmental authorities together with either national or local government and the general population, must promote the above initiatives, based on the insights given by the scientific observations from the studied gold mining environments.

An examination of the insights gained from the studies in Sucio river basin, with a detailed evaluation of the cost-benefits in the gold production, must be approached to an abatement of the pollution in order to protect people and their environment.

Conclusions

The insights gained from the investigations carried out in the Sucio river basin call for

an environmental and human health care and apply for an environmental monitoring. Together with other findings reported by other studies, the insights can be a core of useful information to implement alternatives in the abatement of the contamination in the river basin.

The study of the fluvial movement of mercury in the small gold mining area dealt with: a) the mercury fluxes variations in the impacted stream and the heterogeneous accumulation of mercury in sediments, b) the anthropogenic levels of mercury in water and river sediments, c) the extent of the mercury contamination in a basin scale, d) the extent of the ground water contamination and the hydraulic communication between it and the contaminated surface water, and e) the risk associated with the mercury exposure in human and stream organisms

The temporal variations of the aqueous mercury concentrations reflect the episodic release of mercury by gold mining activity in the river basin. The findings also reveal that the long transport of mercury is due to dissolved mercury concentrations and that particulate concentrations contribute to the mercury sedimentation in the river system. These observations can be used to develop a monitoring program in order to control the mercury emission.

The fluvial transport of mercury associated with mined ores is characterized by a downstream hotspot of mercury concentration in sediments. The low sedimentation and the high total mercury concentrations observed in shallow sediments suggest a recent decline in ore processing, but an extensive use of mercury. These mercury concentrations in the sediment call for improvements of the artisanal practices in gold recovering or for

the implementation of clean alternatives to reduce or eliminate the mercury emissions.

Simultaneous measurements of surface areas of sediment particles, dissolved organic carbon concentrations, and bacterial cell numbers, are useful to predict spatial variation of mercury retention in river sediment and in aquifers. The discernment of mercury partitioning could improve transport modeling in natural systems and enhance the downscaling interpretation of mercury sorption related to particle size. Moreover including mercury-sorbents such as bacteria and organic matter in the prediction of sorption coefficients is important for the description of the transport of mercury.

In a complex hydrogeological area in the studied river, the rainfall infiltration drives the shallow groundwater dynamics in the near channel aquifers along the stream. These observations can be combined with other procedures, such as the methodology implemented to measure the bi-directional flow and flux of water across the interface groundwater/surface water in rivers, which promise to be useful in describing the distribution of upwelling and downwelling areas of the river. This methodology can be used to develop a pattern for mercury transport along the river and across the boundary to the groundwater.

The risk analysis shows that stream organisms are faced with higher risk than human health and groundwater. Exposure assessment for several receptors identifies potential receptors most at risk and provides a basis for risk management decisions in developing strategies to human and environmental protection.

References

- Aberg, B., Ekman, L., Falk, R., Greitz, U., Persson, G., Snihs, J., 1969. Metabolism of methyl mercury (^{203}Hg) compounds in man. *Archives of Environmental Health*. 19, 478-484.
- Abreu, S.N., Pereira, M.E., Duarte, A.C., 1998. The use of a mathematical model to evaluate mercury accumulation in sediments and recovery time in a coastal lagoon (Ria de Aveiro, Portugal). *Water Science and Technology*. 37(6/7), 33-38.
- Akagi, H., Grandjean, P., Takizawa, Y., Weihe, P., 1998. Methylmercury dose estimation from umbilical cord concentrations in patients with Minamata disease. *Environmental Research*. 77(Sec. A), 98-103.
- Akagi, H., Kinjo, Y., Branches, F., Malm, O., Harada, M., Pfeiffer, W.C., Kato, H., 1994. Methylmercury in the Tapajós River Basin, Amazon. *Environmental Science*. 3, 25-32.
- Akagi, H., Malm, O., Branches, F.J.P., Kinjo, Y., Kashima, Y., Guimares, T.R.D., Oliveira, R.B., Haraguchi, K., Pfeiffer, W.C., Takizawa, Y., Kato, H., 1995. Human exposure to mercury due to gold mining in the Tapajós River Basin, Amazon, Brazil: Speciation of mercury in human hair, blood and urine. *Water, Air, and Soil Pollution*. 80, 85-94.
- André, L., Rosén, K., Torstendahl, J., 1997. Minor field study of mercury and lead from gold refining in Central Nicaragua. *Luleå tekniska universitet*.
- Arvidson, B., 1992. Inorganic mercury is transported from muscular nerve

- terminals to spinal and brainstem motoneurons. *Muscle Nerve*. 15, 1080-1094.
- Aschner, M., Aschner, J.L., 1990. Mercury neurotoxicity: Mechanisms of blood-brain barrier transport. *Neuroscience Biobehav Review*. 14(2), 169-176.
- Babiarz, C.L., Hurley, J.P., Benoit, J.M., Shafer, M.M., Andren, A.W., Webb, D.A., 1998. Seasonal influence on partitioning and transport of total mercury in rivers from contrasting watersheds. *Biogeochemistry*. 41, 237-257.
- Babiarz, C.L., Hurley, J.P., Hoffmann, S.R., Andren, A.W., Shafer, M.M., Armstrong, D.E., 2001. Partitioning of total mercury and methylmercury to the colloidal phase in freshwaters. *Environmental Science and Technology*. 35(24), 4773-4782.
- Bakir, F., Damluji, S.F., Amin-Zaki, L., Murtadha, M., Khalidi, A., al-Rawu, N.Y., Tikriti, S., Dhahir, H.I., Clarkson, T.W., Smith, J.C., Doherty, R.A., 1973. Methylmercury poisoning in Iraq. *Science*. 181(96), 230-241.
- Ballaton, N., Clarkson, T.W., 1984. Inorganic mercury secretion into bile as a low molecular weight complex. *Biochemistry Pharmacology*. 33(7), 1087-.
- Balogh, S.J., Mayer, M.L., Johnson, K., 1997. Mercury and suspended sediment loadings in the lower Minnesota River. *Environmental Science and Technology*. 31, 198-202.
- Barringer, J.L., Szabo, Z., Schneider, D., Atkinson, W.D., Gallagher, R.A., 2006. Mercury in groundwater, septage, leach-field effluent, and soils in residential areas, New Jersey coastal plain. *Science of the Total Environment*. 361, 144-162.
- Bidone, E.D., Castilhos, Z.C., Santos, T.J.S., Souza, T.M.C., Lacerda, L.D., 1997. Fish contamination and human exposure to mercury in Tartarugalzinho River, Amapa State, Northern Amazon, Brazil. A screening approach. *Water, Air and Soil Pollution*. 97, 9-15.
- Biestler, H., Zimmer, H., 1998. Solubility and changes of mercury binding forms in contaminated soils after immobilization treatment. *Environmental Science and Technology*. 32, 2755-2762.
- Boening, D.W., 2000. Ecological effects, transport, and fate of mercury: A general review. *Chemosphere*. 40, 1335-1351.
- Brown-Jr, G.E., Henrich, V.E., Casey, W.H., Clark, D.L., Eggleston, C., Felmy, A., Goodman, D.W., Gratzel, M., Maciel, G., MacCarthy, M.I., Nealson, K.H., Sverjensky, D.A., Toney, M.F., Zachara, J.M., 1999. Metal oxide surfaces and their interactions with aqueous solutions and microbial organisms. *Chemical Reviews*. 99(1), 77-174.
- Brown, D.A., Sherriff, B.L., Sawicki, J.A., Sparling, R., 1999. Precipitation of iron minerals by a natural microbial consortium. *Geochimica et Cosmochimica Acta*. 63(15), 2163-2169.
- Callahan, J.E., Miller, J.W., Craig, J.R., 1994. Mercury pollution as a result of gold extraction in North Carolina, U.S.A. *Applied Geochemistry*. 9, 235-241.
- Carrol, R.W.H., Warwick, J.J., Heim, K.J., Bonzongo, J.C., Miller, J.R., 2000. Simulation of mercury transport and fate in the Carson river,

- Nevada. *Ecological Modelling*. 125, 255-278.
- Cavalleri, A., Gobba, F., 1998. Reversible color vision loss in occupational exposure to metallic mercury. *Environmental Research*. 77, 173-177.
- CEQC/CCME, 1999. Canadian Environmental Quality Guidelines/Canadian Council of Ministers of the Environment.
- Clarkson, T.W., 1992. Mercury: Major issues in environmental health. *Environmental Health Perspectives*. 100, 31-38.
- Clarkson, T.W., 1994. The Toxicology of Mercury and Its Compounds. In: C.J. Watras, J.W. Huckabee (Editors), *Mercury Pollution-Integration and Synthesis*. Lewis, pp. 631-641.
- Compeau, G.C., Bartha, R., 1985. Sulfate reducing bacteria: Principal methylator of mercury in anoxic estuarine sediments. *Applied and Environmental Microbiology*. 50, 498-502.
- Coston, J.A., Fuller, C.C., Davis, J.A., 1995. Pb²⁺ and Zn²⁺ adsorption by a natural aluminum- and iron-bearing surface coating on an aquifer sand. *Geochimica et Cosmochimica Acta*. 59(17), 3535-3547.
- Cox, C., Clarkson, T.W., Marsh, D.O., Amin-Zaki, L., Tikriti, S., Myers, G.G., 1989. Dose-response analysis of infants prenatally exposed to methyl mercury: An application of a single compartment model to single-strand hair analysis. *Environmental Research*. 49(2), 318-332.
- Coyne, A., Schäfer, J., Dabrin, A., Girardot, N., Blanc, G., 2007. Groundwater contributions to metal transport in a small river affected by mining and smelting waste. *Water Research*. 41, 3420-3428.
- CTEM, BEST, CLS, NRC, 2000. *Toxicological Effects of Methylmercury*, Washington, D.C.
- Davidson, P.W., Myers, G.J., Cox, C., Axtell, C., Shamlaye, C., Sloane-Reeves, J., Cernichiari, E., Needham, L., Choi, A., Wang, Y., Berlin, M., Clarkson, T.W., 1998. Effects of prenatal and postnatal methylmercury exposure from fish consumption on neurodevelopment: Outcomes at 66 months of age in the Seychelles child development study. *Journal of the American Medical Association*. 280(8), 701-707.
- Divine, K., Ayala-Fierro, F., Barber, D., Carter, D., 1999. Glutathione, albumin, cysteine, and Cys-Gly effects on toxicity and accumulation of mercury chloride in LLC-PK1 cells. *Journal of Toxicology and Environmental Health Part A*. 57(7), 489-505.
- Dolbec, J., Mergier, D., Passos, C.-J.S., Morais, S.S.d., Lebel, J., 2000. Methylmercury exposure affects motor performance of a riverine population of the Tapajós river, Brazilian Amazon. *International Archives of Occupational Environmental Health*. 73, 195-203.
- Dunn, J.D., Clarkson, T.W., Magos, L., 1981. Ethanol reveals novel mercury detoxification step in tissues. *Science*. 213, 1123-.
- Endo, T., Nakaya, S., Kimura, R., 1990. Mechanisms of absorption of inorganic mercury from rat small intestine: III. Comparative absorption studies of inorganic mercuric compounds in vitro.

- Pharmacology Toxicology. 66(5), 347-353.
- EPA, 1995. EPA Section 304 (a). Criteria for the Protection of Aquatic Life from Priority Toxic Pollutants (US Clean Water Act, February 5, 1993; Part 131-Water Quality Standards, Sec. 131.36 proposed amendment April 1995).
- Farid, L.H., Machado, J.E.B., Silva, O.A., 1991. Emission control and mercury recovery from garimpo tailing. In: M. M. Veiga and F. R. C. Fernandez (Editors), Poconé: Un campo de estudos do impacto ambiental do garimpo. CETEM/CNPq, Rio de Janeiro, Brazil. pp.27-44.
- Forbes, E.A., Posner, A.M., Quirk, J.P., 1974. The specific adsorption of inorganic mercury Hg(II) species and Co(III) complex ions on goethite. *Journal of Colloid Interface Science*. 49, 403-409.
- Foulkes, E.C., Bergman, D., 1993. Inorganic mercury absorption in mature and immature Ratjejunum: Transcellular and intercellular pathways in vivo and in everted sacs. *Toxicology and Applied Pharmacology*. 120, 89-95.
- Friberg, L., Group, S.E., 1971. Methylmercury in fish: A toxicological-epidemiologic evaluation of risks report from an expert group. *Nord Hyg Tidskr.* 4(Suppl), 19-364.
- Gilmour, C.C., Henry, E.A., 1991. Mercury methylation in aquatic system affected by acid deposition. *Environmental Pollution*. 71, 131-169.
- Gissinger, P.B.-. Alnot, M., Lickes, J.-P., Ehrhardt, J.-J., Behra, P., 1999. Modeling the adsorption of mercury(II) on (hydr)oxides II: a-FeOOH (goethite) and amorphous silica. *Journal of Colloid and Interface Science*. 215, 313-322.
- Grandjean, P., Weihe, P., White, R.F., Araki, F.S., Yokoyama, K., Murata, K., Sorensen, N., Dahl, R., Jorgensen, P.J., 1997. Cognitive deficit in 7-year-old children with prenatal exposure to methylmercury. *Neurotoxicology and Teratology*. 19(6), 417-428.
- Hall, L.L., Allen, P.V., Fisher, H.L., 1994. The kinetics of intravenously-administered inorganic mercury in humans. In: K.M.S. Subramanian, M.E. Wastney (Editors), *Kinetic Models of Trace Elements and Mineral Metabolism During Development*. CRC Press, Boca Raton, FL, pp. 1-21.
- Harada, M., 1995. Minamata disease: Methylmercury poisoning in Japan caused by environmental pollution. *Critical Reviews in Toxicology*. 25(1), 1-24.
- Harada, M., Akagi, H., Tsuda, T., Kizaki, T., Ohno, H., 1999. Methylmercury level in umbilical cords from patients with congenital Minamata disease. *The Science of the Total Environment*. 234(1-3), 59-62.
- Huckabee, J.W., Elwood, J.W., Hildebrand, S.G., 1979. Accumulation of mercury in freshwater biota. In: J.O.N. (ed) (Editor), *The Biogeochemistry of Mercury in the Environment*. Elsevier/North-Holland Biomedical Press, New York.
- Hurley, J.P., Benoit, J.M., Babiarz, C.L., Shafer, M.M., Andren, A.W., Sullivan, J.R., Hammond, R., Webb, D.A., 1995. Influences of watershed characteristics on mercury levels in Wisconsin rivers.

- Environmental Science and Technology. 29, 1867-1875.
- Hurley, J.P., Cowell, S.E., Shafer, M.M., Hughes, P.E., 1998. Tributary loading of mercury to Lake Michigan: Importance of seasonal events and phase partitioning. *The Science of the Total Environment*. 213, 129-137.
- Hursh, J.B., Clarkson, T.W., Miles, E.F., 1989. Percutaneous absorption of mercury vapor by man. *Archives of Environmental Health*. 44, 120-127.
- Hursh, J.B., Sichak, S.P., Clarkson, T.W., 1988. In vitro oxidation of mercury by the blood. *Pharmacology Toxicology*. 63, 266-273.
- Hylander, L.D., Meili, M., Oliveira, L.J., Silva, E.C., Guimarães, J.R.D., Araujo, D.M., Neves, R.P., Stachiw, R., Barros, A.J.P., Silva, G.D., 2000. Relationship of mercury with aluminum, iron, and manganese oxy-hydroxides in sediments from the Alto Pantanal, Brazil. *The Science of the Total Environment*. 260, 97-107.
- Ikingura, J.R., Mutakyahwa, M.K.D., Kahatano, J.M.J., 1997. Mercury and mining in Africa with special reference to Tanzania. *Water, Air and Soil Pollution*. 97, 223-232.
- Inskip, M.J., Piotrowski, J.K., 1985. Review of the health effects of methylmercury. *Journal of Applied Toxicology*. 5, 113-133.
- Ishihara, N., 2000. Excretion of methyl mercury in human feces. *Archives of Environmental Health*. 55(1), 44-48.
- Islam, J., Singhal, N., O'Sullivan, M., 2001. Modeling biogeochemical processes in leachate-contaminated soils. A review. *Transport in Porous Media*. 43, 407-440.
- Johansson, K., Iverfeldt, Å., 1994. The relation between mercury content in soil and the transport of mercury from small catchments in Sweden. In: C.J. Watras, J.W. Huckabee (Editors), *Mercury Pollution-Integration and Synthesis*. Lewis, pp. 323-328.
- Kajiwara, Y., Yasutake, A., Adachi, T., Hirayama, K., 1996. Methylmercury transport across the placenta via neutral amino acid carrier. *Archives of Toxicology*. 70, 310-314.
- Kerper, L.E., Ballatori, N., Clarkson, T.W., 1992. Methyl mercury transport across the blood-brain barrier by an amino acid carrier. *American Journal of Physiology*. 262(5), R761-R765.
- Kimball, B.A., Broshears, R.E., Bencala, K.E., McKnight, D.M., 1994. Coupling of hydrologic transport and chemical reactions in a stream affected by acid mine drainage. *Environmental Science and Technology*. 28, 2065-2073.
- Krabbenhoft, D.P., Babiarz, C.L., 1992. The role of groundwater transport in aquatic mercury cycling. *Water Resources Research*. 28(12), 3119-3128.
- Kraepiel, A.M.L., Keller, K., Morel, F.M.M., 1999. A model for metal adsorption on montmorillonite. *Journal of Colloid and Interface Science*. 210, 43-54.
- Lacerda, L.D., 1997. Global mercury emission from gold and silver mining. *Water, Air, and Soil Pollution*. 97, 209-221.
- Lacerda, L.D., 2003. Updating global Hg emissions from small-scale gold mining and assessing its environmental impacts.

- Environmental Geology. 43, 308-314.
- Lacerda, L.D., Marins, R.V., 1997. Anthropogenic mercury emission to the atmosphere in Brazil. *Journal of Geochemical Exploration*. 58, 223-229.
- Lacerda, L.D., Ribeiro, M.G., Cordeiro, R.C., Sifeddini, A., Turcq, B., 1999. Atmospheric mercury deposition over Brazil during the past 30,000 years. *Journal of the Brazilian Association for the Advancement of Science*. 51, 363-371.
- Lacerda, L.D., Salomos, W., 1998. Mercury from gold and silver mining. A chemical time-bomb? Springer, Berlin Heidelberg, New York.
- Lawson, N.M., Mason, R.P., 1998. Accumulation of mercury in estuarine food chains. *Biogeochemistry*. 40, 235-247.
- Lebel, J., Mergler, D., Branches, F., Lucotte, M., Amorim, M., Larribe, F., Dolbec, J., 1998. Neurotoxic effects of low-level methylmercury contamination in the Amazonian basin. *Environmental Research*. 79, 20-32.
- Lebel, J., Mergler, D., Lucotte, M., Amorim, M., Dolbec, J., Miranda, D., Arantes, G., Rheault, I., Pichet, P., 1996. Evidence of early nervous system dysfunction in Amazonian population exposed to low-levels of methylmercury. *Neurotoxicology*. 17(1), 157-168.
- Leigh, D.S., 1997. Mercury-tainted oberbank sediment from past gold mining in north Georgia, USA. *Environmental Geology*. 30((3/4)), 244-251.
- Lima, L.R.P.d.A., Bernardez, L.A., Barboza, L.A.D., 2008. Characterization and treatment of artisanal gold mine tailings. *Journal of Hazardous Materials*. 150, 747-753.
- Limbong, D., Kumampung, J., Rimper, J., Arai, T., Miyazaki, N., 2003. Emission and environmental implications of mercury from artisanal gold mining in north Sulawesi, Indonesia. *The Science of the Total Environment*. 302, 227-236.
- Lin, Y., Guo, M., Gan, W., 1997. Mercury pollution from small gold mining in China. *Water, Air, and Soil Pollution*. 97, 233-239.
- Lindqvist, O., 1984. Mercury in the Swedish Environment. Global and Local Sources. National Swedish Environmental Protection Board Report.
- Lipfert, F.W., 1997. Estimating exposure to methylmercury: Effects of uncertainties. *Water, Air, and Soil Pollution*. 97, 119-145.
- Lodenius, M., 1998. Dry and wet deposition of mercury near a chlor-alkali plant. *The Science of the Total Environment*. 213, 53-56.
- Lodenius, M., Seppänen, A., Autio, S., 1987. Sorption of mercury in soils with different humus content. *Bulletin of Environmental Contamination Toxicology*. 39, 593-600.
- Malm, O., 1998. Gold mining as a source of mercury exposure in the Brazil Amazon. *Environmental Research*. 77, 73-78.
- Maprani, A.C., Al, T.A., Macquarrie, K.T., Dalziel, J.A., Shaw, S.A., Yeats, P.A., 2005. Determination of mercury evasion in a contaminated headwater stream. *Environmental Science and Technology*. 39, 1679-1687.

- Marsh, D.O., Clarkson, T.W., Cox, C., Myers, G.J., Amin-Zaki, L., Al-Tikriti, S., 1987. Fetal methylmercury poisoning: Relationship between concentration in a single strands of maternal hair and child effects. *Arch Neurol.* 44(10), 1017-1022.
- Matthiessen, A., 1996. Kinetic aspects of the reduction of mercury ions by humic substances. I. Experimental design. *Fresenius Journal of Analytical Chemistry.* 354, 747-749.
- Maurice-Bourgoin, L., Quemerais, B., M-Turcq, P., Seyler, P., 2003. Transport, distribution and speciation of mercury in the Amazon River at the confluence of black and white waters of the Negro and Solimões Rivers. *Hydrological Processes.* 17, 1405-1417.
- Moore, J.N., Brook, E.D., Johns, C., 1989. Grain size partitioning of metals in contaminated, coarse-grained river floodplain sediment: Clark Fork River, Montana, U.S.A. *Environmental Geology Water Science.* 14(2), 107-115.
- Moreira, J.C., 1996. Threats by heavy metals: Human and environmental contamination in Brazil. *The Science of the Total Environment.* 188 Suppl.(1), S61-S71.
- Morel, F.M.M., Kraepiel, A.M.L., Amyot, M., 1998. The chemical cycle and bioaccumulation of mercury. *Annual Review of Ecology Systematics.* 29, 543-566.
- Mudroch, A., Clair, T.A., 1986. Transport of arsenic and mercury from gold mining activities through and aquatic system. *The Science of the Total Environment.* 57, 205-216.
- Myers, G.J., Davidson, P.W., Cox, C., Shamlaye, C., Cernichiari, E., Clarkson, T.W., 2000. Twenty-seven years studying the human neurotoxicity of methylmercury exposure. *Environmental Research.* 83, 275-285.
- Nazarov, N.A., Demidov, V.N., 2001. Methods and results of numerical modeling of reactive solute transport in river flow. *Water Resources.* 28(1), 34-41.
- Netterstrom, B., Guldager, B., Heeboll, J., 1996. Acute mercury intoxication examined with coordination ability and tremor. *Neurotoxicology and Teratology.* 18(4), 505-509.
- Nimick, D.A., McCleskey, B.R., Gammons, C.H., 2007. Diel mercury-concentration variations in streams affected by mining and geothermal discharge. *Science of the Total Environment.* 373, 344-355.
- Palheta, D., Taylor, A., 1995. Mercury in environmental and biological samples from a gold mining area in the Amazon region of Brazil. *The Science of the Total Environment.* 168, 63-69.
- Pamphlett, R., Waley, P., 1996a. Motor neuron uptake of low dose inorganic mercury. *Journal of Neuro Science.* 135, 63-67.
- Pamphlett, R., Waley, P., 1996b. Uptake of inorganic mercury by the human brain. *Acta Neuropathology.* 92, 525-527.
- Pamphlett, R., Waley, P., 1998. Mercury in human spinal motor neurons. *Acta Neuropathology.* 96, 515-519.
- Paradis, S., Wheatley, B., Boswell-Purdy, J., Bélisle, D., Cole, M., Lickers, H., Hayton, A., Davies, K., 1997. Mercury contamination through fish consumption: A model for

- predicting and preventing hazardous behaviour on a community level. *Water, Air, and Soil Pollution*. 97, 147-158.
- Pfeiffer, W.C., Lacerda, L.D., 1988. Mercury inputs into the Amazon region, Brazil. *Environmental Technology Letter*. 9, 325-330.
- Quémerais, B., Cossa, D., Rondeau, B., Phan, T.T., Gagnon, P., Fortin, B., 1999. Sources and fluxes of mercury in the St. Lawrence river. *Environment Science and Technology*. 33, 840-849.
- Renzoni, A., Zino, F., Fanchi, E., 1998. Mercury levels along the food chain and risk for exposed populations. *Environmental Research*. 77, 68-72.
- Ribeiro, C.A.O., Guimaraes, J.R.D., Pfeiffer, W.C., 1996. Accumulation and distribution of inorganic mercury in a tropical fish (*Trichomycterus zonatus*). *Ecotoxicology and Environmental Safety*. 34, 190-195.
- Rodgers, P., Soulsby, C., Petry, J., Malcom, I., Gibbins, C., Dunn, S., 2004. Groundwater-surface-water interactions in a braided river: a tracer-based assessment. *Hydrological Processes*. 18, 1315-1332.
- Roulet, M., Lucotte, M., Canuel, R., Rheault, I., Tran, S., Goy, Y., Farella, N., Passos, C., Silva, S., Mergler, D., Amorim, M., 1998. Distribution and partition of total mercury in waters of the Tapajós river basin, Brazilian Amazon. *The Science of the Total Environment*. 213, 203-211.
- Roulet, M., Lucotte, M., Saint-Aubin, A., Tran, S., Rheault, I., Silva, E.D.J.D., Dezencourt, J., Passos, C.-J.S., Santos, G., Guimaraes, J.-R.D., Mergler, D., Amorim, M., 1998b. The geochemistry of mercury in central Amazonian soils developed on the Alter-do-Chão formation of the lower Tapajós River Valley, Pará state, Brazil. *The Science of the Total Environment*. 223(1-24).
- Runkel, R.L., Bencala, K.E., Broshears, R.E., 1996. Reactive solute transport in streams 1. Development of an equilibrium-based model. *Water Resources Research*. 32(2), 409-418.
- Runkel, R.L., Kimball, B.A., 1999. Reactive solute transport in streams: A surface complexation approach for trace metal sorption. *Water Resources Research*. 35(12), 3829-3840.
- Salomão, M.S.M.B., Molisani, M.M., Ovalle, A.R.C., Rezende, C.E., Lacerda, L.D., Carvalho, C.E.V., 2001. Particulate heavy metal transport in the lower Paraíba do Sul River basin, southeastern, Brazil. *Hydrological Processes*. 15, 587-593.
- Salonen, J.T., Seppänen, K., Nyyssönen, K., Korpela, H., Kauhanen, J., Kantola, M., Tuomilehto, J., Esterbauer, H., Tatzber, F. R.S., 1995. Intake of mercury from fish, lipid peroxidation, and the risk of myocardial infarction and coronary, cardiovascular, and any death in eastern finnish men. *Circulation*. 91(3), 645-655.
- Sarkar, D., Essington, M.E., Misra, K.C., 1999. Adsorption of mercury(II) by variable charge surfaces of quartz and gibbsite. *Soil Science Society of America Journal*. 63, 1626-1636.
- Sarkar, D., Essington, M.E., Misra, K.C., 2000. Adsorption of mercury(II) by

- kaoline. *Soil Science Society of America Journal*. 64, 1968-1975.
- Schlüter, K., 2000. Review: Evaporation of mercury from soils. An integration and synthesis of current knowledge. *Environmental Geology*. 39(3-4), 249-271.
- Schlüter, K., Gäth, S., 1997. Modelling leaching of inorganic Hg(II) in a Scandinavian iron-humus podzoiil - Validation and long-term leaching under various deposition rates. *Water, Air, and Soil Pollution*. 96, 301-320.
- Sherlock, J., Hislop, J., Newton, D., Topping, G., Whittle, K., 1984. Elevation of mercury in human blood from controlled chronic ingestion of methylmercury in fish. *Human Toxicology*. 3, 117-131.
- Silva, G., 1994. Diagnóstico de la contaminación ambiental generada por la actividad minera sobre los ríos Sucio, Mico y Sineca Nicaragua. Universidad Federal de Pará /Centro de Geociencias.
- Sjöblom, A., Håkansson, K., Allard, B., 2004. River water metal speciation in a mining region-The influence of wetlands, liming, tributaries, and groundwater. *Water, Air, and Soil Pollution*. 152, 173-194.
- Smith, J., Allen, P., Turner, M., 1994. The kinetics of intravenously administered methyl mercury in man. *Toxicology and Applied Pharmacology*. 128, 251-256.
- Sorensen, N., Murata, K., Budtz-Jorgensen, E., Weihe, P., Grandjean, P., 1999. Prenatal methylmercury exposure as a cardiovascular risk factor at seven years of age. *Epidemiology*. 10(4), 370-375.
- Stordal, M.C., Gill, G.A., Wen, L.-S., Santschi, P.H., 1996. Mercury phase speciation in the surface waters of the three Texas estuaries: Importance of colloidal forms. *Limnology Oceanography*. 41(1), 52-61.
- Straaten, P.v., 2000. Mercury contamination associated with small-scale gold mining in Tanzania and Zimbabwe. *The Science of the Total Environment*. 259, 105-113.
- Suda, I., Hirayama, K., 1992. Degradation of methyl- and ethylmercury into inorganic mercury by hydroxyl radical produced from rat liver microsomes. *Arch Toxicol*. 66(6), 398-402.
- Tamashiro, H., Arakaki, M., Futatsuka, M., Lee, E.S., 1986. Methylmercury exposure and mortality in southern Japan: A close look at causes of death. *Journal of Epidemiology Community Health*. 40(2), 181-185.
- Tarras-Wahlberg, N.H., Flachier, A., Lane, S.N., Sangfors, O., 2001. Environmental impacts and metal exposure of aquatic ecosystems in rivers contaminated by small scale gold mining: the Puyango River Basin, Southern Ecuador. *The Science of the Total Environment*. 278, 239-261.
- Telmer, K., Costa, M., Angélica, R.S., Araujo, E.S., Maurice, Y., 2006. The source and fate of sediment and mercury in the Tapajós River, Pará, Brazilian Amazon: Ground- and space-based evidence. *Journal of Environmental Management*. 81, 101-113.
- Tessier, A., Campbell, P.G.C., Bisson, M., 1982. Particulate trace metal speciation in stream sediments and relationships with grain size: Implication for geochemical exploration. *Journal of*

- Geochemical Exploration. 16, 77-104.
- Tsiros, L.X., 2001. A screening model-based study of transport fluxes and fate of airborne mercury deposited onto catchment areas. *Chemosphere*. 44, 99-107.
- Ullrich, S.M., Ilyushchenko, M.A., Uskov, G.A., Tanton, T.W., 2007. Mercury distribution and transport in a contaminated river system in Kazakhstan and associated impacts on aquatic biota. *Applied Geochemistry*. 22, 2706-2734.
- Ullrich, S.M., Tanton, T.W., Abdrashitova, S.A., 2001. Mercury in the aquatic environment: A review of factors affecting methylation. *Critical Reviews in Environmental Science and Technology*. 31(3), 241-293.
- Valenzuela, A., Fytas, K., 2002. Mercury management in small-scale mining. *International Journal of Surface Mining*. 16(1), 2-23.
- Walcarius, A., Devoy, J., Bessiere, J., 1999. Electrochemical recognition of selective mercury adsorption on minerals. *Environmental Science and Technology*. 33, 4278-4284.
- Walling, D.E., 1983. The sediment delivery problem. *Journal of Hydrology*. 65, 209-237.
- Walling, D.E., 1988. Erosion and sediment yield research - Some recent perspectives. *Journal of Hydrology*. 100, 113-141.
- Wallschläger, D., Desai, M.V.M., Spengler, M., Windmüller, C.C., Wilken, R.-D., 1998. How humic substances dominate mercury geochemistry in contaminated floodplain soils and sediments. *Journal of Environmental Quality*. 27(5), 1044-1054.
- Wang, F., Chen, J., Forsling, W., 1997. Modeling sorption of trace metals on natural sediments by surface complexation model. *Environmental Science and Technology*. 31, 448-453.
- Whitney, P.R., 1975. Relationship of manganese-iron oxides and associated heavy metals to grain size in stream sediments. *Journal of Geochemical Exploration*. 4, 251-263.
- WHO, 1989a. *Environmental Health Criteria 86: Mercury, Environmental Aspects*, Geneva.
- WHO, 1989b. *Mercury Environment Aspect, Geneva- Environmental Health Criteria 86*.
- WHO, 1990. *Methyl mercury, International Program on Chemical Safety, Geneva: Environmental Health Criteria 101*.
- Whyte, D.C., Kirchener, J.W., 2000. Assessing water quality impacts and cleanup effectiveness in streams dominated by episodic mercury discharges. *The Science of the Total Environment*. 260, 1-9.
- Wilken, R.D., Horvat, M., 1997. "Mercury as a Global Pollutant" - International Conference. *Fresenius Journal of Analytical Chemistry*. 358, 361-362.
- Winter, T.C., 1999. Relation of streams, lakes, and wetlands to groundwater flow systems. *Hydrological Journal*. 7, 28-45.
- Yin, Y., Allen, H.E., Huang, C.P., 1997. Kinetics of mercury (II) adsorption and desorption on soil. *Environmental Science and Technology*. 31, 496-503.
- Yin, Y., Allen, H.E., Li, Y., Huang, C.P., Sander, P.F., 1996. Adsorption of mercury (II) by soil: Effects of pH, chloride, and organic matter. *Journal of Environmental Quality*. 25, 837-844.

**Temporal and spatial distribution of waterborne
mercury in a gold miner's river**

Picado, F. and Bengtsson, G

Temporal and spatial distribution of waterborne mercury in a gold miner's river

Francisco Picado^{1,2}, Göran Bengtsson².

¹Centro para la Investigación en Recursos Acuáticos de Nicaragua-Universidad Nacional Autónoma de Nicaragua, Apartado Postal 4598, Managua Nicaragua.

²Department of Ecology, Lund University, Sölvegatan 37, SE-22362 Lund, Sweden

Abstract

We examined the spatial and temporal (hourly) variation of aqueous concentrations of mercury in a gold miner's river to determine what factors control transport, accumulation, and export of mercury. The mercury fluxes were calculated to account for episodic inputs of mercury through mining tailings, river flow, and the partitioning of mercury between particulate and dissolved and particulate phase.

Water samples were collected upstream and downstream two mining sites in Sucio river, Nicaragua. The samples were analyzed for dissolved and suspended mercury, total solids, dissolved organic carbon, and total iron in water. Water velocity was also measured at the sampling sites. Mercury was mainly transported in the suspended phase, with a temporal pattern of diurnal peaks corresponding with the amalgamation schedules at the gold mining plants. The concentrations decreased with distance from the mining sites, suggesting dilution by tributaries or sedimentation of particle-bound mercury. The lowest total mercury concentrations were less than 0.1 µg/l and the highest concentrations (5.0 µg/l) were exceeding the WHO maximum permissible limit. Particulate mercury concentrations accounted for the largest variation of mercury fluxes, whereas the dissolved concentrations made up most of the long-ranged transport along the stream. The total mass of mercury accumulated due to sedimentation of suspended solids was 2.7 kg/year and the total mass exported downstream from the mining area was 1.6 kg/year. This study demonstrates the importance of the temporal and spatial resolution of observations in describing the occurrence of mercury in a river affected by anthropogenic activities.

Keywords: Transport, Partitioning, Suspended solids.

Introduction

The process water released into rivers and lakes during homogenization of ore material for gold mining contains fine particles, mostly quartz minerals. During amalgamation of the fine particles, the ore suspension washed into the recipient contains mercury, often in concentrations that are several orders of magnitude greater than the background concentration of local sediments (Wayne et al., 1996).

The released mercury is transported in solution and sorbed to suspended matter (Balogh et al., 1997; Roulet et al., 1998; Maurice-Bourgoin et al., 2003), and the concentrations decrease downstream of a contamination source, in water as well as in the sediments (Wayne et al., 1996; Leigh, 1997; Hylander et al., 2000; Betancourt et al., 2005). In the dissolved phase, mercury occurs as free or hydrated ions and in complexes with dissolved inorganic (chloride, hydroxide, sulphide)

and particularly organic matter, represented by humic and fulvic acids (Ramamoorthy and Kushner, 1975; Morel et al., 1998; Arkhipova et al., 2001; Haitzer et al., 2003). Therefore, a positive relationship between dissolved organic matter (DOM) concentrations and dissolved mercury concentrations is commonly observed in most aquatic systems (Ravichandran, 2004). However, mercury associated with the suspended particulate matter (SPM) dominates the fluxes of mercury in most river systems (Wayne et al., 1996; Balogh et al., 1997; Hurley et al., 1998; Quémérais et al., 1998; Lawson et al., 2001).

Since mercury equilibrates rapidly between the dissolved and particulate phase, the transport of mercury in rivers and streams can be described by the fluxes of dissolved and particulate mercury (Betancourt et al., 2005). The flux of mercury varies with dissolved and particulate matter concentrations, and depends to a great extent on the flow conditions of the stream. For instance, in gold mining areas, the mercury concentration in rivers mainly relies on both the amount of particulate material released (Roulet et al., 1998; Betancourt et al., 2005) and river flow. Mercury associated with finer ore particles usually moves slower than dissolved mercury, and since most of the mercury is particulate (Roulet et al., 1998; Betancourt et al., 2005), the concentrations may gradually decrease in the downstream direction because the particulate mercury sinks onto the riverbed (Roulet et al., 1998; Limbong et al., 2003; Betancourt et al., 2005). As sediment bound mercury increases the probability of long term toxic effects on stream organisms, and in humans through contaminated fish.

In the stream, the spatial and temporal distribution of suspended mercury is mainly controlled by the water velocity (Bishop et al., 1995; Babiarz et al., 1998;

Balogh et al., 1998b; Roulet et al., 1998), but also by the interaction of the suspended mercury with mercury in solution and in the sediment (Roulet et al., 1998; Tarras-Wahlberg et al., 2001; Miller et al., 2002). During periods with high velocity and turbulence, the water may contain high concentrations of mercury due to resuspension of mercury-contaminated particles from the streambed (Bonzongo et al., 1996; Wayne et al., 1996; Hurley et al., 1998; Roulet et al., 1998; Lawson et al., 2001). Fluxes of particulate mercury can also increase due to storm-water runoff, when mercury bound to iron oxy-hydroxides coated-soil particles enters the river channel (Roulet et al., 1998; Betancourt et al., 2005). In contrast, mercury may dissipate during low flow condition due to sedimentation of particle bound mercury; yet, a detectable fraction of mercury remains dissolved in the water phase (Roulet et al., 1998; Limbong et al., 2003; Maurice-Bourgoin et al., 2003). The concentration distribution of mercury along a river is also dependent on dilution by precipitation, upwelling groundwater, and influx from connecting streams (Balogh et al., 1998a; Roulet et al., 1998).

The SPM of e.g tropical rivers contains large quantities of iron and manganese oxyhydroxides (Carvalho et al., 1999) but also particulate organic carbon (POC), which sorbs mercury from the solution (Quémérais et al., 1998; Cai et al., 1999; Yin and Balogh, 2002; Chadwick et al., 2006). However, mined ore particles, which have been in contact with mercury and then discharged into a stream, can mask the mercury-scavenging role of iron-coated particles and other metal sorbents transported by the stream. Therefore, high concentrations of mercury often found in miner's rivers may refer to ore particles (Maurice-Bourgoin et al., 2003; Betancourt et al., 2005; Lima et al., 2008) rather than to terrestrial and autochthonous waterborne SPM

concentrations. These processes are site-specific. For instance, in gold mining areas, short-term amalgamation activities may propagate through a river as temporal pulses of mercury bound to mined ore particles.

Mercury contaminated mill tailings are discharged by gold mining into Sucio river in the St Domingo mining district in central Nicaragua. Since ore crushing is continuous but amalgamation sporadic at the major mills, observations by high temporal and spatial resolution can be helpful i) to elucidate the movement pattern and mass distribution of waterborne mercury and ii) to predict the future accumulation of mercury in the sediment phase and the amount of mercury exported to the neighbour watershed.

This study addresses the spatial and temporal variation of mercury fluxes in Sucio river. We raised five questions: 1) What is the diurnal pattern of mercury concentration in the water? 2) What is the contribution of the suspended material and dissolved organic carbon to the mercury concentration in the water phase? 3) What is the influence of iron concentration on the suspended mercury concentration in the river? 4) What is the spatial pattern of variation of the mercury concentration with distance from the sources? 5) What is the total mass of mercury estimated to accumulate in the river within the St. Domingo area and the total mass exported from the area?

Materials and Methods

Study area

Río Sucio (Río Artiguas) is a small river, historically impacted by the gold mining activity in the St Domingo district. Miners still use mercury in the gold enrichment process. The river basin covers nearly 28 km² and is located in the central mountain region of Nicaragua (Fig. 1). The regimen of precipitation is almost constant in the dry season but it varies in the rainy season. The mean precipitation is about 2400 mm yr⁻¹ (INETER, 1991). The annual temperature varies from 23 to 27 °C. The river drains towards the southwest, and its flow increases downstream due to contributions from several small streams and probably groundwater discharge.

In the river basin, tunnels and shafts are constructed by hand, where gold-bearing deposits are mined (extraction sites in Fig. 1). The ore is transported to gold amalgamation sites and grinded by different tools (e.g. electric mills, water driven stone mills, manual mortars). The amalgamation sites are located along the river at a distance of some few metres from the shore, because the river water is used in the gold recovering process. Mercury vaporizes into the atmosphere when the amalgam is burned, and another fraction is discharged into the river through the mining tailings.

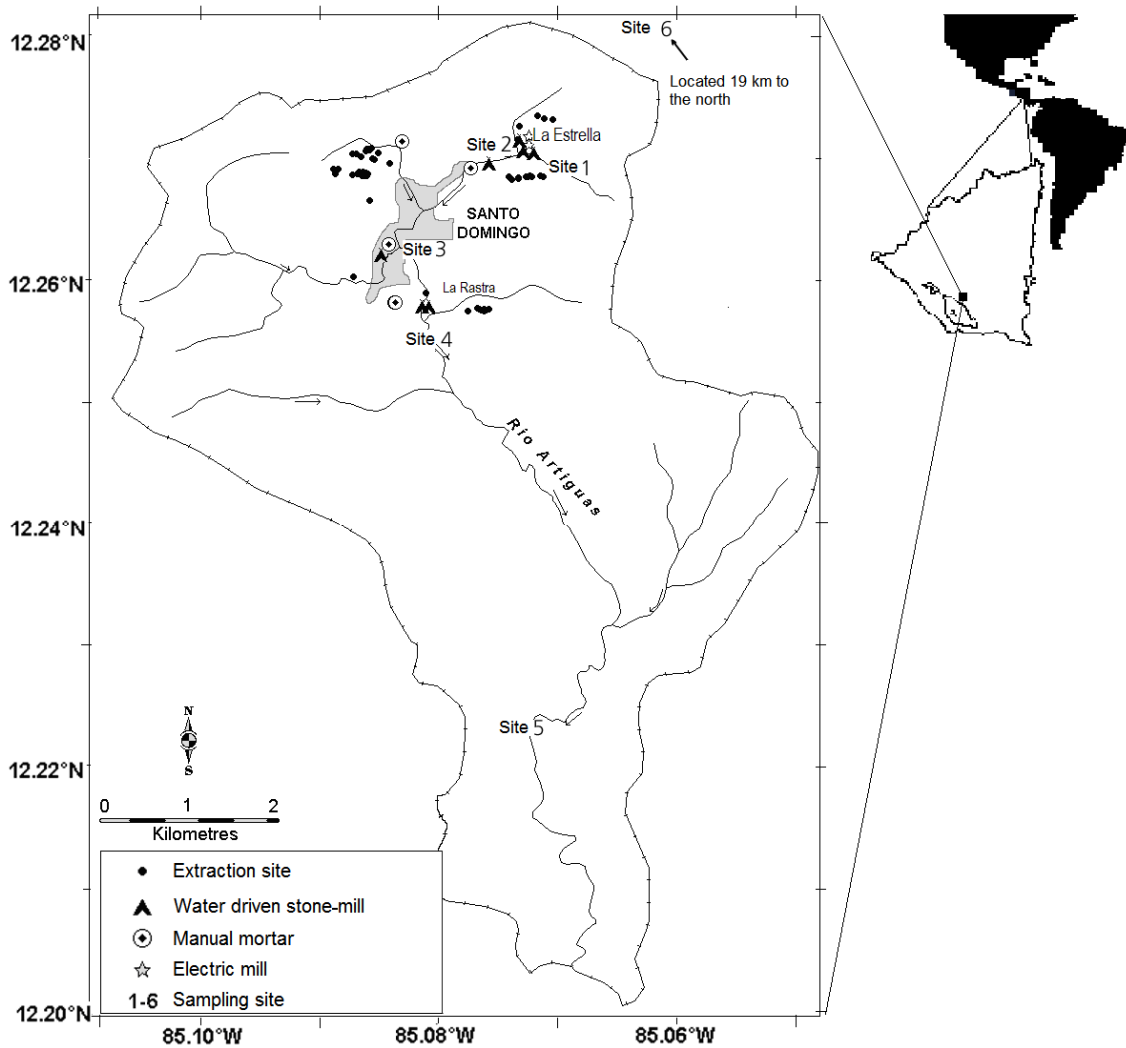


Figure 1. Mercury sources (Mendoza, 2006) and location of sampling sites along the Río Sucio, St Domingo-Chontales, Nicaragua.

Sampling and chemical analyses

Six sites were selected for sampling (Fig. 1, Table 1), based on distance from the point sources of mercury and accessibility for sampling.

Sampling site description

Table 1. Characteristics of sampling sites at the Sucio river.

Sampling site	Site description
Site 1	This is one of two heads of the Sucio river and is located upstream La Estrella gold processing plant. No mining activity was observed in the surroundings. The concentration of mercury was thought to represent ambient conditions.
Site 2	Located 100 m downstream of the processing plant of La Estrella. Mercury concentrations were expected to be high.

Table 1 (*Continuation*)

Site 3	Located in the middle of St Domingo village (2.0 km downstream La Estrella plant). Solid wastes released into the river are domestic, and sometimes blood and rubbishes from cattle that people kill for local consumption are also discharged into the river.
Site 4	Located downstream of the second main processing plant, called La Rastra (3.1 km downstream La Estrella plant). The mining tailings from La Rastra are released directly into the river.
Site 5	Located approximately 8.4 km downstream of La Estrella. It was thought to represent mercury exposure from all major upstream contamination sources
Site 6	Located approximately 45 km downstream of La Estrella. We did not expect to find any traces of the upstream contamination sources.

Water samples

The sites were sampled under baseflow conditions. No precipitation events occurred, and a relatively intense mining activity was observed in the river basin. One litre of water was collected hourly during 24 hr at four of the sites (sites 2, 3, 4, and 5). Water-nitric acid (4:1) washed polyethylene bottles were used, and 500 ml of the sample were preserved in 0.1% HNO₃ and kept on ice until analysed. The unpreserved 500 ml of each water sample were filtered in the field through 0.45 µm Millipore cellulose acetate filters using an all-glass filtration unit. An aliquot of 50 ml was taken from the filtrate, kept on ice in the field and then refrigerated at 0 °C for dissolved organic carbon (DOC) analysis. The remaining filtrate was acid preserved for total dissolved mercury (TDHg) analysis. Mercury and iron concentrations were determined in the unfiltered water. The concentration of particulate mercury (TPHg) was obtained as the differences between the unfiltered (THg) and filtered mercury concentrations.

The concentration of total solids (TS) and total dissolved solids (TDS) was also measured in the unfiltered and unpreserved-filtered water samples, respectively, as outlined in standard methods (APHA, 1999). The total suspended solids (TSS) concentration was

obtained from the difference between the TS and TDS concentrations.

Mercury and iron concentrations were determined by inductively coupled plasma mass spectroscopy (ICP-MS; Perkin Elmer, ELAN-6000) and flame atomic absorption spectrophotometry (AA-20 Varian), respectively. The detection limits were 0.05 mg l⁻¹ and 0.03 µg l⁻¹ for total iron and total mercury, respectively. The ICP-MS was calibrated against a single ²⁰²Hg standard (1 µg l⁻¹). Rhodium was used as internal standard added to the samples and the standard solution.

The DOC concentration was determined in two of the water samples from site 2, 3, 4, and 5 by a Shimadzu TOC-500 analyzer.

Water pH, temperature, and dissolved oxygen (DO) were measured in the field using a portable Orion 210A/electrode, Orion 9107BN pH-meter, and Orion 810A DO-meter. The electric conductivity (EC) was measured using an Orion 105A electrode and an Orion cell 011050 conductivity meter. The uncertainties in measurements of pH, temperature, conductivity, and dissolved oxygen were ± 0.02, ± 1, 0.5%, and ± 1%, respectively. Although these parameters were not considered to have a major influence on the fluxes of mercury in the system, their hourly variations were measured as a contribution to the river characteristics.

The cross-section area of the river at the four sampling sites were determined and the stream velocity was measured with a high-resolution, low-speed rotor flowmeter (2030RG General Oceanic Inc. mechanical flowmeter) when the water samples were taken.

Calculation of the mass of mercury accumulated and exported and the partitioning of total mercury in the river water.

All sources of mercury are between site 1 and 5 (Fig. 1), and the mass of mercury temporally accumulated in the river was assumed to occur between site 2 and 5. It was calculated by the summation of the loss of mercury mass between the sites.

The loss of mass between two sites was calculated by subtracting the mass of mercury (on annual basis) of the downstream site from the mass (on annual basis) of mercury at the nearest upstream site. However, the loss of mass between site 3 and 4 was calculated by assuming the same linear loss rate of dissolved and particulate mercury mass with distance as between site 2 and 3. This assumption was necessary since the mass of mercury at site 4 increased due to input of mercury from the mining tailing of La Rastra.

Since the mercury concentration and the river discharge was measured hourly, daily fluxes at each site were calculated by the summation of the hourly fluxes of total mercury. The hourly flux of total mercury (kg/h) was calculated as total mercury concentration ($\mu\text{g/l}$) ($\text{kg}/10^{-9} \mu\text{g}$) \times river flow (m^3/s) \times ($1000 \text{ l}/\text{m}^3$) \times ($3600 \text{ s}/\text{h}$). The daily mass of total mercury (kg/d) at a site was calculated as the flux of total mercury (kg/h) at the site \times (24 h/d).

To calculate the mass of mercury on an annual basis at a site, it was assumed that the temporal occurrence of mercury in the river water coincides with the work time

of miners, that is, 24 hr a day, 25 days a month and 11 months a year ($\sim 275 \text{ d}/\text{year}$). Then the annual mass of mercury at a site is given by: The daily mass of total mercury (kg/d) at the site \times ($275\text{d}/\text{year}$).

The total mass of waterborne mercury yearly exported from the basin was assumed to correspond to the annual mass of total mercury at site 5.

The partition coefficient for mercury was defined by the ratio between the concentration of particulate mercury in $\mu\text{g}/\text{g}$ (that is normalized to dry total solid mass) and the concentration of dissolved mercury in $\mu\text{g}/\text{ml}$.

Results

The highest total mercury concentrations were found immediately downstream the two amalgamation mills and exceeded the WHO guideline of $1 \mu\text{g}/\text{l}$ for drinking water (WHO, 1996). Whereas the lowest concentration was found at the most remote site (Table 2). The mercury concentrations were highly variable during a day downstream the processing plants (site 2 and 4) (coefficient of variation 0.85-1.03) and much less variable in between (site 3) (Fig. 2).

The flux of particulate mercury varied by a factor of 20 to 40 during the day downstream of the processing plants, with two main peaks at site 2 and four at site 4 (Fig. 3). The two peaks at site 2 were reproduced within the same hour at site 3, at about 1/10 of the flux at site 2. The flux of dissolved mercury varied by a factor of 5-10 during the day, with the largest variation and the highest peak at site 5. Two major peaks, temporally corresponding to those at site 2, were still observed at site 5 (Fig. 3), in spite of an almost threefold increase of the river discharge between site 3 and 5 (Table 2). The occurrence of particulate mercury at

site 5 indicates that the water velocity was sufficiently high to carry particles at least 5 km.

Between 65 and 72% of mercury downstream the processing plants were in the particulate form, whereas dissolved mercury dominated the total pool at the other sites and even made up 100% of the mercury at site 1 (upstream the La Estrella plant) and site 6 (about 45 km downstream of La Estrella) (Table 2).

The concentration of total solids in the water was essentially the same at all sites (Table 2), but the sites downstream the processing plants had higher concentrations of suspended solids than the other sites (Fig. 2), reflecting the ores grinding at the plants. The mean concentration of TSS decreased by approximately 30% over a distance of 5.3 km between site 4 and 5, probably due to sedimentation of mined ore particles or due to the dilution effect, as the river discharge increased by 70% (Fig. 2).

The were significantly correlated with the total suspended solids concentrations across all sites (Table 3), but the correlation between the particulate mercury concentrations and the TSS was stronger. These observations indicate that mercury was effectively sorbed onto grinded ore particles. However, the correlations between the total mercury concentrations and the TSS seemed to be site specific since the correlations are even stronger at the sites 2 and 4 (Table 3).

The partition coefficient for mercury between the particulate and dissolved form ($\log K_d$), ranged from 3.1 to 5.9 ml/g (Table 2). The partition coefficients at sites 2 and 4 varied to the same extent and about 1.5 times as much as the coefficient at site 3. The partition coefficient at site 5 varied most and about twice as much as site 2 and 4, possibly indicating a large heterogeneity in the composition of its

solids. The only significant correlation found for the partition coefficient was with the TSS concentrations at site 5 ($r^2 = -0.40$, $p < 0.05$).

The EC was positively correlated with TSS at sites located near the gold processing plants (site 2 and 4) (Table 4), suggesting that grinding particles brought electrolytes to the water. Consequently, the EC correlated with the TPHg concentrations at those sites. The total dissolved mercury concentrations were positively correlated ($r^2 = 0.62$, $p < 0.05$) with the DOC concentrations.

The total iron concentrations in the river water (Table 4) were not correlated with the TSS concentrations at the upstream sites, because most of the solids in the river water were grinded particles of enriched quartz minerals. Consequently, mercury and iron concentrations were not correlated as mercury was correlated with TSS. However, iron concentrations were correlated with TSS concentrations at site 4 and 5 (Table 4), suggesting that the suspended solids at the downstream sites have different element composition than the those upstream.

The highest iron concentrations were found at site 3 (Table 2), probably due to release of blood and cattle rubbishes by one of the slaughterhouses located at the shore of the river. A single iron peak was observed at 5 am in the morning, reflecting the daily slaughtering activity in the river basin (data not shown).

The electric conductivity and the river pH tended to increase in the downstream direction (Table 2). The prevailing neutral or slightly alkaline conditions (Table 2) may promote the transport of mercury associated to the sediments. In contrast, low pH contributes to the dissolution of mercury in rivers.

The total mass of mercury accumulated in the river was 2.7 kg/year and the total mass exported from the basin was 1.6 kg/year.

Table 2. Mean, standard deviation, and minimum and maximum (in parenthesis) values of *in situ* measurements (Flow, Temp: temperature, pH, EC: electric conductivity, DO: dissolved oxygen), laboratory analyses of water samples (TS: total solids, TDS: total dissolved solids, TSS: total suspended solids, TFe: total iron, DOC: dissolved organic carbon, THg: total mercury, TDHg: total dissolved mercury, TPHg: total particulate mercury) and the mercury partition coefficient ($\log K_d$) in the Río Sucio.

Site	Water velocity (m/s)	Flow (m ³ /s)	Temp (°C)	pH	EC (μS/cm)	DO (mg/l)	TS (mg/l)	TDS (mg/l)	TSS (mg/l)	TFe (mg/l)	DOC (mg/l)	THg (μg/l)	TDHg (μg/l)	TPHg (μg/l)	$\log K_d$ (ml/g)
Site 1	0.45 ± 0.07	0.08 ± 0.01	22.0	6.6	64	6.1	190 ± 70	82 ± 11	104 ± 67	0.19 ± 0.09	-----	0.28	0.32 ± 0.15	0.81 ± 1.13	-----
Site 2	(0.33 - 0.63)	(0.06 - 0.11)	(22.2 - 26.6)	(6.5 - 7.2)	(64 - 71)	(1.1 - 6.0)	(100 - 330)	(48 - 96)	(32 - 240)	(0.09 - 0.42)	(19.3 - 20.1)	(0.30 - 4.90)	(0.05 - 0.63)	(0.00 - 4.49)	(3.37 - 5.07)
Site 3	0.28 ± 0.02	0.09 ± 0.01	24.8 ± 1.6	7.4 ± 0.4	121 ± 20	1.5 ± 1.9	180 ± 60	114 ± 37	60 ± 50	0.67 ± 0.29	-----	0.24 ± 0.14	0.18 ± 0.10	0.06 ± 0.11	3.84 ± 0.31
Site 4	(0.13 - 0.24)	(0.07 - 0.12)	(23.1 - 28.1)	(6.5 - 8.2)	(96 - 72)	(0.2 - 7.8)	(100 - 380)	(28 - 178)	(4 - 204)	(0.22 - 1.66)	(7.0 - 7.5)	(0.07 - 0.60)	(0.04 - 0.42)	(0.00 - 0.42)	(3.43 - 4.37)
Site 5	0.19 ± 0.04	0.15 ± 0.03	24.7 ± 1.6	7.4 ± 0.2	118 ± 18	4.0 ± 1.8	180 ± 70	100 ± 37	75 ± 69	0.63 ± 0.33	-----	0.63 ± 0.53	0.22 ± 0.12	0.41 ± 0.55	4.57 ± 0.38
Site 6	(0.13 - 0.29)	(0.10 - 0.23)	(22.6 - 27.5)	(7.1 - 7.6)	(95 - 169)	(2.0 - 6.5)	(60 - 320)	(28 - 164)	(2 - 232)	(0.20 - 1.15)	(3.8 - 16.6)	(0.11 - 2.19)	(0.01 - 0.57)	(0.00 - 2.08)	(3.99 - 5.42)
Site 7	0.49 ± 0.13	0.26 ± 0.07	25.1 ± 0.7	8.1 ± 0.4	134 ± 3	7.5 ± 0.7	190 ± 10	166 ± 8	21 ± 7	0.20 ± 0.03	-----	0.25 ± 0.10	0.21 ± 0.12	0.04 ± 0.06	4.35 ± 0.85
Site 8	(0.33 - 0.77)	(0.17 - 0.41)	(24.1 - 26.6)	(6.9 - 8.8)	(129 - 137)	(6.0 - 8.4)	(170 - 200)	(146 - 186)	(4 - 31)	(0.12 - 0.26)	(11.7 - 17.0)	(0.11 - 0.57)	(0.04 - 0.57)	(0.00 - 0.22)	(3.15 - 5.97)
Site 9	-----	-----	26.8	7.9	191	3.9	-----	-----	-----	-----	-----	0.06	0.06	0.00	-----

Table 3. Coefficient of correlation (r^2) for the linear relationship between mercury concentrations (THg: total mercury, TDHg: total dissolved mercury, TPHg: total particulate mercury) and EC (electric conductivity), TS (total solids), TSS (total suspended solids), and TDS (total dissolved solids) in Río Sucio.

	THg			TDHg	TPHg			
	TS	TSS	EC	EC	TS	TDS	TSS	EC
All samples	0.28*	0.55*	-----	-----	0.33*	-----	0.61*	-----
By Site								
Site 2	0.74*	0.63*	0.74*	-----	0.63*	-----	0.63*	0.74*
Site 3	0.28**	0.26***	-----	-----	0.61*	-----	0.77*	-----
Site 4	0.60*	0.71*	0.89*	-----	0.57*	-----	0.76*	0.87*
Site 5	-----	-----	0.69*	0.43*	-----	-----	-----	-----

* $p < 0.005$, ** $p < 0.01$, *** $p < 0.05$

Table 4. Coefficient of correlations (r^2) for the linear regression between iron concentration (TFe), electric conductivity (EC) and TS (total solids), TDS (total dissolved solids, TSS (total suspended solids), at four sites in Río Sucio.

Site	TFe			EC		
	TS	TDS	TSS	TS	TDS	TSS
All samples	-----	-----	-----	-----	0.40*	-----
By Site						
Site 2	-----	-----	-----	0.44*	-----	0.43*
Site 3	-----	-----	-----	0.31*	0.50*	-----
Site 4	0.52*	-----	0.56*	0.67*	-----	0.77*
Site 5	0.35*	-----	0.78*	-----	-----	-----

* $p < 0.005$, ** $p < 0.01$, *** $p < 0.05$

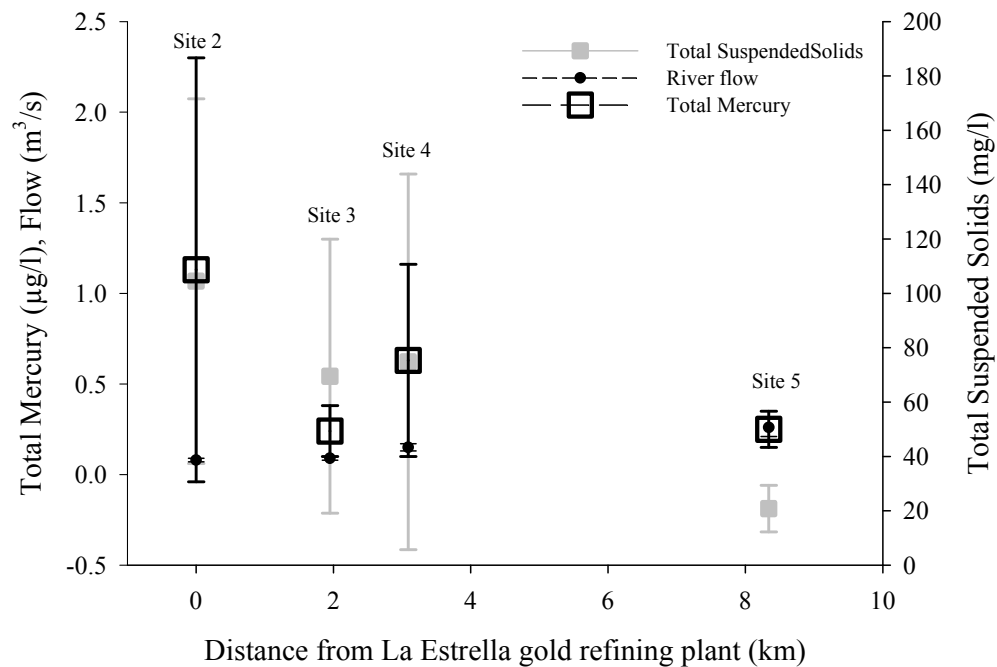


Figure 2. Spatial variation of mercury concentrations, total suspended solids concentrations, and water flow along Sucio river, based on a day of hourly sampling; bars indicate the standard deviation.

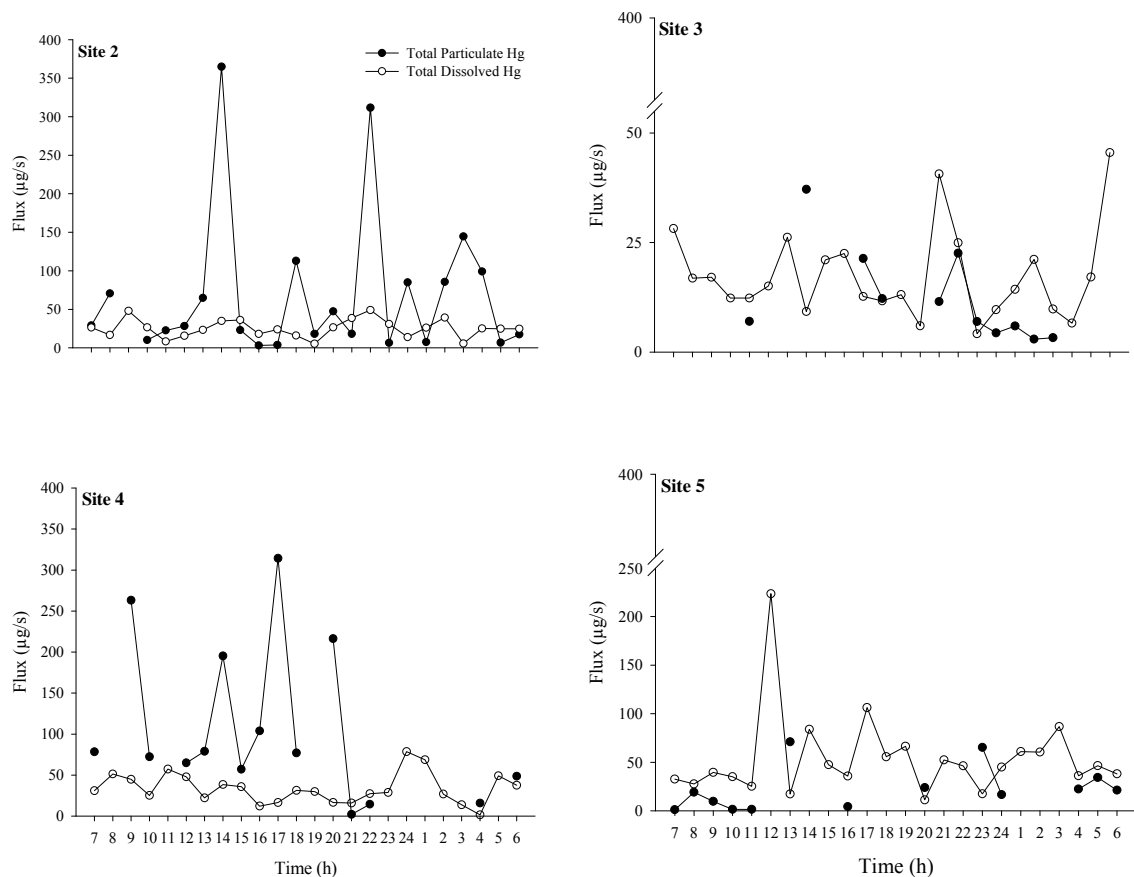


Figure 3. Hourly variation of mercury fluxes at four sampling sites in the Río Sucio. Particulate concentrations equal to zero are not included.

Discussion

The temporal variations of mercury concentrations in rivers are commonly described on monthly and annual scales (Roulet et al., 1998; Betancourt et al., 2005; Ullrich et al., 2007). However, these scales may limit the description of transport processes to large and long term events (Mason and Sullivan, 1998; Miller and Lechler, 2003) and not capture the dynamics of whereas metal transport in rivers in mining areas. In these particular environments, the fluxes of mercury respond to the hourly timed-input of mining tailings rather than to the input of mercury from other external sources, as it was observed, e.g in Sucio river. Mining tailing discharges are characterized by rapid fluctuations, and the associated mercury concentrations are almost unpredictable; therefore, low-frequency

sampling can result in erroneous estimations of the fluxes of mercury in the stream (Mason and Sullivan, 1998), and high temporal and spatial resolution of the mercury fluxes may improve the estimation of mercury loads (Whyte and Kirchener, 2000). Moreover, when a strategy for long term monitoring is needed, the cost of sampling and laboratory analysis can be minimized by examining the pattern of variation of the mercury fluxes in the river.

The diurnal pattern of particulate mercury fluxes in Sucio river most likely reflects the operation schedule at the processing plants. The four prominent peaks at site 2 (Fig. 3) coincide with the mercury-gold amalgamation events at every 4th and 5th hour at La Estrella plant (personal communication with miners), and the four peaks at site 4 may also coincide with the

amalgamation events at the second processing plant. As in other rivers in mining areas (Roulet et al., 1998; Betancourt et al., 2005), the transport of mercury in Sucio river is controlled by the amount of suspended material, which is a mobile sorbent for mercury (Maurice-Bourgoin et al., 2003). The positive correlation between the TSS concentrations of the whole data set and the THg concentrations and between TSS and TPHg concentrations at sites 2, 3 and 4 (Table 3) suggests that transport of mercury is mostly associated with the suspended material from the ore processing (Maurice-Bourgoin et al., 2003; Betancourt et al., 2005).

Since the TDHg concentrations at all sampling sites varied within the same range of (0.01-0.63 $\mu\text{g/l}$) (Table 2), the downstream reduction of the total mercury concentrations can be attributed to sedimentation of mercury-bound particles (Limbong et al., 2003; Maurice-Bourgoin et al., 2003; Ullrich et al., 2007). The distance to site 5 was sufficiently large to allow the particulate mercury released from site 4 to settle, such that 84% of mercury was dissolved (Table 2). Other factors than sedimentation, such as the influx of connecting streams, may contribute by dilution of the particulate mercury concentrations in the river (Balogh et al., 1998a; Roulet et al., 1998). For instance, the downstream decrease of both TDHg and TPHg concentrations from site 2 to site 3 can be due to the increased river flow (Table 2). In contrast, although the river flow increased almost twofold from site 4 to site 5 (Table 2) due to influx from two tributaries (Fig.1), the TDHg concentrations were not diluted between the two sites, perhaps because the connecting tributaries add mercury to Sucio river.

The composition of suspended solids may vary depending on river basin characteristics, but the partition

coefficient for mercury between suspended solids and the aqueous phase has similar range of variation in different rivers, e.g. Amazonian rivers (3.6 to 5.5) (Maurice-Bourgoin et al., 2003) and Wisconsin rivers (2.8 to 5.5) (Babiarz et al., 1998). Although TPHg and TSS were positively correlated (Table 3), K_d and TSS were not (data not shown), most likely because K_d is invariable with the amount of SPM (Stordal et al., 1996), but it can decrease when the concentration of dissolved mercury increases. The negative correlation between K_d and TSS ($r^2 = 0.62$, $p < 0.05$) at site 5, where most of the SPM probably is of non-anthropogenic origin, may come from the effect of filter-passing smaller particles ($< 0.45 \mu\text{m}$), which concentrations can increase as SPM increases (Qu  merais et al., 1998) (I cannot follow this argument). In addition, in some rivers the mercury concentrations associated with colloidal particles comprise more than 40% of the unfiltered concentrations (Babiarz et al., 2001).

The very low water velocity (Table 2) and the relatively long resident time for water between sites 2 and 3 (~ 2 h) and between sites 4 and 5 (~ 4 h) indicates that most of the mercury associated with mined ore particles may undergo sedimentation (Betancourt et al., 2005), greatly reducing the fluxes of TPHg between the sites (Fig. 3). The mechanism of removal of TPHg from the aqueous phase by sedimentation (Maurice-Bourgoin et al., 2003) is supported by the spatial pattern of TSS concentrations, with large losses between site 2 and 3 and between site 4 and 5 (Fig. 2). In contrast, the flux of dissolved mercury tends to increase downstream from site 3 to site 5, such that the mean flux at site 5 ($\sim 55 \mu\text{g/s}$) is threefold the flux at site 3 ($\sim 16 \mu\text{g/s}$). The positive correlation between DOC and TDHg concentrations could indicate a strong interaction between mercury and dissolved organic matter in the river (Ravichandran, 2004).

The major oxides in the suspended material (particles retained by 0.45 μm filter) in the Río Sucio are SiO_2 , Al_2O_2 and Fe_2O_2 , which comprise 48%, 29% and 17% of the suspended oxides respectively (André et al., 1997). Particles coated with iron oxides are common in tropical rivers and efficiently bind mercury (Quémerais et al., 1998; Roulet et al., 1998b; Cai et al., 1999; Yin and Balogh, 2002). However, we found no correlations between THg and TFe concentrations or between TSS and TFe concentrations, probably because suspended iron concentrations are not represented by the measured total iron concentrations. It seems that the large amount of discharged mined particles masks the role of mineral oxides in the transport of mercury and that mercury is mostly associated with grinded quartz particles (Lima et al., 2008) or with waterborne, relatively dense amalgam grains (Au-other metals-Hg) (Miller and Lechler, 2003). This is in contrast to the conditions at site 5, which is without mining activity and where iron concentrations correlated very well with the TSS concentrations (Table 4). The correlation indicates that the suspended particles contain a large fraction of iron oxides. In addition, the daily mean concentrations of TFe at sites 2 and 5 (Table 2) shows that the anthropogenic suspended particulate matter from the mining activity is not a major source of iron to the stream.

Because the calculation did not include the accumulation due to sedimentation of mercury bound to denser mined particles, the reported mass of mercury accumulated in the river seems to be relatively small.

The rapid and very short distance settling of denser Hg-amalgam ore grains followed by the sedimentation of mercury bound to finer ore particles over relative large distances in combination of low flow condition are probably the mechanisms controlling the accumulation of mercury

in Río Sucio, whereas, mercury is mostly exported as dissolved and probably associated to dissolved organic matter.

Although, there are several point sources of mercury in the Río Sucio basin (Fig. 1) the dynamic transport of mercury was mainly characterized by the release of mercury by the two main pollution sources, such that, the spatial and temporal variation of mercury along the river largely responds to the episodic release of mercury through the mining tailings.

Conclusions

Temporal and spatial dynamics of mercury fluxes in Sucio river were controlled by the release of suspended solids from gold mining activities and the sedimentation of the solids in the river bed. The downstream export is by dissolved mercury.

The pattern of mercury fluxes and mercury exposure to the river ecosystem is totally tied to the gold amalgamation practices in the river basin, as demonstrated by the hourly water sampling. Without the high resolution of sampling, prediction of the fate of mercury, whether accumulated or exported, in a gold miner's river will be erroneous.

Acknowledgements

The Swedish International Development Agency (SIDA/SAREC) supported this study through the "Environmental Research Multidisciplinary Programme". It is a cooperative project involving the National Autonomous University of Nicaragua (UNAN-Managua) and Lund University.

References

- André, L., Rosén, K., Torstendahl, J., 1997. Minor field study of mercury and lead from gold refining in Central Nicaragua. Luleå tekniska universitet.
- APHA, 1999. Standard Methods for the Examination of Water and Wastewater. American Public Health Association, AWWA and the WEF, Whashington.
- Arkipova, N.A., Venitsianov, E.V., Kocharyan, A.G., Dmitrieva, I.L., 2001. Experimental study and mathematical modeling of Hg and Cu transformations in the water-bottom sediment system. *Water Resources*. 28(1), 63-67.
- Babiarz, C.L., Hurley, J.P., Benoit, J.M., Shafer, M.M., Andren, A.W., Webb, D.A., 1998. Seasonal influence on partitioning and transport of total mercury in rivers from contrasting watersheds. *Biogeochemistry*. 41, 237-257.
- Babiarz, C.L., Hurley, J.P., Hoffmann, S.R., Andren, A.W., Shafer, M.M., Armstrong, D.E., 2001. Partitioning of total mercury and methylmercury to the colloidal phase in freshwaters. *Environmental Science and Technology*. 35(24), 4773-4782.
- Balogh, S.J., Mayer, M.L., Johnson, K., 1997. Mercury and suspended sediment loadings in the lower Minnesota River. *Environmental Science and Technology*. 31, 198-202.
- Balogh, S.J., Meyer, M.L., Johnson, D.K., 1998a. Diffuse and point source mercury inputs to the Mississippi, Minnesota, and St. Croix rivers. *The Science of the Total Environment*. 213, 109-113.
- Balogh, S.J., Meyer, M.L., Johnson, D.K., 1998b. Transport of mercury in three contrasting river basins. *Environmental Science and Technology*. 32, 456-462.
- Betancourt, O., Narváez, A., Roulet, M., 2005. Small-scale gold mining in the Puyango river basin, Southern Ecuador: A study of environmental impacts and human exposures. *EcoHealth*. 2, 323-332.
- Bishop, K., Lee, Y.-H., Pettersson, C., Allard, B., 1995. Terrestrial sources of methylmercury in surface waters: The importance of the riparian zone on the Svartberget catchment. *Water, Air, and Soil Pollution*. 80, 435-444.
- Bonzongo, J.-C.J., Heim, K.J., Chen, Y., Lyons, W.B., Warwick, J.J., Miller, G.C., Lechler, P.J., 1996. Mercury pathways in the Carson River-Lahontan reservoir system, Nevada, USA. *Environmental Toxicology and Chemistry*. 15(5), 677-683.
- Cai, Y., Jaffé, R., Jones, R.D., 1999. Interactions between dissolved organic carbon and mercury species in surface water of the Florida Everglades. *Applied Geochemistry*. 14, 395-407.
- Carvalho, C.E.V., Ovalle, A.R.C., Rezende, C.E., Molisani, M.M., Salomão, M.S.M.B., Lacerda, L.D., 1999. Seasonal variation of particulate heavy metals in the lower Paraíba do Sul river, R. J., Brazil. *Environmental Geology*. 37(4), 297-302.
- Chadwick, S.P., Babiarz, C.L., Hurley, J.P., Armstrong, D.E., 2006. Influences of iron, manganese, and dissolved organic carbon on the hypolimnetic cycling of amended mercury. *Science of the Total Environment*. 368, 177-188.
- Haitzer, M., Aiken, G.R., Ryan, J.N., 2003. Binding of mercury(II) to aquatic humic substances: Influence of pH and source of humic substances. *Environmental*

- Science and Technology. 37, 2436-2441.
- Hurley, J.P., Cowell, S.E., Shafer, M.M., Hughes, P.E., 1998. Partitioning and transport of total methyl mercury in the lower Fox river, Wisconsin. *Environment Science and Technology*. 32, 1424-1432.
- Hylander, L.D., Meili, M., Oliveira, L.J., Silva, E.C., Guimarães, J.R.D., Araujo, D.M., Neves, R.P., Stachiw, R., Barros, A.J.P., Silva, G.D., 2000. Relationship of mercury with aluminum, iron, and manganese oxy-hydroxides in sediments from the Alto Pantanal, Brazil. *The Science of the Total Environment*. 260, 97-107.
- INETER, 1991. Anuarios meteorológicos (1990,1991). Catastro e Inventarios de Recursos Naturales: Nicaragua.
- Lawson, N.M., Mason, R.P., Laporte, J.-M., 2001. The fate and transport of mercury, methylmercury, and other trace metals in Chesapeake Bay tributaries. *Water Resources*. 35(2), 501-515.
- Leigh, D.S., 1997. Mercury-tainted oberbank sediment from past gold mining in north Georgia, USA. *Environmental Geology*. 30((3/4)), 244-251.
- Lima, L.R.P.d.A., Bernardez, L.A., Barboza, L.A.D., 2008. Characterization and treatment of artisanal gold mine tailings. *Journal of Hazardous Materials*. 150, 747-753.
- Limbong, D., Kumampung, J., Rimper, J., Arai, T., Miyazaki, N., 2003. Emission and environmental implications of mercury from artisanal gold mining in north Sulawesi, Indonesia. *The Science of the Total Environment*. 302, 227-236.
- Mason, R.P., Sullivan, K.A., 1998. Mercury and methylmercury transport through and urban watershed. *Water Research*. 32(2), 321-330.
- Maurice-Bourgoin, L., Quemerais, B., M-Turcq, P., Seyler, P., 2003. Transport, distribution and speciation of mercury in the Amazon River at the confluence of black and white waters of the Negro and Solimões Rivers. *Hydrological Processes*. 17, 1405-1417.
- Mendoza, J.A., 2006. Groundwater occurrence and risk of pollution in a mountain watershed of Nicaragua. Doctoral thesis Thesis, Lund University, Lund, 132 pp.
- Miller, J.R., Lechler, P.J., 2003. Importance of temporal and spatial scale in the analysis of mercury transport and fate; an example from the Carson River system, Nevada. *Environmental Geology*. 43, 315-325.
- Miller, J.W., Callahan, J.E., Craig, J.R., 2002. Mercury interactions in a simulated gold placer. *Applied Geochemistry*. 17, 21-28.
- Morel, F.M.M., Kraepiel, A.M.L., Amyot, M., 1998. The chemical cycle and bioaccumulation of mercury. *Annual Review of Ecology Systematics*. 29, 543-566.
- Quémerais, B., Cossa, D., Rondeau, B., Phan, T.T., Fortin, B., 1998. Mercury distribution in relation to iron and manganese in the waters of the St. Lawrence river. *The Science of the Total Environment*. 213(1-3), 193-201.
- Ramamoorthy, S., Kushner, D.J., 1975. Heavy metal binding components of river water. *Journal of Fish Research Board Canadian*. 32(10), 1755-1766.
- Ravichandran, M., 2004. Interactions between mercury and dissolved organic matter-a review. *Chemosphere*. 55, 319-331.
- Roulet, M., Lucotte, M., Canuel, R., Rheault, I., Tran, S., Goy, Y.,

- Farella, N., Passos, C., Silva, S., Mergler, D., Amorim, M., 1998. Distribution and partition of total mercury in waters of the Tapajós river basin, Brazilian Amazon. *The Science of the Total Environment*. 213, 203-211.
- Roulet, M., Lucotte, M., Saint-Aubin, A., Tran, S., Rheault, I., Silva, E.D.J.D., Dezencourt, J., Passos, C.-J.S., Santos, G., Guimaraes, J.-R.D., Mergler, D., Amorim, M., 1998b. The geochemistry of mercury in central Amazonian soils developed on the Alter-do-Chão formation of the lower Tapajós River Valley, Pará state, Brazil. *The Science of the Total Environment*. 223(1-24).
- Stordal, M.C., Gill, G.A., Wen, L.-S., Santschi, P.H., 1996. Mercury phase speciation in the surface waters of the three Texas estuaries: Importance of colloidal forms. *Limnology Oceanography*. 41(1), 52-61.
- Tarras-Wahlberg, N.H., Flachier, A., Lane, S.N., Sangfors, O., 2001. Environmental impacts and metal exposure of aquatic ecosystems in rivers contaminated by small scale gold mining: the Puyango River Basin, Southern Ecuador. *The Science of the Total Environment*. 278, 239-261.
- Ullrich, S.M., Ilyushchenko, M.A., Uskov, G.A., Tanton, T.W., 2007. Mercury distribution and transport in a contaminated river system in Kazakhstan and associated impacts on aquatic biota. *Applied Geochemistry*. 22, 2706-2734.
- Wayne, D.M., Warwick, J.J., Lechler, P.J., Gill, G.A., Lyons, W.B., 1996. Mercury contamination in the Carson River, Nevada: A preliminary study of the impact of mining wastes. *Water, Air, and Soil Pollution*. 92, 391-408.
- WHO, 1996. *Guidelines for Drinking Water Quality*, 2nd ed., VOL. 2., Geneva.
- Whyte, D.C., Kirchener, J.W., 2000. Assessing water quality impacts and cleanup effectiveness in streams dominated by episodic mercury discharges. *The Science of the Total Environment*. 260, 1-9.
- Yin, X., Balogh, S.J., 2002. Mercury concentrations in stream and river water: An analytical framework applied to Minnesota and Wisconsin (USA). *Water, Air, and Soil Pollution*. 138, 79-100.

**Sedimentation and resuspension of particle bound
mercury in a polluted river**

Bengtsson, G. and Picado, P.

Sedimentation and resuspension of particle bound mercury in a polluted river

Göran Bengtsson² and Francisco Picado^{1,2}

¹Department of Ecology, Lund University, Sölvegatan 37, SE-223 62 Lund, Sweden

²Centro para la Investigación en Recursos Acuáticos de Nicaragua-Universidad Nacional Autónoma de Nicaragua, Apartado Postal 4598, Managua Nicaragua.

Abstract

Mercury associated with suspended material undergoes sedimentation and contributes to the accumulation of mercury in river sediments. However, settled particles may become resuspended and move mercury downstream until a new temporal sedimentation occurs. This work was intended to examine the spatial pattern of gross and net accumulation and resuspension of mercury in a small river in Nicaragua, used as discharge by ~100 years of gold mining activity based on gold extraction by amalgamation.

Sediment and mercury net accumulation was examined in sediment cores from six sites of the river. Gross accumulation and resuspension was calculated from short-term assays of changes of mercury concentration and weight of sediment exposed to the river flow in sediment traps. The sediment age and net sedimentation was calculated based on Pb-210 analysis. The organic content of depth sediments was also determined. We found: i) The highest mercury concentrations (about 10 µg/g) were found 2-3 km downstream of the two processing plants, and the lowest concentrations (about 0.1 µg/g) 45 km downstream. The mercury concentrations were positively correlated with the organic carbon content of the sediment and accumulated in the uppermost 5 cm of the sediment in the most exposed parts of the river, ii) The vertical distribution of the net sedimentation rate of particles had a peak at all of the examined sites, but the quantities accumulated and the year the main peak took place varied but coincided at the mercury contaminated sites with high activities at the processing plants in the 1980's and 1990's. The mean of the mass of mercury accumulated by sedimentation and the mass of sediment accumulated, varied from 19.5 to 1,628.5. mg/m² and from 128 to 215 kg dw/m² between sites, respectively, iii) sediment and mercury bound particles were resuspended even by a very low water velocity (0.01 m/s), but no gross sedimentation was observed. The resuspension rate of sediment varied from 6 to 12 mg/s and the resuspension rate of mercury from 0.04 to 0.2 µg/s, and iv) the rate of sediment resuspension and mercury resuspension to the bulk water in the river was positively correlated, suggesting that resuspension is a transport mechanism for mercury in the river.

Keywords: *Mining, sediment traps, contamination*

Introduction

Tailings from gold mining are sources of sediments, mercury, and other metals in surface water, e.g. rivers (Wayne et al., 1996; Tarras-Wahlberg et al., 2001; Serfor-Armah et al., 2004), and of high concentrations of particle bound mercury observed in gold miner's rivers (Wayne et al., 1996; Roulet et al., 1998; Telmer et al., 2006). Concentrations of particulate bound mercury may decrease over short distances as the particulate matter adds to streambed (Roulet et al., 1998), but mercury contamination may extent far downstream in river sediments (Wayne et al., 1996; Ullrich et al., 2007) probably by resuspension of mercury bound to sediment closer to contamination sources (Mudroch and Clair, 1986; Roulet et al., 1998; Ullrich et al., 2007).

Sediments serve as the ultimate repository of the particle scavenged mercury, and the concentrations of mercury in river sediments are several orders of magnitude greater than in the water phase (Wayne et al., 1996; Serfor-Armah et al., 2004; Ullrich et al., 2007). Therefore, the sediment phase becomes the major source of mercury in benthic organisms (Tarras-Wahlberg et al., 2001). Concentrations in the water phase increase during high flow events, when mercury moves to the water column by resuspension from the streambed (Bonzongo et al., 1996; Hurley et al., 1998; Lawson et al., 2001). Although the resuspension process becomes less pronounced at low flow conditions, there is still a fraction of mercury concentrated in finer particles of unconsolidated sediment that moves in a looping behavior along a stream (Roulet et al., 1998). The transport of mercury by particles resuspension is initiated and controlled by the flowing water forces,

which pull mercury into a mobile phase, especially in shallow streams. This mechanism is not often acknowledged in description of the transport process. The downstream transport of particle bound mercury is limited when the hydraulic conditions facilitate sedimentation, resulting in mercury accumulation and aging the sediment. The net transport of mercury in a river generally results in a patchy downstream accumulation and a distinct depth profile in the sediment (Callahan et al., 1994; Leigh, 1997), observed in mining-exposed river sediments, suggesting that resuspension and sedimentation of particle bound mercury are site specific phenomena.

The sedimentation of particle bound mercury and the downstream transport of mercury by sediment resuspension mostly depends on the sediment load, particle size and organic content of the sediment, river hydraulic conditions (Roulet et al., 1998; Lima et al., 2008), and external factors, e.g. precipitation events (Balogh et al., 1997). For instance, the long distance transport of particulate mercury during high water velocities is controlled by temporal and spatial changes of the water flow (Bishop et al., 1995; Babiarz et al., 1998; Balogh et al., 1998; Roulet et al., 1998). However, at any flow condition, the mass of mercury added to the water phase due to resuspension could be depending on sediment particle densities, because most of the resuspended sediment is composed by fine particles, and mercury is not homogeneously distributed on mined ore particles (Lima et al., 2008).

Gradients of mercury concentrations and sediment age are archives of the historical accumulation of mercury in rivers (Leigh, 1997). Higher concentrations are always due to anthropogenic release of mercury,

and the accumulation pattern of mercury is a result of the final arrangement of the scavenged particles when they find their way to the streambed. Since most mercury is organically bound coinciding with the vertical distribution of organic matter in sediment cores (Benoit et al., 1998; Biester et al., 2002), and since grain size controls its spatial variation in river sediments by adsorption, mercury accumulation depends on organic content and sediment particle size (Wayne et al., 1996; Bengtsson and Picado, 2008). Mercury concentration is inversely correlated with the particle size (Wayne et al., 1996; Deacon and Driver, 1999; Huang and Lin, 2003; Bengtsson and Picado, 2008), such that in mining rivers, the highest concentrations of mercury are found in silty and clay rich sediment located downstream of gold mining sites (Bonzongo et al., 1996; Wayne et al., 1996; Gray et al., 2000; Hylander et al., 2000). Silty and clay rich sediment accumulates more mercury and other metals than sandy sediments (Wayne et al., 1996; Deacon and Driver, 1999; Goncalves et al., 2000; Huang and Lin, 2003), due to high content of organic carbon (Tsai et al., 2002).

Sucio river is a small river that has been affected by more than 100 years of gold mining activity in St Domingo, Nicaragua. Mercury fluxes in the river have been reported by a previous study (Paper I), the results show suspended particles as the major pathway of stream-borne mercury, and that the fluxes decrease downstream of mercury sources suggesting a mass of mercury loss due the deposition of particulate mercury. Here we examine the depth distribution of mercury in sediments at different distances from contamination sources, the gross and net accumulation

and resuspension of suspended particles and associated mercury.

Materials and Methods

Study area and description of the sampling sites

Río Artigas (locally known as Río Sucio) is a small, brown coloured stream. The river basin is approximately 28 km² and is located in the central mountain region of Nicaragua (Fig. 1). Past and present mining activities in the basin include the extraction of gold and silver. The soils in the basin are often brown-red coloured and originate from basalt and andesite rocks. The colour of the soil is probably due to iron oxides and turns redder in the surrounding of quartz veins. The river sediments are mainly composed by quartz minerals. The lowest stream water flow river is from January to April. Large amounts of grinded ore particles are often observed along the stream far away from the gold processing sites. Grinded ores containing mercury and other metals are continuously released into the stream by the gold mining activities (Paper I). The river also transports domestic wastes from the village. The mercury is spread downstream, and the aqueous concentrations are diluted by the water inflow of small tributaries (Paper I). A large fraction of mercury in the river is associated with suspended solids from mining activities (Paper I). Particulate mercury sedimentation and both sediment and mercury accumulation deteriorates the water quality and affects the river biota.

Table 1. Characteristic of sampling sites at the Sucio river.

Sampling site	Site description
1	The sediment accumulation at this site may be due natural eroded soil particles, because no mining activity was observed in the surroundings. The concentration of mercury in sediment is thought to be due to a local wet deposition of the airborne mercury.
2	It is nearby (100 m downstream) the processing plant of La Estrella. High sedimentation is mostly due to a directly release on mined ores from the mining activity. Mercury concentration in sediment was expected to be high.
3	Located 2.0 km downstream La Estrella plant and most of the sediment come from the upstream gold processing sites and sediment transported by upstream tributaries. Solid wastes released into the river are also domestic.
4	It is located downstream of the second main processing plant, called La Rastra. It is though that mass of mercury accumulated at this site mainly comes from the mining tailings of La Rastra and from the upstream sediment fluxes. The mass of eroded soil particles incorporated to the riverbed can be very small in comparison with the amount of solid material discharge by the upstream mining activity.
5	Located approximately 8.4 km downstream of La Estrella. Little suspended material is observed at this site. However, bottom sediments are still composed by mined ores particles.
6	Located approximately 45 km downstream of La Estrella. We did not expect to find traces of mercury in the sediment, because it is though that most sediment accumulated at this site comes from naturally eroded soil particles.

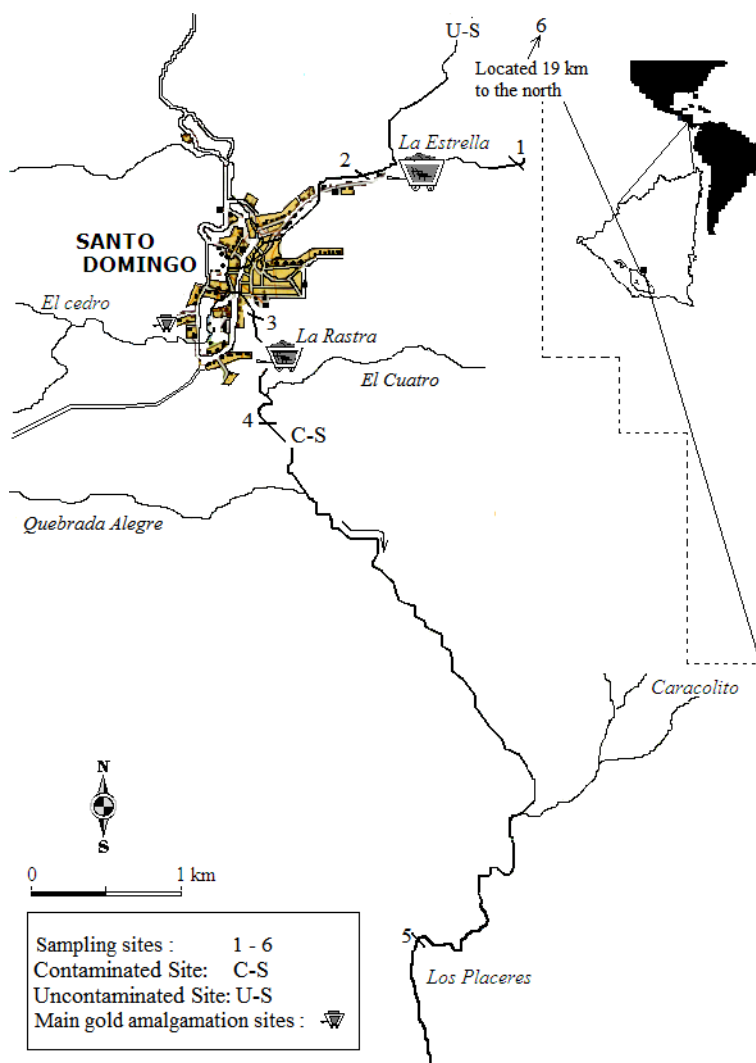


Figure 1. Sediment core sampling and sediment resuspension assay locations at the Sucio river. Sampling sites are numbered from 1 to 6. The sediment resuspension assay was done at a downstream site where river water is contaminated with mercury (C-S) (Paper I) and at upstream uncontaminated site (U-S).

Sampling, chemical analyses and field measurements

Sediment sampling and chemical analyses

Three replicate sediment cores were collected from undisturbed wetted depositional areas in the river channel at six sites (Table 1, Fig. 1), using PVC core tubes (5.08 cm in diameter, 50.8 cm length) in a gravity stainless steel Kajak-Brinkhurst. Core Sampler. The core tubes were sealed with rubber plugs and

transported on ice to the laboratory for analysis. The cores were gently placed on the side and the end caps removed. A rubber piston plunger was used to push the sediment cores from the bottom of the core tube. In this way, one sediment core from each of the six sites was sliced in 1 cm sections and the others in 5 cm sections. The core sections were placed separately in aluminum foil containers and dried at room temperature (30 °C).

The sediment age was determined in the 1 cm sliced cores using the lead-210 dating method by alpha counting the activity of its alpha-emitting grand-daughter nuclide, Polonium-210. A Polonium-209 spike was added to approximately 2 g of dry and finely ground sediment prior to leaching with a mixture of HNO₃ and HCl (1:1). The Polonium isotopes were plated onto a silver disc, and the disc activity was counted with a Canberra-Quad/7404 alpha spectrometer connected to a Canberra 1520 Mixer/Route. The age of the sediment and net sedimentation was calculated from the radioactive decay of Lead-210 and the constant rate of supply (CRS) model (Appleby and Oldfield, 1978).

One gram of the sediment slices from the 5 cm un-dated and 1 cm dated cores was digested with HNO₃ at 120 °C for 1 h in an autoclave. The mercury in the solution was analyzed by inductively coupled plasma mass spectroscopy (ICP-MS; Perkin Elmer, ELAN-6000). The ICP-MS was calibrated against a single ²⁰²Hg standard (1 µg/l). Rhodium was used as internal standard added to the samples and standard solution. The instrument detection limits was 0.03 µg/l total mercury.

The organic content of the sediment was determined by oxidation. Ten ml of 1 N potassium dichromate and 20 ml sulfuric acid were added to one gram of sediment in a 500 ml flask. After 30 min, the solution was diluted to 200 ml with distilled water, and 10 ml of phosphoric acid, 0.2 g of sodium fluoride and 1 ml of diphenylamine were added prior to titration with 0.5 N ammonium iron sulfate (Jackson, 1982).

Gross accumulation and sediment resuspension assay

Based on prior observations of small diurnal variations in the river flow (Paper I), the sedimentation/resuspension experiment was carried out within 8 h at one uncontaminated (U-S) and one mercury contaminated (C-S) site in the river (Fig. 1). The principal idea for the experiment was to use mercury contaminated sediment in a trap at the uncontaminated site and uncontaminated sediment in a trap at the contaminated site, and exposes the trap to exchange and dilution. The changes in sediment weight and mercury concentration were observed and used to interpret different outcomes of the experiment. For instance, a weight loss synchronized with a constant mercury concentration of the remaining sediment in the trap at the U-S site would be interpreted as resuspension of the original sediment, whereas, let's say, a halving of the weight with a corresponding halving of the mercury concentration of the sediment in the trap, would be interpreted as a total resuspension of the original sediment in the trap and replacement as sedimentation of half of its weight by uncontaminated suspended material.

A large portion (~10 kg) of undisturbed sediment was collected at the U-S site and at the C-S site in the river. The maximum water depth at the sites was 18 and 42 cm, respectively. The sediment samples were homogenized separately and dried at room temperature (30 °C). One gram of U-S and P-S sediment was digested with HNO₃ at 120 °C for 1 h in an autoclave, the mercury concentration in the solution was measured by ICP-MS, and the mass of mercury in the sediment calculated.

The particles size distribution of the sediment was determined by passing portions of U-S and C-S sediment samples through sieves ranging from < 63 to 2000

μm . The size distribution of smaller particles than $63 \mu\text{m}$ was determined following the Pipette Method (Day, 1965).

The sedimentation/resuspension assay was made during two consecutive field campaigns.

Sediment traps of $14 \times 4.5 \times 18.5$ centimetres with a maximum storage capacity of ~ 700 g of sediment were constructed from PVC (Fig. 2). The traps were fitted on concrete bricks. Four replicates with a known amount of undisturbed U-S sediment (~ 550 g) were prepared in the field on an Ohaus Adventure Pro Av2101 precision balance (maximum capacity of 2100 g and a readability of 0.01 g) and placed in sediment traps. The sediment in the traps was wetted with distilled water. The traps were closed and carefully placed on the river bottom sediment in a horizontal position parallel to the stream at the C-S site. No loss of sediment in the traps was observed during their installation. Once placed in the river, the trap covers were gently and partially opened by pulling a fine nylon cord (fixed to them) towards the river flow direction to allow water to flow in, and when the traps were full of water, the covers were gently and completely opened and the sediment was exposed to the river flow for 2 hours. Another eight replicates were exposed to the stream in the same way for the same time period. The procedure was repeated on another set of replicates, exposed for 4, 6 and 8 hr. The undisturbed C-S sediments were exposed to the river flow at the U-S site, following the same field procedure as for the U-S sediments.

After the exposure time the traps were gently closed and removed from the river. The sediment traps were left horizontally on the ground until the supernatant was clear. It was carefully decanted, and the

wet sediment samples were dried at room temperature. The dry sediment was weighted on an Ohaus Adventure Pro Av2101 precision balance, and one gram was acid digested and the mercury concentration determined by ICP-MS.

In order to estimate the temporal variation of the river discharge, the cross sections of the river were measured at both sites and the stream velocity was measured with a high-resolution, low-speed rotor flow meter (2030RG General Oceanic Inc. mechanical flowmeter) every 30 minutes during the exposure period of time. Means values of the river discharge were used in the data analysis.

Data on the change of sediment weight in the traps and the changes in mercury concentration of the remaining sediment after exposure were used to calculate the mercury resuspension and gross sedimentation.



Figure 2. Sediment traps used for the gross accumulation and sediment resuspension assay in the Sucio river.

Results

The sediments were contaminated with mercury from site 2, immediately downstream of the upper processing plant, to site 5, more than 8 km downstream of the upper processing plant (Fig. 3). The highest mercury concentrations (about 10 µg/g) were found at site 4, downstream both of the processing plants, and the lowest concentrations at site 6, 45 km downstream of the upper processing plant. The mercury concentrations at these two sites, as well as site 1, upstream of the upper processing plant, were evenly distributed with the depth to 20 cm, whereas the other three sites had maximum concentrations in the uppermost 5 cm of the sediment. Thus, the sites immediately downstream of the processing plants have retained mercury mostly from the last ten years (Fig. 3, year axis), whereas site 4 may act as a mercury sink in the river basin. The mercury and organic carbon concentrations at all depths and sites together were positively correlated ($r^2 = 0.64$, $p < 0.00005$).

The vertical distribution of net sedimentation rate of particles had a peak at all of the sites, but the quantities accumulated and the year the main peak took place was largely different (Fig. 3). The largest quantities of particle mass were accumulated at the downstream sites 4-6 and at site 2, and least quantities were accumulated at the upstream site 1 and at site 3, between the processing plants, just downstream of the village. The low sedimentation rate at site 1 was expected, since there is no anthropogenic activity upstream of it, and it is essentially a creek with a short distance to the spring. Site 3 was expected to have a higher sedimentation rate, since it has the same flow as site 2 and the same concentration

of total suspended solids in the water as site 6 (Picado and Bengtsson, paper I). Since the net accumulation of particles was calculated from the Pb-210 analysis, the age of the sediment at a certain depth varied with the same pattern as the accumulation rate. For instance, the year of deposition of the sediment at 15 cm depth was 1975, 1950, 1962, and 1972 at sites 2, 4, 5, and 6, respectively, and it was 1920 and 1930 at sites 1 and 3, respectively (Fig. 3). There were at least three age groups for peaks of accumulation rate to occur among the sites. The downstream sites, 4, 5, and 6, had their sedimentation peaks in 1989, 1991 and 1992 plus 1998, respectively, that is, essentially in the 1990's, and the upstream sites, 1 and 2, trapped most particles in 1975 plus 1980 and in 1983, respectively. Thus, it seems as if the sedimentation peak in 1983 probably associated with the upper processing plant, La Estrella, was not detected at the other sites, whereas the peak in sedimentation in 1989 just downstream of the second processing plant, La Rastra, may have been transmitted to sites 5 and 6 in the following 2-3 years.

There was no gross accumulation of sediment observed in any of the traps, but all of them had resuspension of both sediment particles and mercury (Table 2). The contaminated site had twice as high resuspension of sediment as the uncontaminated, but the variability was large, with coefficient of variation 65-70 %. The resuspended mass at the uncontaminated site carried 5.7 times as much mercury as the resuspended mass at the contaminated site. The difference between the sediments in resuspended mercury was slightly larger than the difference between them in mercury concentration (4.5×), mainly because the contaminated sediment lost a larger

fraction (2.4%) of its mercury load than the uncontaminated sediment (1.9%) during resuspension. The resuspension of mass rates in Table 2 can be converted to an area basis by dividing with the bottom area of the trap, 259 cm². The yearly average resuspension rate at the contaminated site then becomes 1460 g/cm², year, which is orders of magnitude larger than the net accumulation, calculated from the sediment dating (Fig. 3).

The mass resuspended mercury is positively correlated with the mass of resuspended sediment resuspended at both the unpolluted ($r^2 = 0.77$, $p < 0.00005$) and polluted ($r^2 = 0.88$, $p < 0.00005$) sites (Fig.

4), and the fluxes of resuspended mercury ($\mu\text{g/s}$) is positively correlated with the fluxes of resuspended sediment (mg/s) at both the unpolluted ($r^2 = 0.71$, $p < 0.00005$) and polluted ($r^2 = 0.82$, $p < 0.00005$) sites (Fig. 4). That means that the fluxes of resuspended mercury and sediments were better correlated for the sediment with low mercury content. There was much scatter and weak positive correlations between river flow on one hand and resuspended sediment ($r^2 = 0.54$, $p < 0.00005$) and resuspended mercury ($r^2 = 0.46$, $p < 0.00005$) on the other at the uncontaminated site (Fig. 4). The correlations were worse at the contaminated site.

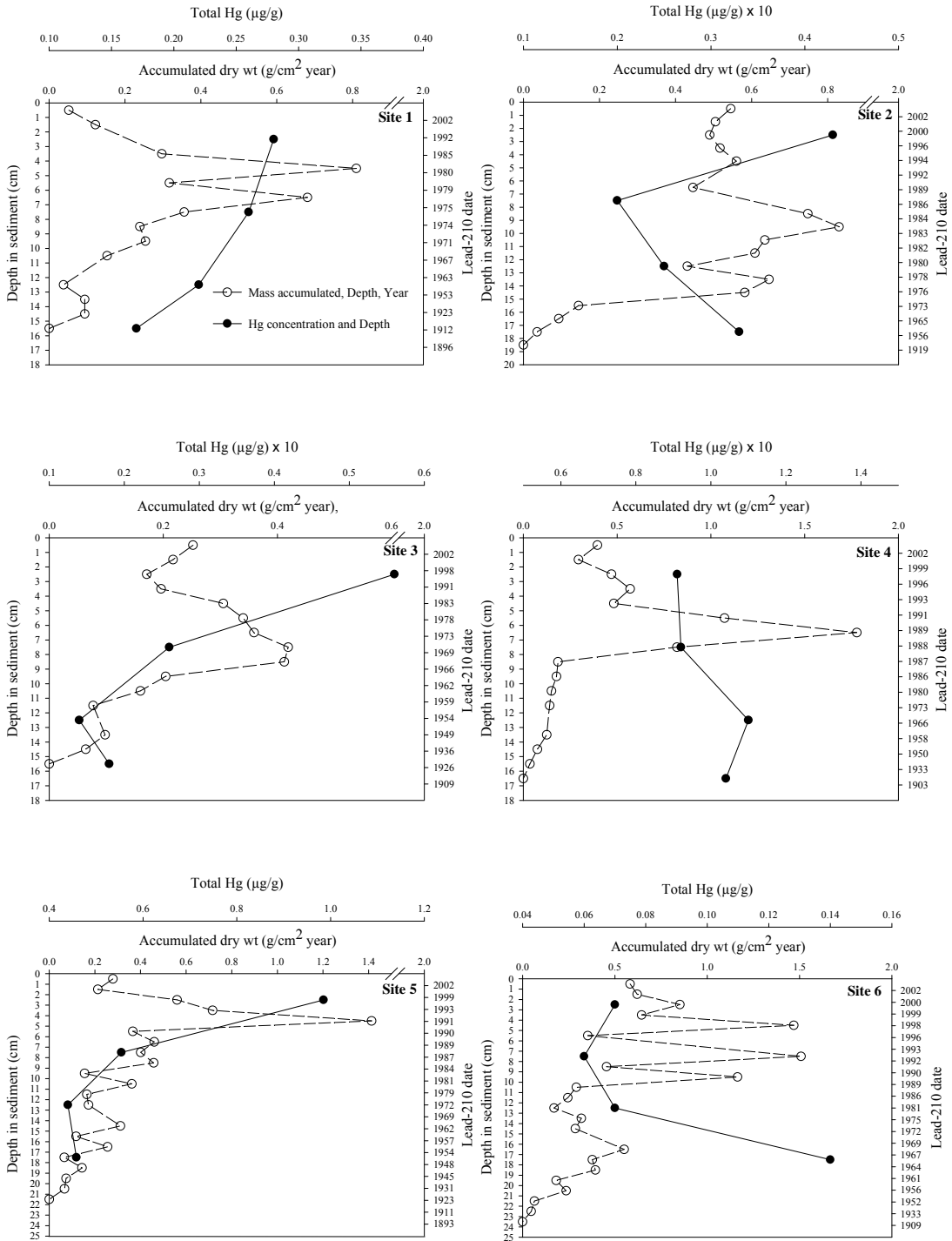


Figure 3. Historical records of net mass accumulation ($\text{g/cm}^2 \text{ year}$) (\circ) of sediment during different years and at different depths in the sediment, and mean of total mercury concentration (\bullet), in Sucio river sediments. Notice that the mercury concentration at sites 2-4 are up by a factor of 10.

Table 2. Mean river flow, particle size distribution and mean total mercury (THg) concentration of the sediments used in the resuspension experiment, and mean resuspension rates of sediment and mercury from the sediment traps to the water column.

Site	River flow (m ³ /s)	Water velocity (m/s)	Sediment			Resuspension rate		
			Sand	% Silt	Clay	THg (μg/g)	Mercury (μg/s)	Sediment (mg/s)
*U-S	0.08 ± 0.06 (0.004 – 0.213)	0.26 ± 0.17 (0.01 – 0.66)	77	19	4	2.12	0.23 ± 0.14 (0.09 - 0.60)	5.99 ± 4.28 (1.24 – 15.54)
*C-S	0.61 ± 0.21 (0.16 – 1.10)	0.36 ± 0.13 (0.10 – 0.66)	78	17	5	9.52	0.04 ± 0.02 (0.02 - 0.12)	12.16 ± 7.96 (3.56 – 40.79)

*Uncontaminated site (U-S), Contaminated site(C-S)

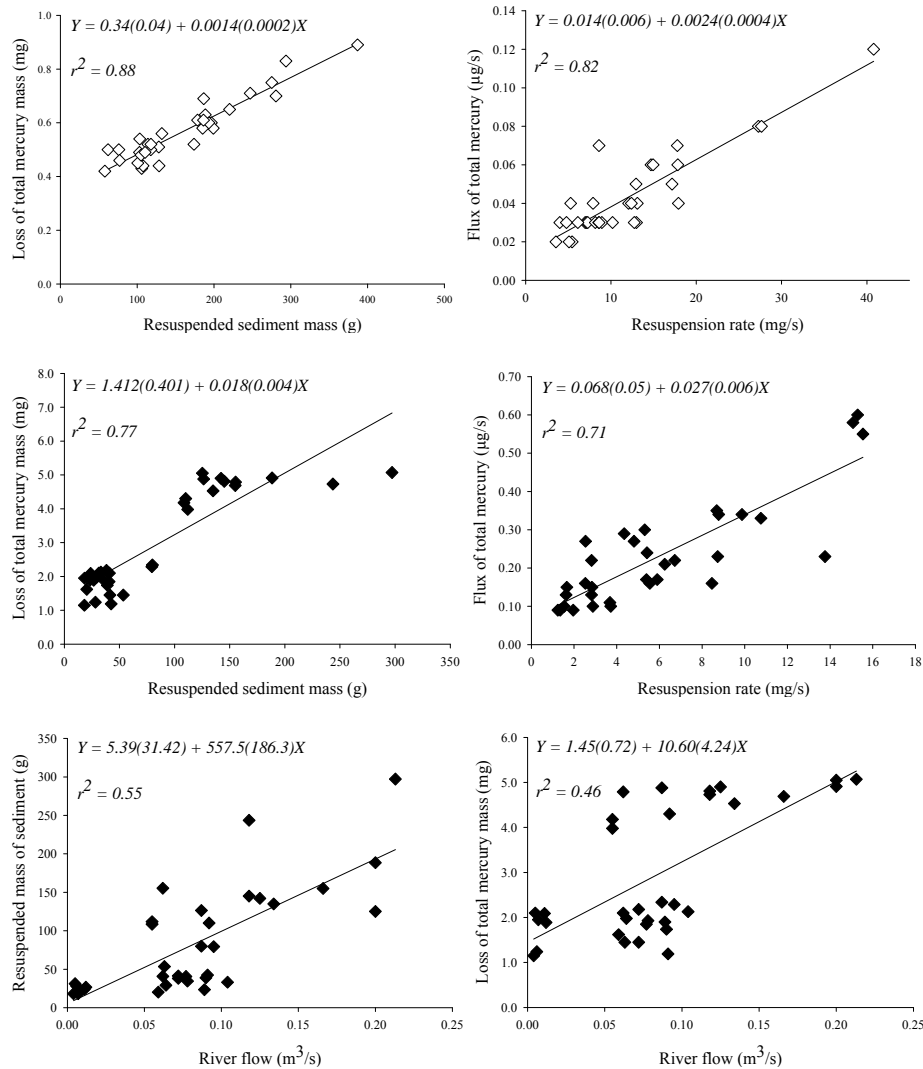


Figure 4. Sediment and sediment particle bound mercury resuspension at a contaminated site (◇) and an uncontaminated site (◆) in Suciio river. Numbers within parentheses in the linear models are the ± 95% confidence intervals for intercepts and slopes.

Discussion

Gold mining activity uses surface waters to dispose large amounts of sedimentary wastes containing mercury and other metals, such that mercury accumulates in river sediments. It is hoped that rivers and streams dilute the contamination by means of a downstream spreading of the mercury mass, but low flow conditions and the presence of stagnant areas facilitate a gradual sedimentation and the subsequent accumulation of particle bound mercury. In contrast, high flow promotes resuspension of sediment particles, which may be an important mechanism for mercury transport in rivers and streams.

Whatever the extent and the mechanisms of the fluvial transport may be, mercury is always found in sediments as inorganic species or at very low concentrations as methylated species (Ullrich et al., 2001). Depth sediment profiles are commonly analysed to elucidate the historic conditions of aquatic systems with respect to sedimentation processes (Jha et al., 1999) and contamination (Leigh, 1997; Lockhart et al., 2000; Ullrich et al., 2001). The sediment cores from Sucio river reflect the deposition of suspended solids into sediments and the accumulation of mercury in the streambed (Fig. 3) from 100 years of gold mining activity in St Domingo. The observed peaks of net sedimentation indicate the direct release of mined ores into the river by an intense mining activity in the past. The yearly net sedimentation gradually increased from 1910 to 1955, probably due to increased ore processing by two gold mining companies. The first mining company settled in 1910 and the second one went in operation in 1928, when the former closed down. The mining activity became more intense between 1940 and 1950 due to an

increase in the international gold demand. However, the net sedimentation rate along the river was less than 0.1 g/cm^2 per year and lower than in the next three decades (Fig. 3) when a large sedimentation ($\sim 0.9 \text{ g/cm}^2 \text{ year}$) peak was observed at site 2, probably due to an increase in ore processing at La Estrella plant (Fig. 1, 3). The increasing net sedimentation rates after 1980 coincides with the local gold production, which increased between 1980 and 1990. Therefore, a large sedimentation peak is observed in all sites during that period (Fig. 3). The gold recovery at the industrial level ceased after 1990 and the mining activity was continued on semi industrial and artisanal bases, such that the net sedimentation rate in the riverbed remained below $0.6 \text{ g/cm}^2 \text{ year}$. A decline in mining activity due to difficulties in ore extraction from vein structures was another factor associated with the latter low sediment deposition.

Since the upstream sediments are gradually resuspended by the river flow, the large net sediment accumulation between 8 and 16 cm depth, with a peak at 10 cm at site 2, is transmitted to the downstream sites (Fig. 3). However, the highest peak at 7 cm depth at site 4 was due to the upstream sediment resuspension and probably due to the release of mined ores by a new ores processing site established in the early 1990's, w locally known as La Rastra (Fig. 1).

Mercury accumulation increases upward in a sediment profile (Fig. 3) and the top 5 cm concentrations of most contaminated sites (2, 3,5) are higher than the concentration of $0.45 \text{ } \mu\text{g/g dw}$ associated with probable effect on freshwater organisms (CEQC/CCME, 1999). Nevertheless, the vertical pattern of the mean total mercury concentrations is not the same as for the

net accumulation rate (Fig. 3), probably because the ratio between the mass of mercury and the amount of ore in the mining tailings released into the river is not always the same or the sediment mercury concentrations are diluted by episodic inputs of soil particles eroded from the catchment. In addition, even though the spatial distribution of the settling of sediment particles, which is driven by the flow conditions and influenced by particles density (Wayne et al., 1996), can also account for the vertical distribution of mercury in sediments, the organic content of the sediment is considered to be a primary factor for the accumulation of mercury in a vertical sediment profile (Benoit et al., 1998; Biester et al., 2002).

The transport of sedimentary wastes and their accumulation in the riverbed is observed 45 km away from the ore processing sites (site 6), but during heavy rains, the soil eroded by runoff and the influx of suspended material from the connecting streams may also contribute to the mass of sediment deposited at the downstream sites, e.g. site 5 and 6. The concentrations of mercury at site 5 and the detectable concentrations at ~37 km downstream of the processing plant (site 6) suggests the sediment bound mercury resuspension as an important mechanism for mercury transport in Sucio river. This mechanism is indicated by the relatively strong correlation between the resuspension of mercury mass and resuspension of sediment at the two sites of the river (Fig. 4). The correlation can be influenced by the sediment particle size and the organic content of the sediments, because smaller particles are removed faster than larger particles at any flow condition and mercury is preferentially associated with smaller particles and with

high high organic content. Inasmuch, river flow can differently affect the resuspension of particles bound mercury and the sediment resuspension. This was observed by the correlation found at the unpolluted sites (Fig. 4). Although resuspension of mercury and sediment is correlated at both low and high flow rates in Sucio river (Fig. 4), there were only weak correlations between the river flow and resuspension of mercury and sediment mass at the high flow rate at the polluted site (Table 3), probably due to the suddenly up and down events in water velocity, which were not recorded, that promote a suddenly large and faster resuspension of sediment particles.

An estimation based on data from cores gives mean values of 128, 195, 166, 164, 202, and 215 kg dw/m² and 29.5, 592.8, 473.1, 1628.5, 123.2, and 19.4 mg/m² respectively at site 1, 2, 3, 4, 5 and 6 for 100 years of net sedimentation of particle mass and mercury. The low mercury concentrations at site 6 can be attributed to a dilution effect due to the input of sediment from other sources or to the absence of organic matter in the sediments (Table 2). A mass of mercury about 59.2 kg/m² accumulated in the top 5 cm at this site indicates a recent contamination and that mercury-sediment resuspension greatly contributes to the downstream spreading of the pollution. If we assume that the accumulation of mercury in the river occurs between site 2 and site 5 and the mass of mercury downstream of site 5 is exported to other basins, 1.5 and 0.7 kg/year are respectively the estimated masses assuming a mean river width of 5 m and using the distance between sites given in Table 1.

Sediment resuspension is slightly dependent on water flow and particles

density and it contributes to the transport of mercury in rivers and streams. Here, the particle bound mercury resuspension from the sediment to the bulk water was measured during eight hours of exposure under reasonably constant river flow condition. However, the up scaling from hour to year in calculating the resuspension may result in inaccurate estimations. Long term sedimentation-sediment resuspension measurements over an appropriate temporal and spatial scales along the river will give further insights in both mechanisms, involved in the net fluvial transport of mercury.

Conclusions

The transport of mercury associated with mined ore in Sucio river is characterized by a downstream hotspot of mercury concentration in sediments. The patchy spatial accumulation probably is a result of a combination of upstream mercury-sediment resuspension and a downstream sedimentation.

Since the mass of mercury that is transported by the resuspension of particles bound mercury can vary spatially along the

river due to changes in water velocity and sediment particles size distribution, more measurements of resuspension in combination with the mercury-particles sedimentation are needed to quantify the net contribution of the former mechanism to mercury transport in the river.

The low sediment deposition and the higher total mercury concentrations found in the shallow sediment indicates a relatively recent decline in ore processing, but an extensive use of mercury. These mercury concentrations in the sediment call for improvements of the artisanal practices in gold recovering or for the implementation of clean alternatives to reduce or eliminate the mercury emissions.

Acknowledgments

The Swedish International Development Agency (SIDA/SAREC) supported this study through the “Environmental Research Multidisciplinary Programme”. It is a cooperative project involving the National Autonomous University of Nicaragua (UNAN-Managua) and Lund University.

Appendix

Mean total mercury concentration and organic content of depth sediments from Sucio river.

Sampling site	Depth (cm)	Total Hg ($\mu\text{g/g}$)		Organic Content (%)	
		Mean	Standard Deviation	Mean	Standard Deviation
Site 1	0-5	0.28	0.16	2.3	1.2
	5-10	0.26	0.23	1.5	1.1
	10-15	0.22	0.17	1.4	1.0
	15-20	0.17	0.09	1.2	0.8
Site 2	0-5	4.35	3.11	0.4	0.1
	5-10	2.00	0.30	0.4	0.2
	10-15	2.47	1.16	0.3	0.1
	15-20	3.34	1.39	0.4	0.1
Site 3	0-5	5.59	0.66	1.6	0.3
	5-10	2.57	0.89	1.2	0.7
	10-15	1.43	0.49	1.0	0.3
	15-18.5	1.79	0.52	1.3	0.2
Site 4	0-5	9.10	1.75	1.5	0.2
	5-10	9.23	2.19	1.2	0.1
	10-15	11.05	1.94	1.6	0.3
	15-18.5	10.36	2.42	1.6	0.2
Site 5	0-5	0.98	0.21	0.6	0.0
	5-10	0.55	0.16	0.3	0.1
	10-15	0.44	0.10	0.2	0.0
	15-20	0.46	0.19	0.1	0.0
Site 6	0-5	0.07	0.01	0.0	0.0
	5-10	0.06	0.02	0.0	0.0
	10-15	0.07	0.02	0.1	0.1
	15-20	0.14	0.13	0.1	0.1

References

- Appleby, P.G., Oldfield, F., 1978. The calculation of lead-210 dates assuming a constant rate of supply of unsupported ^{210}Pb to the sediment. *Catena*. 5, 1-8.
- Arkhipova, N.A., Venitsianov, E.V., Kocharyan, A.G., Dmitrieva, I.L., 2001. Experimental study and mathematical modeling of Hg and Cu transformations in the water-bottom sediment system. *Water Resources*. 28(1), 63-67.
- Babiarz, C.L., Hurley, J.P., Benoit, J.M., Shafer, M.M., Andren, A.W., Webb, D.A., 1998. Seasonal influence on partitioning and transport of total mercury in rivers from contrasting watersheds. *Biogeochemistry*. 41, 237-257.
- Balogh, S.J., Mayer, M.L., Johnson, K., 1997. Mercury and suspended sediment loadings in the lower Minnesota River. *Environmental Science and Technology*. 31, 198-202.
- Balogh, S.J., Meyer, M.L., Johnson, D.K., 1998. Transport of mercury in three contrasting river basins. *Environmental Science and Technology*. 32, 456-462.
- Bengtsson, G., Picado, F., 2008. Mercury sorption to sediments: Dependence on grain size, dissolved organic

- carbon, and suspended bacteria. *Chemosphere*. doi:10.1016/j.chemosphere.2008.06.017.
- Benoit, J.M., Gilmor, C.C., Mason, R.P., Riedel, G.S., Riedel, G.F., 1998. Behavior of mercury in the Patuxent river estuary. *Biochemistry*. 40, 249-265.
- Biester, H., Muller, G., Scholer, H.F., 2002. Binding and mobility of mercury in soils contaminated by emissions from chlor-alkali plants. *The Science of the Total Environment*. 284 (191-203).
- Bishop, K., Lee, Y.-H., Pettersson, C., Allard, B., 1995. Terrestrial sources of methylmercury in surface waters: The importance of the riparian zone on the Svartberget catchment. *Water, Air, and Soil Pollution*. 80, 435-444.
- Bonzongo, J.-C.J., Heim, K.J., Chen, Y., Lyons, W.B., Warwick, J.J., Miller, G.C., Lechler, P.J., 1996. Mercury pathways in the Carson River-Lahontan reservoir system, Nevada, USA. *Environmental Toxicology and Chemistry*. 15(5), 677-683.
- Callahan, J.E., Miller, J.W., Craig, J.R., 1994. Mercury pollution as a result of gold extraction in North Carolina, U.S.A. *Applied Geochemistry*. 9, 235-241.
- CEQC/CCME, 1999. Canadian Environmental Quality Guidelines/Canadian Council of Ministers of the Environment.
- Day, P.R., 1965. Particle fractionation and particle-size analysis. In: C.A. Black (Editor), *Methods of soil analysis, Part 1*. American Society of Agronomy, Inc, Madison, Wisconsin, pp. 545-567.
- Deacon, J.R., Driver, N.E., 1999. Distribution of trace elements in streambed sediment associated with mining activities in the Upper Colorado River basin, Colorado, USA, 1995-96. *Archives of Environmental Contamination and Toxicology*. 37, 7-18.
- Goncalves, C., Fávoro, D.I.T., Melfi, A.J., Oliveira, S.M.B.d., Vasconcellos, M.B.A., Fostier, A.H., Guimarães, J.R.D., Boulet, R., Forti, M.C., 2000. Evaluation of mercury levels in sediment and soil samples from Vila Nova river basin, in Amapá State, Brazil, using radiochemical neutron activation analysis. *Journal of Radioanalytical and Nuclear Chemistry*. 243(3), 789-796.
- Gray, J.E., Theodorakos, P.M., Bailey, E.A., Turner, R.R., 2000. Distribution, speciation, and transport of mercury in stream-sediment, stream-water, and fish collected near abandoned mercury mines in southwestern Alaska, USA. *The Science of the Total Environment*. 260, 21-33.
- Huang, K.-M., Lin, S., 2003. Consequences and implication of heavy metal spatial variations in sediments of the Keelung River drainage basin, Taiwan. *Chemosphere*. 53, 1113-1121.
- Hurley, J.P., Cowell, S.E., Shafer, M.M., Hughes, P.E., 1998. Partitioning and transport of total methyl mercury in the lower Fox river, Wisconsin. *Environment Science and Technology*. 32, 1424-1432.
- Hylander, L.D., Meili, M., Oliveira, L.J., Silva, E.C., Guimarães, J.R.D., Araujo, D.M., Neves, R.P., Stachiw, R., Barros, A.J.P., Silva, G.D., 2000. Relationship of mercury with aluminum, iron, and

- manganese oxy-hydroxides in sediments from the Alto Pantanal, Brazil. *The Science of the Total Environment*. 260, 97-107.
- Jackson, M.L., 1982. *Análisis Químico de Suelo*, Barcelona.
- Jha, S.K., Krishnamoorthy, T.M., Pandit, G.G., Nambi, K.S.V., 1999. History of accumulation of mercury and nickel in Thane Creek, Mumbai, using ^{210}Pb dating technique. *The Science of the Total Environment*. 236, 91-99.
- Lawson, N.M., Mason, R.P., Laporte, J.-M., 2001. The fate and transport of mercury, methylmercury, and other trace metals in Chesapeake Bay tributaries. *Water Resources*. 35(2), 501-515.
- Leigh, D.S., 1997. Mercury-tainted oberbank sediment from past gold mining in north Georgia, USA. *Environmental Geology*. 30((3/4)), 244-251.
- Lima, L.R.P.d.A., Bernardez, L.A., Barboza, L.A.D., 2008. Characterization and treatment of artisanal gold mine tailings. *Journal of Hazardous Materials*. 150, 747-753.
- Lockhart, W.L., Macdonald, R.W., Outridge, P.M., Wilkinson, P., DeLaronde, J.B., Rudd, J.W.M., 2000. Tests of the fidelity of lake sediment core records of mercury deposition to known histories of mercury contamination. *The Science of the Total Environment*. 260, 171-180.
- Mudroch, A., Clair, T.A., 1986. Transport of arsenic and mercury from gold mining activities through and aquatic system. *The Science of the Total Environment*. 57, 205-216.
- Roulet, M., Lucotte, M., Canuel, R., Rheault, I., Tran, S., Goy, Y., Farella, N., Passos, C., Silva, S., Mergler, D., Amorin, M., 1998. Distribution and partition of total mercury in waters of the Tapajós river basin, Brazilian Amazon. *The Science of the Total Environment*. 213, 203-211.
- Serfor-Armah, Y., Nyarko, B.J.B., Adotey, D.K., Adomako, D., Akaho, E.H.K., 2004. The impact of small-scale mining activities on the levels of mercury in the environment: The case of Prestea and its environs. *Journal of Radioanalytical and Nuclear Chemistry*. 262(3), 685-690.
- Tarras-Wahlberg, N.H., Flachier, A., Lane, S.N., Sangfors, O., 2001. Environmental impacts and metal exposure of aquatic ecosystems in rivers contaminated by small scale gold mining: the Puyango River Basin, Southern Ecuador. *The Science of the Total Environment*. 278, 239-261.
- Telmer, K., Costa, M., Angélica, R.S., Araujo, E.S., Maurice, Y., 2006. The source and fate of sediment and mercury in the Tapajós River, Pará, Brazilian Amazon: Ground- and space-based evidence. *Journal of Environmental Management*. 81, 101-113.
- Tsai, L.-J., Yu, K.-C., Huang, J.-S., Ho, S.-T., 2002. Distribution of heavy metals in contaminated river sediment. *Journal of Environmental Science and Health*. A37(8), 1421-1439.
- Ullrich, S.M., Ilyushchenko, M.A., Uskov, G.A., Tanton, T.W., 2007. Mercury distribution and transport in a contaminated river system in Kazakhstan and associated impacts on aquatic biota. *Applied Geochemistry*. 22, 2706-2734.

Ullrich, S.M., Tanton, T.W., Abdrashitova, S.A., 2001. Mercury in the aquatic environment: A review of factors affecting methylation. *Critical Reviews in Environmental Science and Technology*. 31(3), 241-293.

Wayne, D.M., Warwick, J.J., Lechler, P.J., Gill, G.A., Lyons, W.B., 1996. Mercury contamination in the Carson River, Nevada: A preliminary study of the impact of mining wastes. *Water, Air, and Soil Pollution*. 92, 391-408.

**Mercury sorption to sediments: Dependence on
grain size, dissolved organic carbon, and
suspended bacteria**

Bengtsson, G. and Picado, F.



Mercury sorption to sediments: Dependence on grain size, dissolved organic carbon, and suspended bacteria

Göran Bengtsson^{a,*}, Francisco Picado^{a,b}

^a Department of Ecology, Lund University, Sölvegatan 37, SE-223 62 Lund, Sweden

^b Centro para la Investigación en Recursos Acuáticos, Universidad Nacional Autónoma de Nicaragua (CIRA-UNAN), Apdo. Postal 4598, Managua, Nicaragua

ARTICLE INFO

Article history:

Received 4 February 2008

Received in revised form 8 June 2008

Accepted 9 June 2008

Available online xxx

Keywords:

Hg
Transport
Groundwater
River
DOC
Bacteria

ABSTRACT

A combination of laboratory scale derived correlations and measurements of grain size distribution, DOC (dissolved organic carbon) concentration, and density of suspended bacteria promises to be useful in estimating Hg(II) sorption in heterogeneous streambeds and groundwater environments. This was found by shaking intact sediment and fractions thereof (<63–2000 μm) with solutions of HgCl_2 (1.0–10.0 ng ml^{-1}). The intact sediment was also shaken with the Hg(II) solutions separately in presence of DOC (6.5–90.2 $\mu\text{g ml}^{-1}$) or brought in contact with suspensions of a strain of groundwater bacteria (2×10^4 – 2×10^6 cells ml^{-1}). Hg(II) sorption was rather weak and positively correlated with the grain size, and the sorption coefficient (K_d) varied between about 300 and 600 ml g^{-1} . By using the relative surface areas of the fractions, K_d for the intact sediment was back calculated with 2% deviation. K_d was negatively correlated with the concentration of DOC and positively correlated with the number of bacteria. A multiple regression showed that K_d was significantly more influenced by the number of bacteria than by the grain size. The findings imply that common DOC concentrations in groundwater and streambeds, 5–20 $\mu\text{g ml}^{-1}$, will halve the K_d obtained from standard sorption assays of Hg(II), and that K_d will almost double when the cell numbers are doubled at densities that are common in aquifers. The findings suggest that simultaneous measurements of surface areas of sediment particles, DOC concentrations, and bacterial numbers are useful to predict spatial variation of Hg(II) sorption in aquifers and sandy sediments.

© 2008 Elsevier Ltd. All rights reserved.

1. Introduction

Concern about the distribution and fate of mercury (Hg) and the likelihood that it reaches health risk levels in food and drinking water has directed research towards understanding Hg transport in soil and water (DeMarco et al., 2006; Kongchum et al., 2006). Models can describe Hg transport by advective–dispersive equations modified to account for retention processes, such as sorption (Yin et al., 1997a; Sarkar et al., 1999; Carrol et al., 2000; Kim and Corapcioglu, 2002) and sedimentation (Carrol et al., 2000; DiLeonardo et al., 2006). One of the major challenges for this approach is the spatial variability in hydraulic, geologic, and geochemical parameters. Of particular importance is the heterogeneity of the sorption capacity of the geological material, which may vary by an order of magnitude at the centimetre scale for nonionic organic compounds in sediments (Elabd et al., 1986).

Characteristics of soil and sediment particles, such as mineral composition, clay and organic matter content, and metal coatings (Schlüter, 1997), influence sorption of Hg. Minerals, such as quartz and feldspar, which are predominantly found in medium to coarse

particle sizes (Barber et al., 1992), have a permanent negative charge and may retain cationic Hg by electrostatic forces. Likewise, temporary and patchy cover of mineral surfaces by anions, such as hydroxyl and sulphate ions, clay minerals, oxyhydroxides of Al, Fe, and Mn (Coston et al., 1995; Brown et al., 1999), and soil organic carbon (SOC) (Wen et al., 1998; Brown et al., 1999), retains Hg by electrostatic forces and complexation (Yin et al., 1996). Furthermore, the size of the solid particle may affect sorption and concentration of Hg (Fukue et al., 2006), since smaller sized particles are mainly composed of weathering-resistant, net positively charged minerals of Fe and Al (Coston et al., 1995).

The sorption of mercury to natural soils and mineral surfaces is affected by particulate (POC) and dissolved organic carbon (DOC) due to their strong adsorption affinity for Hg (Yin et al., 1996; Ravichandran, 2004; Jing et al., 2007). DOC sorbs to mineral surfaces of Al and Fe oxides-hydroxides by either electrostatic attraction or ligand exchange between carboxyl and hydroxyl groups of DOC and OH and OH_2 groups of the surface minerals (Kaiser and Zech, 1998), and when SOC dissolves, mainly at higher pH, it forms DOC–Hg complexes (Yin et al., 1996; Schlüter, 1997).

Likewise, the presence of bacteria suspended in the aqueous phase or sorbed to the solid can influence the sorption of Hg. Most bacteria have an overall anionic cell surface at common

* Corresponding author. Tel.: +46 462223777.

E-mail address: goran.bengtsson@ekol.lu.se (G. Bengtsson).

environmental pH's as a result of the pK_a 's of carboxyl (4–6) and phosphoryl (~ 7) groups of peptidoglycans, lipopolysaccharides, and phospholipids in the cell wall (Schiewer and Volesky, 2000). These ligands form complexes with metals (Daughney et al., 2002). The high sorption capacity is one of the characteristics that make bacteria a valuable sorbent for removal of metals from wastewater and polluted areas (Chen and Wilson, 1997; Schiewer and Volesky, 2000), e.g. where mercury is released from gold extraction.

One of the challenges in the development of methodologies to account for spatially variable flow and sorption parameters is to identify correlations between flow and sorption parameters and between sorption coefficients and geologic and geochemical parameters. With the latter, laboratory scale derived correlations at hand, laborious preparations of sorption isotherms may be replaced by indirect methods allowing for more rapid screening of field samples. With this in mind, a study was designed to establish quantitative relationships between sorption of Hg(II) to a saturated sediment and the size distribution of the sediment particles, DOC concentration, and cell density of bacteria.

We hypothesized that sorption of Hg(II) to the solid phase would be (i) negatively related to the particle size since cation exchange was assumed to be an important sorption mechanism, with smaller particles sizes having greater capacity than larger particles; (ii) negatively related to DOC concentrations since Hg(II) was assumed to have high affinity for DOC; (iii) negatively related to the density of suspended bacteria as a result of Hg(II) complexation at net negatively charged cell surfaces of suspended bacteria.

2. Materials and methods

2.1. Sediment

The sediment was collected from a depth of 15 cm at the bottom of a temporarily drained water infiltration pond at the lake Vombsjön infiltration area near Lund, south of Sweden. It was a sandy sediment mostly composed of quartz. Kaolinite, amphibole, and feldspar were also found in the sediment (Bengtsson and Ekere, 2001). The sediment was air-dried at room temperature (22 °C). Portions of the sediment were mechanically sieved in a JEL electric shaker into six size fractions, ranging from <63–2000 μm . The ambient total mercury concentration (C_A) in each fraction was determined by inductively coupled plasma mass spectrometry (ICP-MS; Perkin-Elmer, ELAN-6000). The detection limit of the ICP-MS was 0.03 ng total Hg ml^{-1} . It was calibrated against a single ^{202}Hg standard (1 ng ml^{-1}). Rhodium, which is rarely found in water samples, was used as internal standard in the samples and the standard solution.

The cation exchange capacity (CEC) was determined in two grams of each size fraction. The fractions were shaken for 2 h with 10 ml of 0.1 M BaCl_2 in 15 ml Kimax test tubes, using an end-over-end shaker. The aqueous phase was filtered onto a 0.22 μm nitrocellulose Millipore filter and the filtrate used to determine the concentration of cations (Na^+ , K^+ , Ca^{2+} , Mg^{2+} , Mn^{2+} , Fe^{3+} , Al^{3+}) by inductively coupled plasma atomic emission spectrometry (ICP-AES; Perkin-Elmer, Optima 3000 DV). The pH of the filtrate was determined by an Orion SA-720 pH-meter. The ICP-AES was calibrated using a mixture of multi-component standards at three concentrations within a factor of 50. The calibration was controlled with independent standards. CEC was calculated as the sum of the concentrations of each cation (cmol kg^{-1}) and the hydrogen ion concentration.

The total carbon (TC) concentration of each size fraction was determined by weighing 0.01 g of hand-milled sediment in tin cups. The samples were analysed by continuous-flow isotope ratio mass spectrometry (CF-IRMS) using an ANCA 20–20 mass spectrometer with a solid/liquid preparation module (PDZ Europa).

The standard curve was obtained by analysis of sucrose solutions prepared at concentrations ranging from 2.0 to 40.0 mg ml^{-1} .

The specific surface area (SSA) of the fractions was previously calculated for the same sediment sample (Bengtsson and Ekere, 2001). The sediment was reconstructed by mixing the fractions in the original weight proportions.

2.2. Sorption of Hg to sediment

Solutions of Hg(II) were prepared from HgCl_2 in groundwater (pH 7.2) at four different concentrations between 1.0 and 10.0 ng ml^{-1} , to represent contaminated aquifers and streambed environments. Groundwater was taken from a well at the lake Vombsjön infiltration area and filtered onto a 0.45 μm nitrocellulose Millipore filter. One gram of a size fraction, intact sediment, or reconstructed sediment was mixed with 5 ml of the Hg solution in 10 ml Kimax test tubes. This solid/solvent ratio ensured that detectable quantities of Hg were recovered in the solvent phase after equilibration of 1.0 and 10.0 ng ml^{-1} (EPA, 2004). The test tubes were left on an end-over-end shaker for a period of 24 h, with five replicates for each treatment (adsorption kinetics of mercury on pure minerals and sediment and soil particles shows that a period of 24 h is sufficient to obtain equilibrium (Yin et al., 1997a; Sarkar et al., 1999; Miretzky et al., 2005)). They were then centrifuged in a Labofuge 200 (Heraeus Instruments) at 971g for 30 min. The supernatant was transferred to a 5 ml polypropylene vial, preserved in 0.1% HNO_3 and stored in a refrigerator at 5 °C. Hg was quantified by ICP-MS as described above.

The concentration of adsorbed Hg (C_S , ng g^{-1}) was calculated by subtracting the concentration of Hg remaining in the aqueous phase after equilibration (C_W , ng ml^{-1}) and the ambient Hg concentration of the sediment samples (C_A , ng g^{-1}) from the concentration initially added to the test tube (C_0 , ng ml^{-1}): $C_S = (C_0 - C_W) \times (V/W) - C_A$, where V (mL) is the solution volume and W is the weight of air-dried sediment (g). The equilibrium sorption coefficient K_d (mL g^{-1}) was calculated as C_S/C_W .

The K_d in the intact and reconstructed sediment was back calculated from the K_d 's in the fractions to estimate the contribution of the particle sizes to the Hg(II) sorption in intact sediment. We assumed that each particle size fraction contributed to sediment sorption in proportion to its specific surface area (SSA): $K_d = \sum_i K_{di} \times F_{SSA_i}$, in which K_{di} is the K_d for the i th particle size range in mL g^{-1} and F_{SSA_i} is the relative specific surface area fraction of the i th particle size range of the intact sediment (dimensionless).

2.3. Sorption of Hg in presence of DOC

DOC was obtained by shaking 500 g of carbon rich soil (Hasselfors garden soil; a mixture of 60 vol.% low humified peat, 30 vol.% highly humified peat, 5 vol.% composted bark and 5 vol.% sand) with 1500 ml of groundwater on a horizontal Labasco KS-500 shaker at 50 rpm for 100 h. The slurry was centrifuged for 30 min at 4629g in 300 ml aliquots in 500 ml Nalgene screw capped plastic tubes in a Sorvall RC 5B centrifuge at 10 °C. The supernatant was filtered onto GF/A glass fibre filters and then onto 0.45 μm nitrocellulose filters. The filtrate was concentrated at low dry rate by vacuum centrifugation in a Savant SC10A speed vacuum system at 22 °C for 4 h to approximately 400 $\mu\text{g ml}^{-1}$ of DOC. The DOC concentration was measured in a Shimadzu TOC-500 analyzer.

Six DOC solutions (pH 6.8–7.2) were prepared in the range 6.5–90.2 $\mu\text{g ml}^{-1}$ from the DOC concentrate, with groundwater as solvent. The lowest DOC concentration (6.5 $\mu\text{g ml}^{-1}$) was that found in the groundwater. Five replicates of four concentrations (1.0–10.0 ng ml^{-1}) of HgCl_2 were prepared in each of the DOC solutions

in 50 ml Pyrex volumetric flasks. The DOC–Hg(II) solutions were shaken slowly at 60 rpm on a horizontal Labassco KS-500 shaker for 24 h. From each DOC–Hg(II) solution, 5.0 ml were added to 10 ml test tubes, each with one gram of intact sediment. The test tubes were shaken and centrifuged as described in the procedure for sorption of Hg(II) on size fractions, and Hg remaining in the aqueous phase was analysed by ICP-MS.

2.4. Sorption of DOC to sediment

Five millilitres of the DOC solutions prepared for sorption of Hg(II) in presence of DOC were mixed with one gram of intact sediment in 10 ml test tubes, with five replicates for each concentration. The test tubes were shaken and centrifuged as in the procedure for sorption of Hg(II) on size fractions. The DOC in the aqueous phase was measured in the Shimadzu TOC-500 analyzer. The concentration of adsorbed organic carbon (C_{s-OC} , $\mu\text{g g}^{-1}$) was calculated from the difference between the concentration initially added to the test tube (C_{0-OC} , $\mu\text{g ml}^{-1}$) and that remaining in the aqueous phase after equilibration (C_{w-OC} , $\mu\text{g ml}^{-1}$): $C_{s-OC} = (C_{0-OC} - C_{w-OC}) \times (V/W)$, where V (mL) is the solution volume and W is the weight of air-dried sediment (g).

2.5. Sorption of Hg in presence of bacteria

An indigenous groundwater bacterium, *Stenotrophomonas maltophilia* (CCUG 49037), previously isolated from a depth of 7–8 m in the aquifer at the lake Vombsjön infiltration area, was cultured for 2 days at room temperature (22 °C) in 20 ml of 20% peptone–yeast–glucose medium (PYG) by gently shaking on a Labassco KS-500 shaker. The number of cells was determined by counting in a Bürker chamber using a phase contrast microscope (Axioskop 20, Zeiss).

Six dilutions of cultured bacteria, which were washed twice and then resuspended in groundwater, were prepared in the range 2.0×10^4 – 2.0×10^6 cells ml^{-1} . Four concentrations (1.0–10.0 ng ml^{-1}) of HgCl₂ were prepared for each of the bacteria suspensions in 50 ml Pyrex volumetric flasks (pH 7.0–7.4). The bacteria–Hg(II) suspensions were shaken slowly at 50 rpm on a horizontal Labassco KS-500 shaker for 24 h. From each bacteria–Hg(II) suspension, 5.0 ml were added to 10 ml Kimax test tubes, each with one gram of intact sediment. The test tubes were shaken as in the procedure for sorption of Hg(II) on size fractions and then centrifuged at 1157g at 10 °C for 30 min in the Sorvall RC 5B centrifuge. Hg remaining in the aqueous phase was analysed by ICP-MS.

To separate Hg sorbed to cells from dissolved Hg(II) in the supernatant, the aqueous phase was centrifuged at 5432g at 10 °C for 15 min in the Sorvall RC 5B centrifuge. The pellet of bac-

teria was resuspended in 5 ml of groundwater, preserved in 1.0% HCl and analysed for Hg by ICP-MS. All reagents and glassware were sterilized by autoclaving.

Replicated blank samples of 5 ml filtered groundwater and one gram of intact sediment were also equilibrated for 24 h to test for the potential influence of e.g., soil drying on sorption and mobilization of nutrients, metals, and dissolved organic compounds (Rechcigl et al., 1992; Baskaran et al., 1994; Klitzke and Lang, 2007). Mercury was not detected in the aqueous phase, and the DOC concentration ($5.1 \pm 0.4 \mu\text{g ml}^{-1}$) was lower than the ambient DOC concentration initially measured in the groundwater ($6.5 \mu\text{g ml}^{-1}$). Two test tubes with 5 ml of 0.2 ng ml^{-1} of HgCl₂ were also shaken and centrifuged. The Hg concentration did not change, suggesting that no mass losses occurred during the sorption assays.

2.6. Statistical calculations

Means, standard deviations, and the 95% confidence intervals were calculated for each data set of five replicates. Data within the confidence intervals were used to calculate the linear sorption coefficients.

Multiple linear regression (MLR) (Statistica 6.1) was carried out to evaluate the contribution of particle size and number of bacteria to mercury sorption to the sediment.

3. Results

The sorption isotherms for Hg(II) were linear in the concentration range examined, with r^2 values above 0.7 (Table 1). The calculated sorption coefficients varied between about 300 and 600 ml g^{-1} for the size fractions (Table 1). The strength of the linearity of the sorption isotherms was weakened by little sorption of the lowest mercury concentration added, 1.0 ng ml^{-1} . The sorption coefficients were positively correlated with the particle size, with a shallow slope of a linear relationship ($K_d = 419.5(\pm 70.6) + 0.0896(\pm 0.081) \times \text{particle size}$; $r^2 = 0.62$). The 95% confidence interval for the correlation was wide, and particle sizes in the interval of, e.g. 212–500 μm could be assigned a sorption coefficient between 380 and 520 ml g^{-1} with the same probability. The uncertainty was mainly attributed to the relatively small sorption coefficient with the second smallest particle size. The sorption coefficient for Hg(II) with the intact sediment was 409 (Table 1), exceeding the K_d with the sediment reconstructed from the fractions by 0.7%.

The sorption coefficients were negatively and weakly correlated with the ambient Hg concentration ($K_d = 532 - 4.9 \times C$; $r^2 = 0.44$), CEC ($K_d = 520 - 20.6 \times \text{CEC}$; $r^2 = 0.35$) and the TC content ($K_d = 519 - 16.7 \times \text{TC}$; $r^2 = 0.43$). The last two were positively correlated with the ambient Hg concentration ($\text{CEC} = 0.8 + 4.7 \times C_A$; $r^2 = 0.97$,

Table 1

Sediment particle size characteristics and linear sorption coefficients (K_d) for observed Hg sorption to sediment and sediment fractions

Particle size (μm)	Relative weight of fraction	CEC (Cmol kg^{-1})	Total carbon (mg g^{-1})	Net charge ^a ($\times 10^{-7}$ Mequiv. cm^{-2})	K_d (ml g^{-1})	r^2	SSA ($\text{m}^2 \text{g}^{-1}$)	Relative SSA of fraction	Ambient total Hg concentration (ng g^{-1} sediment)
0–63	0.01	6.8	8.4	6.2	453	0.91	21.1	0.35	31.5
63–106	0.01	5.0	6.8	5.1	333	0.77	19.1	0.32	27.1
106–212	0.01	3.3	3.9	5.8	413	0.98	11.0	0.18	14.7
212–500	0.13	1.7	1.8	9.6	457	0.90	3.5	0.06	8.9
500–1000	0.47	1.4	1.5	8.3	500	0.92	3.3	0.05	8.8
1000–2000	0.37	1.3	1.1	9.7	564	0.83	2.5 ^b	0.04	5.6
Intact sediment		1.5	–	–	409	0.86	–	–	8.0
Reconstructed sediment			–	–	406	0.86	–	–	–

^a Calculated from SSA and CEC data according to Uehara and Gillman (1980).

^b Data for SSA were only available for the 1000–1500 μm range but assumed to be representative for the 1000–2000 μm range.

* p -Values < 0.005.

TC = $2.4 + 3.5 \times C_A$; $r^2 = 0.99$, respectively) but negatively related to the particle size (Table 1), with most of the negative effect attributed to smaller particles than 200 μm . The size fractions were separated into two groups by the net charge of the particles. One had lower charges (<212 μm) and the other larger (>212 μm).

The CEC and ambient Hg concentration of the intact sediment was accurately calculated from the values of the individual fractions multiplied with their relative weights (1.5 and 8.1, respectively; cf. observed values in Table 1). The K_d back calculated from K_d of the fractions and their relative weights was erroneous (515), suggesting that the particle size distribution would not be an appropriate predictor of the spatial variability of Hg(II) sorption in the field. The back calculation of K_d for the reconstructed sediment from the K_d 's and relative surface areas of the fractions gave $K_d = 415(453 \times 0.35 + 333 \times 0.32 + 413 \times 0.18 + 457 \times 0.06 + 500 \times 0.05 + 564 \times 0.04)$, which was about 2% above both the K_d calculated from sorption to the reconstructed sediment or the K_d for the intact sediment (Table 1).

Linear sorption isotherms were obtained for Hg(II) with the intact sediment in presence of varying concentrations of DOC. The presence of DOC reduced Hg(II) sorption to the intact sediment by 31–90% (cf. Tables 1 and 2). The resulting negative correlation between DOC concentration and K_d was linear with a fairly steep slope ($K_d = 253(\pm 75.1) - 2.5(\pm 1.4) \times \text{DOC}$; $r^2 = 0.86$). DOC had a low affinity for the mineral sediment, with a sorption coefficient of about 3 ml g^{-1} ($C_{S-OC} = -19.2 + 3.3 \times C_{W-OC}$; $r^2 = 0.94$, where C_{S-OC} is the concentration of organic carbon adsorbed to the sediment and C_{W-OC} is the concentration of dissolved organic carbon in the aqueous phase). It is interesting to notice that K_d of the intact sediment (Table 1) was obtained with the same solvent composition as the 31% lower K_d of the assay with the lowest DOC concentration (Table 2). The reduction most likely came from the step of bringing Hg(II) in contact with DOC in the groundwater for 24 h before the sorbate was combined with the sediment.

In contrast to sorption of Hg(II) to DOC, the number of suspended cells and the sorption coefficient for Hg(II) were positively correlated ($K_d = 401(\pm 112) + 0.00014(\pm 0.0001) \times \text{bacterial number}$; $r^2 = 0.79$), and the Hg(II) sorption was greater in presence of the bacteria than in their absence (cf. Tables 1 and 2). The amount of Hg(II) sorbed to the suspended bacteria varied from less than the ICP-MS detection limit (0.03 ng) for the lowest density of cells to 0.21 ng for the highest.

Multiple linear regression showed that Hg(II) sorption could be predicted from data on the particle size distribution and the numbers of bacteria per ml ($F_{2,3} = 20.3$, $r^2 = 0.93$, $p = 0.018$), which were estimated from the K_d value for bacteria corresponding to a particle size (Table 1). The Hg(II) sorption was significantly affected by the cell numbers ($p < 0.05$) and less by the particle size ($p = 0.40$) ($K_d = 369 - 0.41 \text{ particle size} + 1.34 \text{ number of bacteria ml}^{-1}$). The relatively small partial regression coefficient for the particle size made its contribution to the predicted sorption coefficient less significant compared with the number of bacteria.

Table 2

Sorption coefficients (K_d) for Hg(II) with the intact sediment in presence of DOC at different concentrations and in presence of bacteria cells at different initial densities in the aqueous phase

DOC ($\mu\text{g ml}^{-1}$)	K_d (ml g^{-1})	r^2	No. of bacteria ($\times 10^6 \text{ cell ml}^{-1}$)	K_d (ml g^{-1})	r^2
6.5	283	0.75*	0.02	410	0.91*
20.0	191	0.94*	0.5	525	0.89*
36.1	131	0.73*	1.0	427	0.95*
45.1	103	0.98*	1.5	618	0.37**
72.2	89	0.97*	2.0	717	0.90*
90.2	41	0.86*			

* p -Values < 0.005.

** p -Values < 0.05.

4. Discussion

Mineral composition, CEC, electrostatic forces, complexation with coated organic matter and other physical/chemical characteristics of particle surfaces take a range of values for each size fraction in sediments and natural soils (Yin et al., 1997b; Wen et al., 1998; doValle et al., 2006; Ramalhosa et al., 2006), which is one of the bases for sorption heterogeneity. Particles in the range of clay mostly have unsatisfied surface charge, high CEC, and more surface area per unit of weight than most other sediment fractions (Table 1). The cation exchange is thought to have a major influence on sorption of most metals. For instance, the negative correlation between the particle size and ambient Hg concentrations (Table 1; particle size = $35 - 5.4 \times C_A$; $r^2 = 0.90$) reflects the control of Hg(II) sorption by a combination of cation exchange and complexation with TC. External surfaces of smaller particles often trap more organic carbon than larger particles, and the SOC acts in tandem with the cation exchange capacity to enhance their sorption capacity for mercury, at least at low pH (Yin et al., 1997b).

Yet, Hg(II) sorption was positively and linearly correlated with the particle size in the experiment, suggesting that sorption of added mercury was dependent on the differences in net negative charges between smaller particles and larger (Table 1) and associated with the surfaces either via electrostatic interactions or via chemical reactions between mercury and functional groups at the particle surface. It is possible that mercury was preferentially adsorbed via electrostatic interaction once the cation exchange had been satisfied (e.g. by the adsorbed ambient mercury concentration), but the phenomenon is difficult to generalize, since the development of positive and negative charges depends on pH and the mineral characteristics of the particles (Uehara and Gillman, 1980; McBride, 1994). The formation of Hg(II) complexes e.g. with chloride or DOC in the filtered groundwater might also be a limiting factor for sorption of Hg(II) via CEC.

The distribution of organic matter and clay content was probably responsible for the negative relationship between the particle size and CEC (Table 1). The neutral pH in our assays probably facilitated the solubilization of surface bound organic matter (Anderson, 1979), further decreasing the low concentration of organic carbon (Table 1) and reducing the affinities of mercury for small particles. Moreover, the large variability of K_d with the 0–63 μm particles suggests that they had a heterogeneous surface composition, with some sub-fraction being more sorptive than others. This would be in agreement with suggestions of Altin et al. (1998) that particles of the same size might have different mineral composition and CEC.

The large impact of DOC on K_d for mercury in this study (Table 2) was probably a result of a combination of strong complexation of Hg(II) with anionic DOC groups, and competition between DOC and free ionic mercury for sorption sites on the sediment particles (Yin et al., 1996; Schlüter, 1997). At least three orders of magnitude more DOC ($\mu\text{g g}^{-1}$) became sorbed to the particles compared with mercury (8–60 ng g^{-1}), and the sorbed DOC increased the organic carbon content of the particles by 0.5–2% depending on the added quantity (Table 1). This may effectively have blocked the charged particle sites and made the particles less attractive for Hg(II) sorption compared with the DOC fraction as more DOC was added to the aqueous phase.

The net negatively charged cell surface of many bacteria is an efficient trap for metal cations. This was evident in the assays even with the lowest density of bacteria, in which K_d increased by 0.2% compared with K_d of the intact sediment (cf. Tables 1 and 2). *S. maltophilia* has a net negative charge and preferentially sorbs to soil particles by charge interactions (Lindqvist and Bengtsson, 1995), with a sorption coefficient that is negatively correlated with the particle size (Bengtsson and Ekere, 2001). By assuming a cell

weight of 10^{-13} g and a batch sorption coefficient in groundwater of 13 ml g^{-1} (Lindqvist and Bengtsson, 1991), we estimated that bacteria would make a marginal contribution to the organic carbon content of the sediment particles, even at their highest density (less than $3 \mu\text{g g}^{-1}$) and rather add to the anionic complexing capacity of the particles. If all of the cell weight is assumed to represent organic carbon, the density of suspended cells would be equivalent to about $2\text{--}200 \text{ ng ml}^{-1}$ of DOC, that is, at least three orders of magnitude less than the DOC used in the DOC experiment. The complexing capacity of the suspended bacterial carbon was obviously marginal at that concentration, but the highest concentration, corresponding to $2 \times 10^6 \text{ cells ml}^{-1}$, increased K_d by 75% compared with a cell-free environment. The highest concentration of DOC, corresponding to 450 times as much organic carbon as the bacteria, decreased K_d by 90%. Whether one or the other source of organic carbon had most influence on K_d is difficult to say, but both contributed to similar but opposite K_d changes at concentrations that are commonly found for each of the sources at field sites.

5. Conclusions

Some general insights were gained from the experiments about Hg(II) sorption to sediments. First, the correlation of the sorption coefficient with the net charge of the particles suggests that sorption mechanisms, such as ion bonding, control sorption of Hg(II) in excess of ambient background concentrations, whereas cationic exchange and complexation with SOC seem to be the prevailing mechanisms at ambient concentrations. Second, the heterogeneity of the sorption coefficient for Hg(II) cannot be predicted from the particle size distribution, but sorption is more dependent on the distribution of the specific surface area of particles than of their weight. That is a consequence of the dependence of the sorption process in sandy sediments on surface characteristics of the particles, such as charge, so that smaller particles make a greater contribution to variations of the sorption coefficient than expected from their weight. Third, at concentrations of DOC commonly found in groundwater, $5\text{--}20 \mu\text{g ml}^{-1}$, the anionic and complexing capacity of DOC may halve K_d for Hg(II), and at higher concentrations, e.g. in the plume of a solid waste site, K_d may be a fourth or less than calculated from standard sorption assays. Fourth, bacteria may counteract this effect by sorbing Hg(II) and themselves to the sediment particles to the extent that the sorption coefficient is almost doubled when the cell numbers are doubled at densities that are common in aquifers. The findings suggest that simultaneous measurements of surface areas of sediment particles, DOC concentrations, and bacterial cell numbers are useful to predict spatial variation of Hg(II) sorption in aquifers and sandy sediments. Rather than relying upon laborious sorption assays to address the heterogeneity in Hg(II) retention in mineral dominated sediments, a field survey can accomplish more accurate information from an examination of the spatial distribution of grain surface areas, DOC concentration, and density of pore water bacteria.

Acknowledgements

The Swedish International Development Agency (SIDA/SAREC) supported this study through the "Environmental Research Multi-disciplinary Programme". It is a cooperative project involving the National Autonomous University of Nicaragua (UNAN-Managua) and Lund University. We thank Olof Regnell at our department for comments on an earlier version of the manuscript.

References

Altin, O., Özbelgue, H.Ö., Dogu, T., 1998. Use of general purpose adsorption isotherms for heavy metals-clay mineral interactions. *J. Colloid Interf. Sci.* 198, 130–140.

- Anderson, A., 1979. Mercury in soil. In: Nriagu (Ed.), *The Biogeochemistry of Mercury in the Environment*. Biomedical Press, Amsterdam, The Netherlands, North-Holland, pp. 79–112.
- Barber, L.B., Thurman, E.M., Runnells, D.D., 1992. Geochemical heterogeneity in a sand and gravel aquifer. Effect of sediment mineralogy and particle size on the sorption of chlorobenzenes. *J. Contam. Hydrol.* 9, 34–35.
- Baskaran, S., Bolan, N.S., Rahman, A., Tillman, R.W., MacGregor, A.N., 1994. Effect of drying of soils on the adsorption and leaching of phosphate and 2,4-dichlorophenoxyacetic acid. *Aust. J. Soil Res.* 32, 491–502.
- Bengtsson, G., Ekere, L., 2001. Predicting sorption of groundwater bacteria from size distribution, surface area, and magnetic susceptibility of soil particles. *Water Resour. Res.* 37, 1795–1812.
- Brown Jr., G.E., Henrich, V.E., Casey, W.H., Clark, D.L., Eggleston, C., Felmy, A., Goodman, D.W., Gratzel, M., Maciel, G., MacCarthy, M.I., Nealson, K.H., Sverjensky, D.A., Toney, M.F., Zachara, J.M., 1999. Metal oxide surfaces and their interactions with aqueous solutions and microbial organisms. *Chem. Rev.* 99, 77–174.
- Carroll, R.W.H., Warwick, J.J., Heim, K.J., Bonzongo, J.C., Miller, J.R., 2000. Simulation of mercury transport and fate in the Carson river, Nevada. *Ecol. Model.* 125, 255–278.
- Chen, S., Wilson, D.B., 1997. Genetic engineering of bacteria and their potential for Hg²⁺ bioremediation. *Biodegradation* 8, 97–103.
- Coston, J.A., Fuller, C.C., Davis, J.A., 1995. Pb²⁺ and Zn²⁺ adsorption by a natural aluminum- and iron-bearing surface coating on an aquifer sand. *Geochim. Cosmochim. Acta* 59, 3535–3547.
- Daughney, C.J., Siciliano, S.D., Rencz, A.N., Lean, D., Fortin, D., 2002. Hg(II) adsorption by bacteria: a surface complexation model and its application to shallow acidic lakes and wetlands in Kejimikujik National Park, Nova Scotia, Canada. *Environ. Sci. Technol.* 36, 1546–1553.
- DeMarco, S.D., Botté, S.E., Marcovecchio, J.E., 2006. Mercury distribution in abiotic and biological compartments within several estuarine systems from Argentina: 1980–2005 period. *Chemosphere* 65, 213–223.
- DiLeonardo, R., Tranchida, G., Bellanca, A., Neri, R., Angelone, M., Mazzola, S., 2006. Mercury levels in sediments of central Mediterranean Sea: a 150+ year record from box-cores recovered in the Strait of Sicily. *Chemosphere* 65, 2366–2376.
- doValle, C.M., Santana, G.P., Windmöller, C.C., 2006. Mercury conversion processes in Amazon soils evaluated by thermodesorption analysis. *Chemosphere* 65, 1966–1975.
- Elabd, H., Jury, W.A., Cliath, M.M., 1986. Spatial variability of pesticide adsorption parameters. *Environ. Sci. Technol.* 20, 256–260.
- EPA, 2004. Code of Federal Regulation-Protection of Environment; Chap. 1: Environment Protection Agency; Part 796: Chemical Fate Testing Guidelines; Subpart C; Sec. 796.2750: Sediment and Soil Adsorption Isotherm, pp. 87–90; Ref. 40 CFR 796.2750 (7-1-03 edition).
- Fukue, M., Yanai, M., Sato, Y., Fujikawa, T., Furukawa, Y., Tani, S., 2006. Background values for evaluation of heavy metal contamination in sediments. *J. Hazard. Mater.* 136, 111–119.
- Jing, Y.D., He, Z.L., Yang, X.E., 2007. Effects of pH, organic acids, and competitive cations on mercury desorption in soils. *Chemosphere* 69, 1662–1669.
- Kaiser, K., Zech, W., 1998. Soil dissolved organic matter sorption as influenced by organic and sesquioxide coatings and sorbed sulfate. *Soil Sci. Soc. Am. J.* 62, 129–136.
- Kim, S.-B., Corapcioglu, M.Y., 2002. Contaminant transport in riverbank filtration in the presence of dissolved organic matter and bacteria: a kinetic approach. *J. Hydrol.* 266, 269–283.
- Klitzke, S., Lang, F., 2007. Hydrophobicity of soil colloids and heavy metal mobilization: effects of drying. *J. Environ. Qual.* 36, 1187–1193.
- Kongchum, M., Devai, I., DeLaune, R.D., Jugsujinda, A., 2006. Total mercury and methylmercury in freshwater and salt marsh soils of the Mississippi river deltaic plain. *Chemosphere* 63, 1300–1303.
- Lindqvist, R., Bengtsson, G., 1991. Dispersal dynamics of groundwater bacteria. *Micro. Ecol.* 21, 49–72.
- Lindqvist, R., Bengtsson, G., 1995. Diffusion limited and chemical-interaction-dependent sorption of soil bacteria and microspheres. *Soil Biol. Biochem.* 27, 941–948.
- McBride, M.B. (Ed.), 1994. *Environmental Chemistry in Soils*. Oxford University Press, Oxford.
- Miretzky, P., Bisinoti, M.C., Jardim, W.F., Rocha, J.C., 2005. Factors affecting Hg(II) adsorption in soils from the Rio Negro basin (Amazon). *Quim. Nova* 28, 438–443.
- Ramalhosa, E., Segade, S.R., Pereira, E., Vale, C., Duarte, A., 2006. Mercury cycling between the water column and surface sediments in a contaminated area. *Water Res.* 40, 2893–2900.
- Ravichandran, M., 2004. Interactions between mercury and dissolved organic matter – a review. *Chemosphere* 55, 319–331.
- Rechcigl, J.E., Payne, G.G., Sanchez, C.A., 1992. Comparison of various soil drying techniques on extractable nutrients. *Commun. Soil Sci. Plan.* 23, 2347–2363.
- Sarkar, D., Essington, M.E., Misra, K.C., 1999. Adsorption of mercury(II) by variable charge surfaces of quartz and gibbsite. *Soil Sci. Soc. Am. J.* 63, 1626–1636.
- Schiewer, S., Volesky, B., 2000. *Environmental Microbe-Metal Interactions*. ASM Press, Washington, DC, pp. 329–362.
- Schlüter, K., 1997. Sorption of inorganic mercury and monomethyl mercury in an iron-humus podzol soil of southern Norway studied by batch experiments. *Environ. Geol.* 30, 266–279.
- Uehara, G., Gillman, G.P., 1980. Charge characteristics of soils with variable and permanent charge minerals. I. Theory. *Soil Sci. Soc. Am. J.* 44, 250–252.

Wen, X., Du, Q., Tang, H., 1998. Surface complexation model for heavy metal adsorption on natural sediment. *Environ. Sci. Technol.* 32, 870–875.

Yin, Y., Allen, H.E., Huang, C.P., 1997a. Kinetics of mercury (II) adsorption and desorption on soil. *Environ. Sci. Technol.* 31, 496–503.

Yin, Y., Allen, H.E., Huang, C.P., Sanders, P.F., 1997b. Adsorption/desorption isotherms of Hg(II) by soil. *Soil Sci.* 162, 35–45.

Yin, Y., Allen, H.E., Li, Y., Huang, C.P., Sander, P.F., 1996. Adsorption of mercury (II) by soil: effects of pH, chloride, and organic matter. *J. Environ. Qual.* 25, 837–844.

**Aquifer interactions with a polluted mountain river
of Nicaragua**

Medoza, J. A., Ulriksen, P., Picado, F., and Dahlin, T.

Aquifer interactions with a polluted mountain river of Nicaragua

Jose Alfredo Mendoza,^{1,2*} Peter Ulriksen,² Francisco Picado³ and Torleif Dahlin²

¹ Universidad Nacional Autónoma de Nicaragua - Centro de Investigaciones Geocientíficas Recinto Universitario Rubén Darío Managua, Apdo. Postal E-1 Managua, Nicaragua

² Lund University, Department of Engineering Geology, John Ericsson v1 Lund 22100, Sweden

³ UNAN-Managua - Centro de Investigación en Recursos Acuáticos, Managua, Nicaragua

Abstract:

The interactions between a stream and nearby shallow aquifers were investigated in a mountain basin being polluted by mercury released during mining in central Nicaragua. Hourly data series of water levels and temperatures were analysed using cross-correlation. Resistivity imaging was used to map the subsurface and to complement the hydrological data interpretation. The results show the complex hydrogeological conditions that characterize the region, with weathering and fractured rock as main contributors to groundwater transport. The resistivity images suggest the presence of two vertical dykes perpendicular to the stream, and zones rich in clay. The data series indicate a rapid response from the aquifers to recharge events, followed by immediate discharge on a yearly basis. Furthermore, alternating periods of stream infiltration and aquifer discharge were identified. This work demonstrates that surface water pollution is a threat to groundwater quality in the area. Copyright © 2007 John Wiley & Sons, Ltd.

KEY WORDS time series analysis; resistivity imaging; cross-correlation; surface water; groundwater; pollution; Nicaragua

Received 6 March 2006; Accepted 1 May 2007

INTRODUCTION

Understanding the relationship between surface waters and groundwater is an important task in hydrological sciences. Characterizing this interaction becomes critical as environmental stress on surface waters increases and may be transferred to subsurface waters. Commonly, the interactions occur in the in-stream and near-stream areas where exchange of water and biological processes take place (Sophocleous, 2002). In streams there can be three modes of interaction; gaining flow sections, losing flow sections and steady pressure (Winter *et al.*, 1998). When pollutants are present they may contaminate either resource.

Mining using the mercury method to refine gold has led to continuous contamination of streams in the central region of Nicaragua since the 19th century. The most polluted river is Río Artiguas (known locally as Sucio, meaning dirty), where a cluster of small-scale mills releases mining waste directly into the river water. Thus, the mercury concentrations in the river water are frequently above the guidelines for drinkable water (Silva, 1994; Albuquerque, 1996; Romero, 1996; André *et al.*, 1997). In addition, sewage from the nearby village of Santo Domingo is discharged into the river (Figure 1). An understanding of the connections between the stream waters and the nearby channel aquifers is necessary

because the water supply to the population is provided from sources located close to the polluted streams.

Among the methods for studying stream–aquifer connections, a frequently used approach is the surface water gains–losses method (Lerner, 1997). This method is based on the identification of gain and loss sections along the river channel by estimating the differences in stream flow budgets. Mendoza (2002) used the gains–losses method in the Río Artiguas channel but no conclusive results were obtained because of measurement errors and rapid changes in stream velocities. Additional attempts using seepage meters failed due to the river rocky bed (Grunander and Nordenberg, 2004).

The study of time series data can reveal temporal variations and impulse response characteristics in aquifers (Duffy and Gelhar, 1986; Padilla and Pulido-Bosch, 1995). During the last two decades various studies have shown the applicability of time series analyses for understanding hydrological processes. For instance, time series analyses of piezometric data have been used to identify recharge mechanisms (Lee and Lee, 2000), forecast the water level in wells (Bierkens *et al.*, 2001), study river base flow and estimate groundwater recharge (Zhang and Schilling, 2004; Crosbie *et al.*, 2005). Generally, the measured parameter used for the time series analyses is hydraulic head but electric conductivity and temperature have also been used (Laroque *et al.*, 1998; Sheets *et al.*, 2002; Kim *et al.*, 2005).

Geophysical mapping of the subsurface can provide complementary information on the subsurface geology, which can be used for interpretation of the hydrological

* Correspondence to: Jose Alfredo Mendoza, Universidad Nacional Autónoma de Nicaragua - Centro de Investigaciones Geocientíficas Recinto Universitario Rubén Darío Managua, Apdo. Postal E-1 Managua, Nicaragua. E-mail: alfredo@terrambiente.se; alfredo.mendoza@tg.lth.se

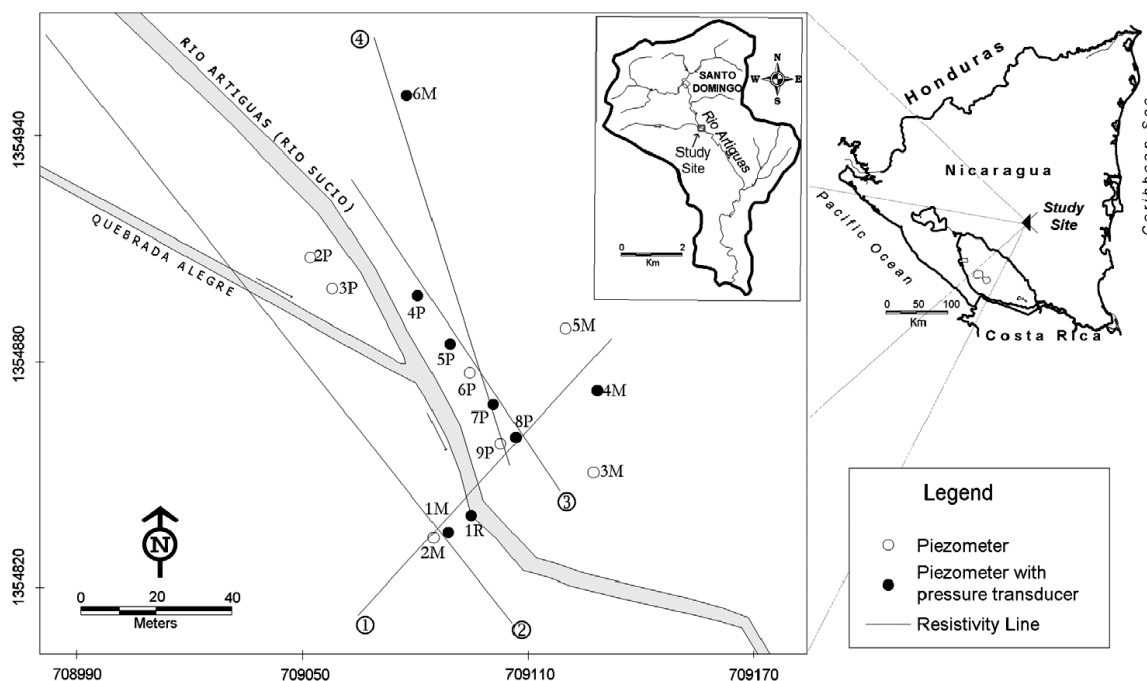


Figure 1. Location of the study site in the Río Artiguas basin (inset), central Nicaragua

data. Resistivity imaging is a suitable method for hydrogeological mapping as the electrical resistivity of earth materials is dependent on electrolytic conduction through the pore fluid. The multi-electrode technique permits the acquisition of large amounts of resistivity data (Dahlin, 1996) and fast inversion methods allow interpretation of the subsurface resistivity distribution (deGroot-Hedlin and Constable, 1990; Ellis and Oldenburg 1994, Loke and Barker, 1996). Recently, resistivity imaging has been used for hydrogeological mapping in the Río Artiguas basin (Mendoza, 2002; Mendoza *et al.*, 2005).

The objective of this study is to examine time series of hydraulic heads and water temperature data in combination with resistivity imaging to determine the factors controlling the shallow groundwater dynamics at the study site. A second objective is to verify if the river water infiltrates the near channel aquifers carrying heavy metals to pollute the local groundwater. This information is important in promoting groundwater protection in the central regions of Nicaragua, where the majority of the population depends on both groundwater and surface water for human consumption. This article presents an application of time series analysis and resistivity imaging to explain a relevant environmental and hydrogeological problem. The work has been developed within the framework of a broad environmental programme funded by the Swedish International Development Agency (Sida/SAREC) with the aim of assessing the environmental effects of mining activity in Nicaragua.

THE RÍO ARTIGUAS BASIN AND THE STUDY SITE

The study site is located in the Río Artiguas basin, in the eastern part of the central highlands of Nicaragua.

The basin has experienced a century of gold mining using the mercury extraction method. A weather station recently installed in the basin reports temperatures with a minimum of 15 °C and maximum of 34 °C, for the period November 2004 to March 2005. Historic average precipitations of 2400 mm year⁻¹ have been recorded in the area by INETER (1991). The rainy season extends for nine months from April to December having a large influence on the river flow, which indicates a discharge from 2×10^4 m³ day⁻¹ during the dry season to 9×10^4 m³ day⁻¹ during the wet season. The young drainage system for surface waters has developed under a structural control where faults, fractures and joints lead to a geometrically rectangular flow pattern.

Geologically, most of the Río Artiguas basin is covered by Tertiary volcanic rocks, mainly basalts and andesitic lava flows. These lava flows overlie rhyolitic-dacitic pyroclastic flows towards the south of the basin (Hodgson, 1972). The quartz veins and tectonic zones, in combination with fracturing and weathering, are considered the major factors contributing to groundwater occurrence and transport. Consequently, the saturated zone is a composite horizon of both weathered layers and fractured bedrock. Mendoza *et al.* (2005) suggested a hydrogeological model for the basin; water infiltrating the weathered nonsaturated zone travels through the saturated zone but quickly discharges in a spring or along the streams. If water infiltrates through open fractures, tectonic contacts or bed contacts, it can travel longer distances and eventually form regional groundwater flows. However, such a hydrogeological model is insufficient to explain the interactions between surface waters and groundwater and a smaller area had to be investigated in detail.

A site in the centre of the basin was selected for this study because it is regarded as a typical tectonic

setting, with fracturing along the river (Hodgson, 1972) and a smooth valley that allowed accessibility and drilling in the otherwise rough relief of the basin. Aerial photographs indicate fracturing perpendicular to the river, and field documentation verified that fractured bedrock underlies, on average, 3 m thick soils. The groundwater table is usually found within 3 m and much of the shallow groundwater is expected to discharge into the river (Mendoza *et al.*, 2004). The Río Artiguas is joined by the generally clean Quebrada Alegre tributary at the site. The area is used for grazing and grass covers a wetland on the east side of the river (Figure 1).

METHODOLOGY

Fourteen piezometers were installed at the site and one level gauge in the river (1R). The piezometers are cased with 6 cm diameter PVC pipe, and in the uppermost part 1-m metal tubes with a lock to prevent theft. The piezometers were packed with a mixture of gravel and clay and the upper part sealed with cement to prevent direct infiltration along the casing. The maximum depth to the fractured bedrock in the piezometers is 2.35 m, occurring at piezometer 6M. The piezometers located closer to the river channel have shallower depth as they reach the bedrock. Most piezometers are located on even terrain but piezometers 6M, 5M and 4M are located on hillsides. The soil at the outer piezometers had more clay loam content, while greater sand content was found in the piezometers closer to the river. The elevations of the piezometers were determined by differential-GPS (global positioning system) measurements. In cases where the GPS observation error was high, traditional levelling was carried out.

Continuous hydraulic head and temperature measurements were taken hourly in eight piezometers, including the gauge height at the river (1R), using pressure transducers from March 2004 until March 2005. Furthermore, piezometer 4M was equipped with an additional barometric pressure transducer for post-processing correction. The pressure transducers were all Van Essen Divers Instruments with 2 mm and 0.01 °C resolution for hydraulic head and temperature, respectively. Daily precipitation data were measured with a standard rain gauge located 800 m from the site and since November 2004 an automatic weather station located 300 m from the site records hourly precipitation. Data were retrieved from the data loggers every three months and occasionally manual measurements were made for data quality checks.

Preparation of the data series for analysis included (a) removing values from occasional perturbations in water levels following slug tests and water sampling, and (b) applying a high-pass filter to remove seasonal trends and DC components from the original data. The analysis of the hydrological data was performed using the cross-correlation function as described by Jenkins and Watts (1968), Padilla and Pulido-Bosch (1995) and Laroque *et al.*, (1998). The cross-correlation function establishes

an interrelationship between an input and an output signal. In this study the river data are considered input signals and the water level fluctuation in the piezometers as output signals. A particular case of cross-correlation is autocorrelation, a function which quantifies the linear dependency of successive values over time. Thus, the autocorrelation function checks the data suitability before a cross-correlation analysis is carried out. The main output of correlation is the correlation coefficient (C), which ranges from -1.0 to $+1.0$. The time at maximum C is the lag time between the input and output signal. A coherence function was applied in cases where relevant cross-correlation was found. The coherence function expresses the linear contribution of an input signal to an output signal and is analogous to cross-correlation in the frequency domain (Padilla and Pulido-Bosch, 1995).

For the geophysical survey, the ABEM Lund Imaging System (Dahlin, 1996) was used to explore the electrical resistivity distribution in the subsurface of the site. The system is based on the automation of collection, processing and presentation of resistivity data. The data collection was performed as 2D resistivity imaging by using a roll-along technique, in which cables are moved upward or downward along a succession of stations. As it was important to get information about the resistivity distribution in the upper subsurface, the minimum electrode spacing was 1 m. A multiple gradient electrode array was used for the measurements, since it has proved to have good resolution capability and to be robust in the field (Dahlin and Zhou, 2004, 2006). Four resistivity lines were performed, line 1 was 100 m, line 2 was 160 m, line 3 was 100 m, and line 4 was 120 m (Figure 1).

Once the resistivity survey was carried out, data processing was performed using the Res2Dinv algorithm (Loke, 1997). Interpretation of the 2D resistivity data was performed using the robust (L_1 -norm) inversion method, which minimizes the absolute differences between measured and calculated apparent resistivity values (Loke *et al.*, 2003). This is an appropriate method for interpreting data from areas where subsurface regions separated by sharp boundaries are expected. Furthermore, a finite element grid was used in the data inversion as inclusion of the topography was necessary for precise relation of the object's position in space along the survey lines.

The hydraulic conductivities of the unsaturated and saturated zones were investigated at a few points of the site using a constant head permeameter (Amoozegar, 1989) and slug tests (Hvorslev, 1951), respectively. The permeability can contribute to the interpretation of the cross-correlation analyses.

To complement the time series data and geophysical survey, chemical analyses of hazardous substances were carried out. Four water samples for bacterial analyses were collected from 1M, Río Artiguas, the river at Quebrada Alegre, and from an old mining gallery that serves as water supply for the village and is located just upstream from the site. It is assumed that high presence of coliform bacteria in groundwater would originate from Río Artiguas as this river is highly contaminated

with sewage. The bacterial analyses were carried out at the National University in Managua (UNAN-Managua). Later, 1M, 3P, 8P and the river were sampled for Hg analyses, which were performed with a Perkin Elmer model Elan 6000 ICP Mass Spectrometer (PerkinElmer, Canada).

RESULTS

The water levels of the river indicate a rapid response to precipitation during most of the monitoring period (March 2004–March 2005) (Figure 2). In general, the hydraulic heads in 5P, 7P, 8P and 1M have a tendency to change together with the river levels (1R). A smaller response is observed at 6M, 4P and 4M. The temperatures also have a similar trend among the piezometers during the period studied, except for 4M and 6M, which present a rather straight curve (Figure 2).

The autocorrelation functions show that the changes in water level at 6M, 4M and 4P occur gradually throughout the period studied (Figure 3). Conversely, the changes in water levels in all the other piezometers and the river take place rapidly, within a lag time of 24 h.

The cross-correlation analyses between the river data and each piezometer are presented in Figure 4. The strongest correlation between hydraulic heads is observed at 8P, which has a correlation coefficient (C) of 0.62, followed by 1M ($C = 0.57$), 7P ($C = 0.50$) and 5P ($C = 0.32$). In contrast, low or weak correlation is found with 6M ($C = 0.06$), 4P ($C = 0.22$) and 4M ($C = 0.09$). In the case of temperatures, cross-correlation is strong in all cases, being highest at 8P ($C = 0.93$) and lowest at 6M ($C = 0.70$). The lag times in level fluctuations at the piezometers located near the river channel are short and positive, except for 4P which precedes the river signal by 64 days (Figure 4). The temperatures at 7P, 4P, 8P, 4M

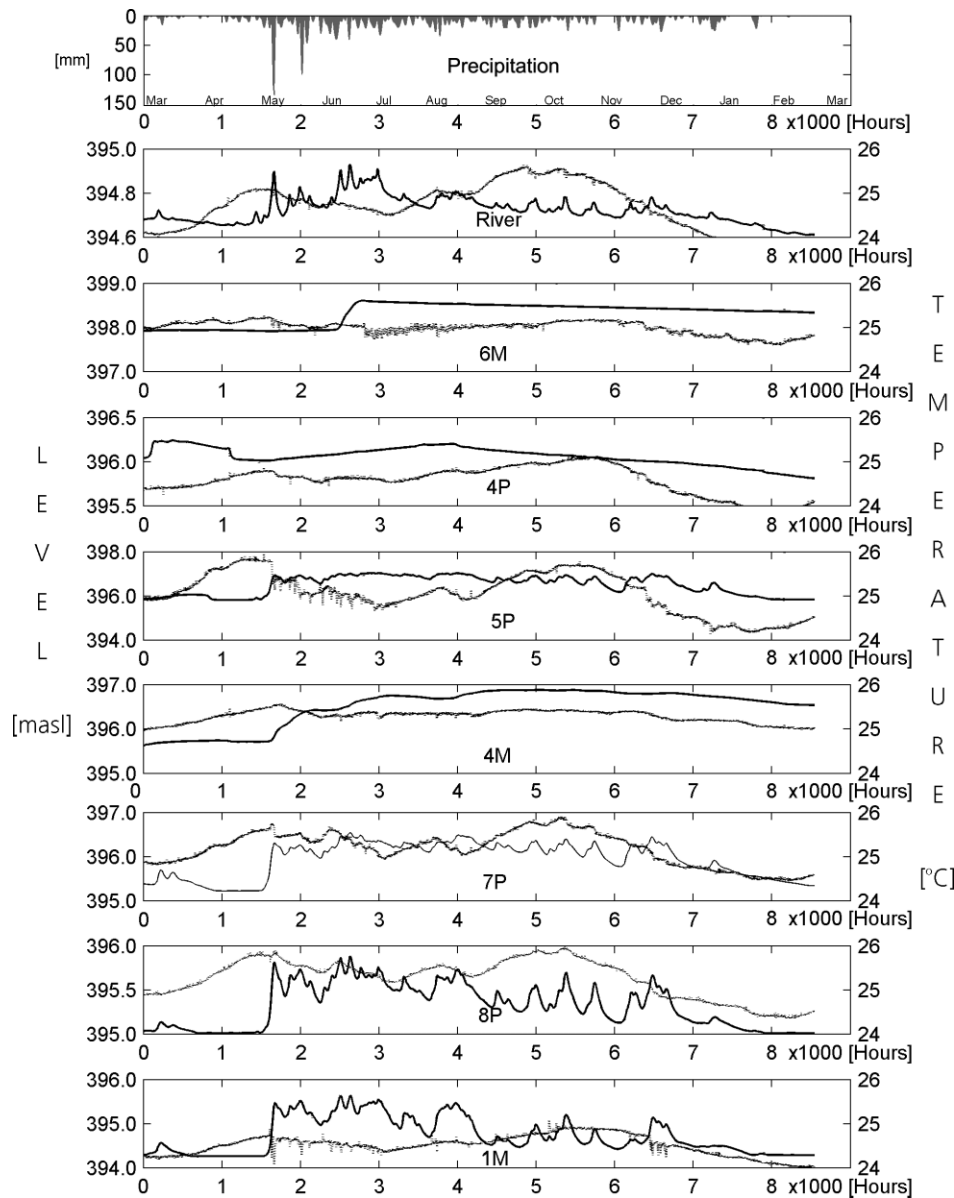


Figure 2. Rainfall, river water and groundwater levels and temperatures measured from March 2004 to March 2005. Continuous lines represent levels and dashed lines represent temperatures

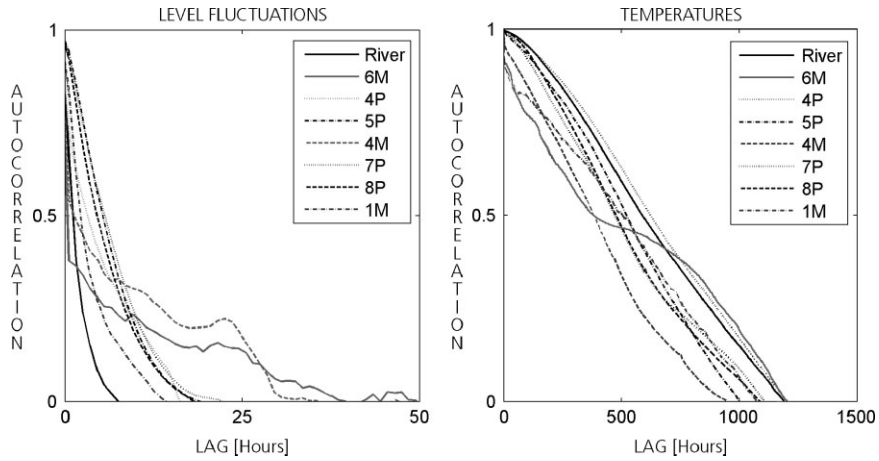


Figure 3. Autocorrelation functions for the groundwater levels (left) and for temperatures (right)

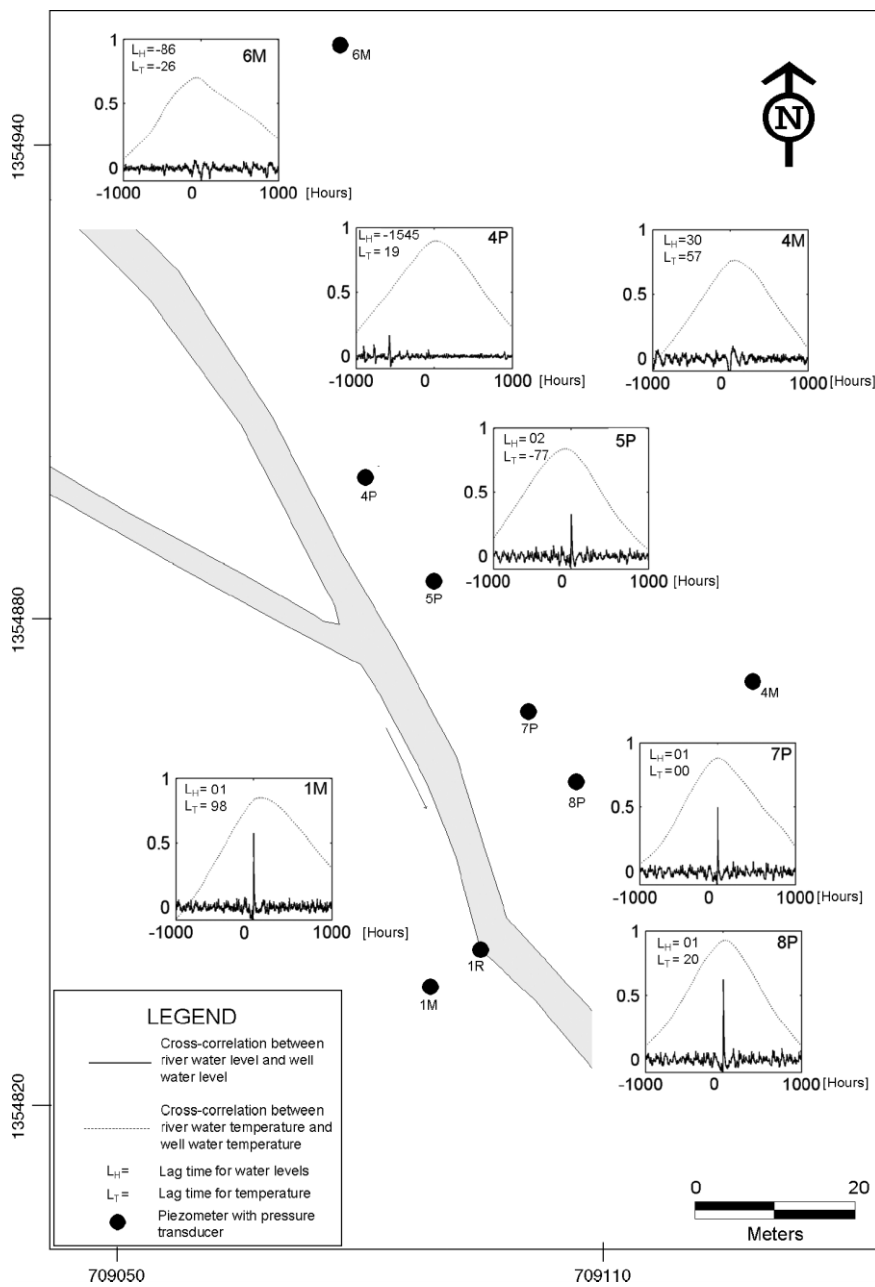


Figure 4. Cross-correlation between river level and each of the monitored piezometers at the site

and 1M lag the temperature in the river, while a negative lag is found for 6M and 5P.

Since the highest cross-correlations were found between the river level and the piezometers situated near the channel, a coherence function was applied to explore the linear connection between those points. The coherence functions shown in Figure 5 indicate that, in general, there is a strong connection between the river levels and piezometers 7P, 9P and 1M at periods of 12 h. Similarly high coherences are found between 7P and 5P, 8P and 1M. However, poor or no coherence was found between the river and 5P and 4M.

Based on the time series data, two scenarios were interpreted for the periods with lowest groundwater level and the periods with higher groundwater level. During the long wet season a clear gradient towards the river is observed (Figure 6a and 6c). During the dry season (January–March 2004) groundwater levels were lower and infiltration from the river to 1M and 2M occurred (Figure 6b and 6c). At the east side of the river, the groundwater gradient does not indicate river intrusion during the dry season.

The inversion results of electrical resistivity surveys are presented in Figure 7. Line 1 was placed crossing Río Artiguas perpendicularly, while lines 2 and 3 were located parallel to the river. Line 2 crosses the tributary stream and line 4 crosses the wetland up to the hillsides. The inversion models indicate the presence of a 3–7 m thick high resistivity top layer ($>160 \Omega\text{m}$) at lines 2

and 1, particularly at the sections where the lines cross the streams. Similarly, high resistivity zones extending vertically are found at the north ends of lines 2 and 4, and at the south side of line 2. Other highly resistive zones appear at the southern extremities of lines 2, 3 and 4. The clay content in a swamp located next to the river has a clear effect, decreasing the resistivity, as shown along the upper zones of line 4 and at the east side of line 1. Deeper low resistivity zones are located below the areas where the lines intersect and at deeper zones below the river beds ($<40 \Omega\text{m}$).

The permeabilities at the site are generally low at the clay-rich vadose zone (upper 1 m), but show an increase at the saturated zone near the river channel (5P, 7P, 8P and 1M). In contrast, permeability tests at the hillsides indicate very low or no measurable permeability (4M, 5M and 6M). Figure 8 shows hydraulic conductivity results obtained at different points along resistivity line 3. Higher permeabilities are found in areas of high electrical resistivity. The hydraulic conductivities of the vadose zone, as estimated with the constant head permeameter, indicate a permeability ranging from $8 \times 10^{-8} \text{ m s}^{-1}$ in the proximity of 5P to 10^{-5} m s^{-1} at the southern extremity of resistivity line 3. A test performed next to 5M show a permeability of 10^{-6} m s^{-1} at that side of the wetland. The slug tests performed in the piezometers indicate permeabilities ranging from $2 \times 10^{-5} \text{ m s}^{-1}$ at 5P to 10^{-4} m s^{-1} at 8P. The estimated permeability at 1M was $5 \times 10^{-6} \text{ m s}^{-1}$.

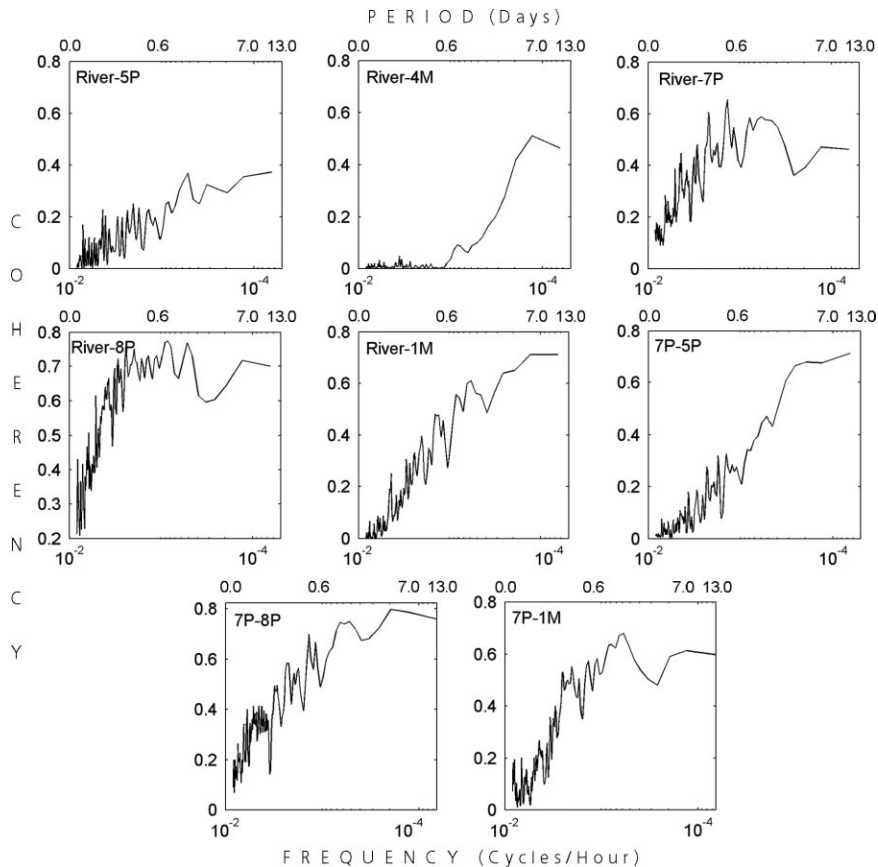


Figure 5. Coherence functions between river and nearest piezometers and between 7P and nearest piezometers

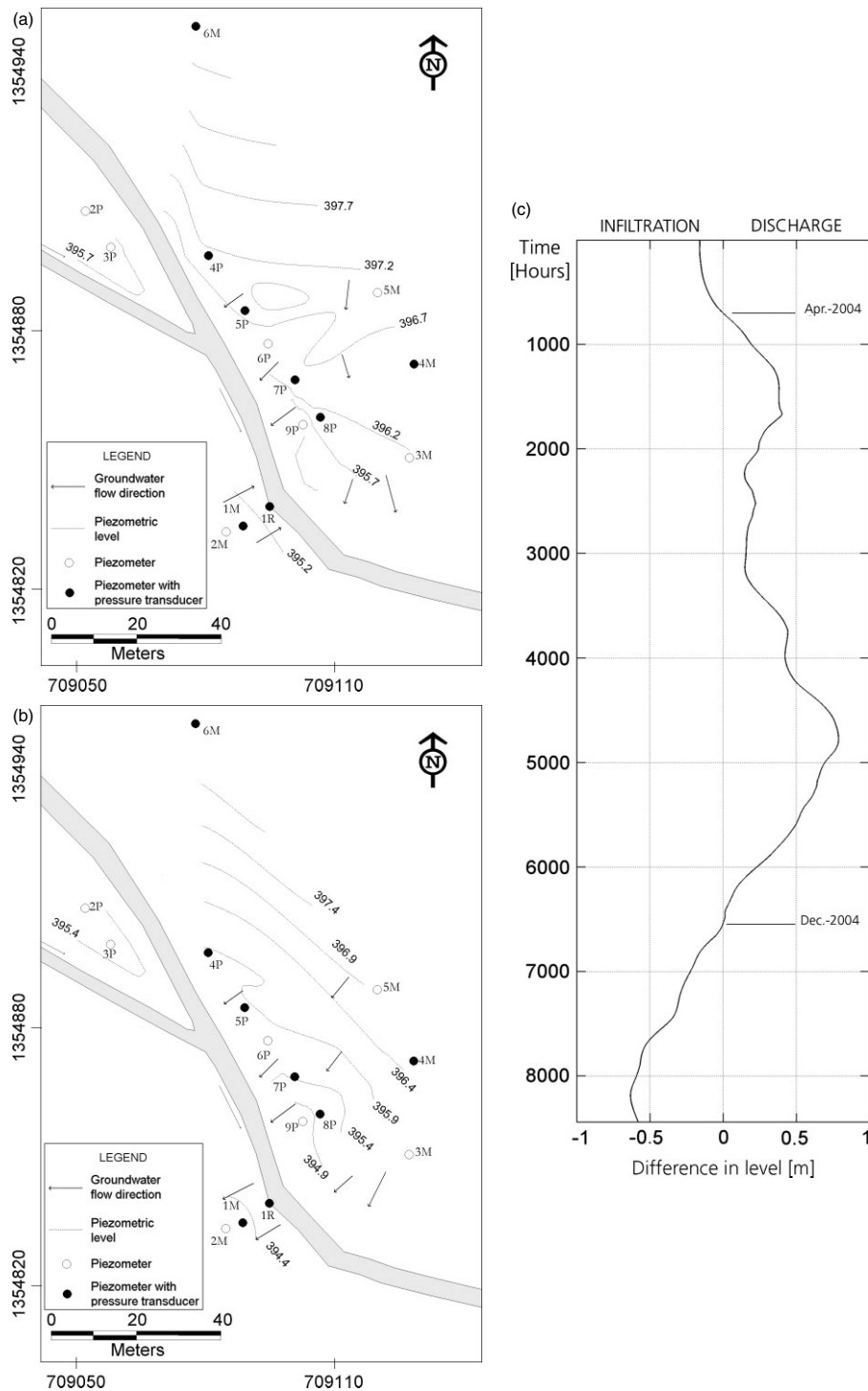


Figure 6. Groundwater table (a) period of highest hydraulic heads and (b) period of lowest hydraulic heads and (c) periods of infiltration from the river and discharge to the river as observed at 1M

Bacterial analyses show a low number of *Escherichia coli* in the main source of drinking water for Santo Domingo (300 bacterial per 100 mL), which it is not a health concern. However, in the Río Artiguas a high concentration of bacteria was found (10^4 – 10^5 bacterial per 100 mL). Moreover, an important concentration of *Escherichia coli* was detected at 2M ($\sim 10^3$ bacteria per 100 mL). Detectable mercury concentrations were found in water samples from the piezometers and the river, the highest value was found at 1M ($0.11 \mu\text{g L}^{-1}$), followed

by the river ($0.04 \mu\text{g L}^{-1}$), 8P ($0.03 \mu\text{g L}^{-1}$) and 3P ($0.01 \mu\text{g L}^{-1}$).

DISCUSSION

The river water level is strongly influenced by the heavy precipitation regime that characterizes the basin. Additionally, the groundwater level fluctuations appear to be controlled by rapid infiltration following rainfall.

This strong link between changes in the river level and groundwater table fluctuation suggests a seasonal character of the shallow aquifers. In the areas near the hillsides (6M and 4M) groundwater fluctuations are less influenced by infiltration, probably due to a high clay content, which also contributes to the formation of the wetland. In contrast, the relatively high cross-correlation ($>C = 0.32$) found in all piezometers located next to the river channel denotes faster infiltration and transport of water through the fractured rock. However, considering the short distance between piezometers and the low cross-correlation found at 4P ($C = 0.22$), high spatial variability of the hydraulic properties should be expected in the area. Moreover, the coherence functions indicate

a marked connection in the frequency domain between fluctuations at the south side of the site (1R-7P-8P-1M), but this strong relationship is not present between the piezometers elsewhere. The strong cross-correlation of temperatures found in all cases reflects the similar origin of river water and groundwater.

The high variability of hydraulic properties at the site is also supported by the electrical resistivity surveys. The resistivity response from the top areas varies from high resistivity zones ($>160 \Omega\text{m}$) associated with coarse-grain material and hard rock to the low resistivity zones rich in clay ($<40 \Omega\text{m}$) (Figures 7 and 8). There are strong lateral variations in the resistivity over short distances, which indicate intense vertical fracturing. Furthermore,

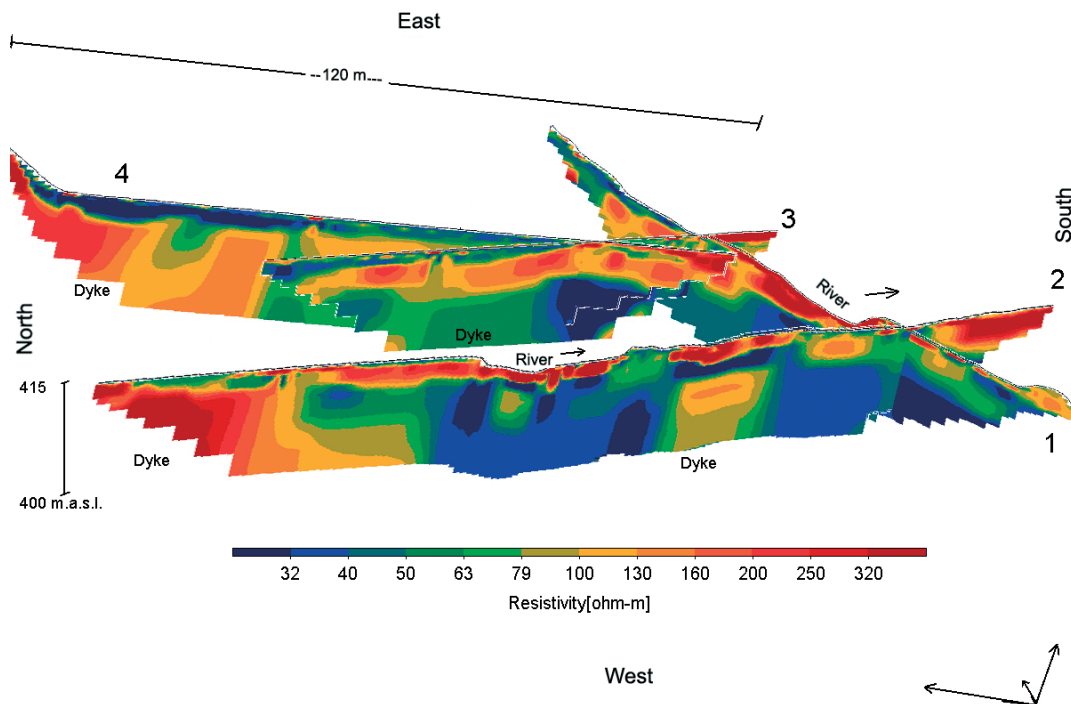


Figure 7. Electrical resistivity images

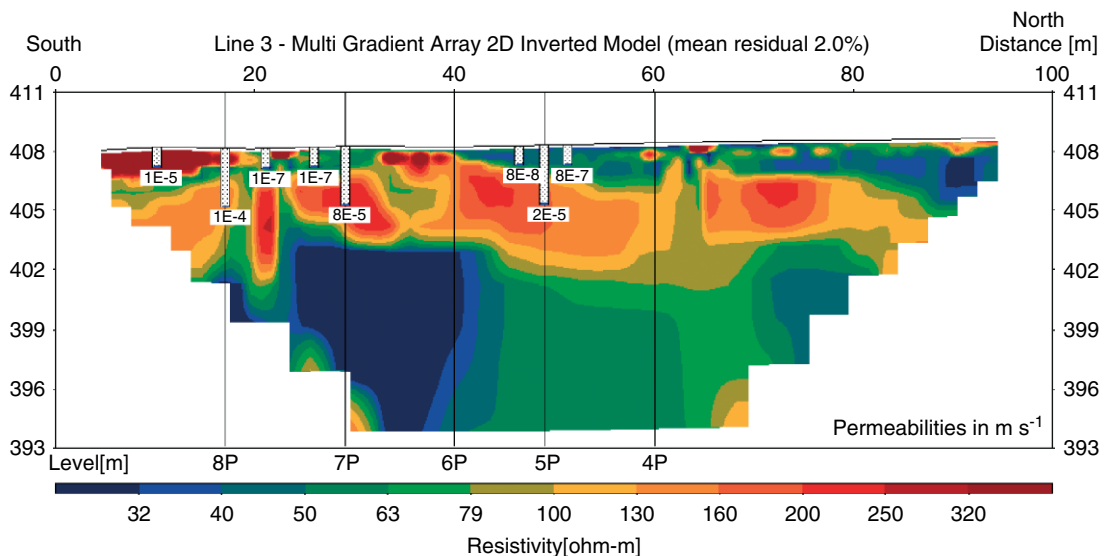


Figure 8. Electrical resistivity image of line 3 including values from permeability tests

previous aerial photointerpretation, field documentation and geophysical surveys in the basin (Mendoza, 2002) suggest that the vertical zones of high resistivity present in the resistivity images of lines 2, 3 and 4 might be associated with two basaltic dykes crossing the river.

Zones of discharge near the channel of the river cannot be interpreted from the resistivity images. Nevertheless, areas with high resistivity values associated with bedrock were observed near the channel in line 1. This may be an indicator that discharge to the river does not occur through sediments but through fractures in the bedrock.

Regarding the groundwater table, there was a hydraulic gradient towards the river for most of the monitoring period. This gradient is maintained by the heavy precipitation and expected high infiltration rate. However, as the rain season finished the hydraulic gradient changed on the west side of the river, allowing river water infiltration (Figure 6). The topographically controlled hydraulic gradient on the north-east side of the river permitted a continuous flow to the south-west during the short dry season. This situation explains the bacterial concentrations in 2M, similar to the concentration found in the river water. The Hg concentrations found in 1M are higher than in 3P and the piezometers located on the other side of the river channel.

The interpretation of hydraulic data and resistivity imaging is supported by the hydraulic conductivities estimated at different points of the site. Higher permeability was found at 8P, which also presents higher cross-correlation (Figure 4). The top layers commonly have lower hydraulic conductivities due to the higher clay content, but there may be an increase when reaching the fractured rock at depth and close to the fractured dykes.

In general, these results are in agreement with the findings of Mendoza *et al.* (2005), who suggested that there is rapid groundwater circulation through the basin. From these local groundwater systems water travels relatively fast when moving through joints and fractures until discharging into the river. When precipitation decreases, the situation could be the inverse, with channel water infiltrating the nearby shallow aquifers.

CONCLUSIONS

This paper has shown that rainfall infiltration is the main factor controlling the shallow groundwater dynamics in the near channel aquifers along the Río Artiguas river. Cross-correlation analyses of river levels against hydraulic heads revealed a rapid response of the groundwater table to river infiltration and direct recharge. The piezometers located far from the river channel showed poor correlation with the river, indicating a lack of contact with the nearby groundwater. This may be caused by the high clay content found at those areas, as interpreted from the electrical resistivity images. Less weathered or fresh rock is related to the deeper high resistivity zones, where flow through fractures may be of major hydrogeological significance.

The high bacteria concentrations found in the river and in the groundwater at 2M confirm that there is a connection between the river and the adjacent shallow aquifers. This is also supported by the hydraulic heads, which suggests that most of the river infiltration to aquifers occurs during the dry season. However, the frequent river floods can also spread the pollutants to the nearby aquifers.

The results presented here showing the exposure of groundwater systems to pollution in basins characterized by fractured media, such as the highlands of Nicaragua, are a major concern. In this case, waste disposal in surface water can also lead to direct pollution of groundwater. The seasonal character of the aquifers suggests limited availability of groundwater resources, as they seem to depend on recent recharge. Further research could be aimed at characterizing the recharge and discharge processes throughout the river basin, which can increase the understanding of groundwater–surface water relationships.

ACKNOWLEDGMENTS

This work was conducted as part of a multidisciplinary research programme funded by the Swedish International Development Agency (Sida/SAREC). Technical and logistical support was provided by the Department of Engineering Geology at Lund University (Sweden) and Centro de Investigaciones Geocientíficas at UNAN-Managua, respectively. Professor Göran Bengtsson suggested valuable ideas for the study. Kjell Andersson assisted in the piezometers installation and Tommy Olsson carried out the mercury analyses at the Department of Ecology, Lund University. Jonas Hedberg installed the meteorological station and Marvin Corriols retrieved divers' data. Family Duarte is specially acknowledged as their assistance made fieldwork less difficult under the tropical conditions at Río Artiguas. Suggestions by an anonymous reviewer helped to improve the manuscript.

REFERENCES

- Albuquerque N. 1996. Estudio de Impacto Ambiental. [Environmental Impact Study] Empresa Asociativa de Pequeños Mineros de SD Chontales.
- Amoozegar A. 1989. A compact constant-head permeameter for measuring saturated hydraulic conductivity of the vadose zone. *Soil Science Society of America Journal* **53**: 1356–1361.
- André L, Rosén K, Torstendahl J. 1997. *Minor field study of mercury and lead pollution from gold refining in Central Nicaragua*. MSc thesis, ISBN 1402–1617. Luleå University of Technology, Sweden.
- Aronsson M, Wallner C. 2002. *Inventory of springs and hydrochemical investigations of groundwater in the drainage basin of Sucio river, Nicaragua*. MSc thesis, ISRN LUTVDG/TVTGTG–5078–SE. Lund University, Sweden.
- Bierkens MFP, Knotters M, Hoogland T. 2001. Space-time modeling of water table depth using a regionalized time series model and the Kalman filter. *Water Resources Research* **37**: 1277–1290.
- Crosbie RS, Binning P, Kalma JD. 2005. A time series approach to inferring groundwater recharge using the water table fluctuation method. *Water Resources Research* **41**(1): W01008. DOI:10.1029/2004WR003077.
- Dahlin T. 1996. 2D resistivity surveying for environmental and engineering applications. *First Break* **14**(7): 275–283.

- Dahlin T, Zhou B. 2004. A numerical comparison of 2D resistivity imaging with 10 electrode arrays. *Geophysical Prospecting* **52**: 379–398.
- Dahlin T, Zhou B. 2006. Gradient array measurements for multi-channel 2D resistivity imaging. *Near Surface Geophysics* **4**: 113–123.
- deGroot-Hedlin C, Constable S. 1990. Occam's inversion to generate smooth, two-dimensional models from magnetotelluric data. *Geophysics* **55**: 1613–1624.
- Duffy CJ, Gelhar LW. 1986. A frequency domain analysis of groundwater quality fluctuations: interpretation of field data. *Water Resources Research* **22**: 1115–1128.
- Ellis RG, Oldenburg DW. 1994. Applied geophysical inversion. *Geophysical Journal International* **116**: 5–11.
- Grunander K, Nordenberg L. 2004. *Investigation of groundwater—surface water interaction in the drainage basin of the River Sucio, Nicaragua*. MSc thesis, ISRN LUTVDG/TVTG–5090–SE. Lund University, Sweden.
- Hodgson G. 1972. Geological map of La Libertad, Catastro e Inventario de Recursos Naturales: Nicaragua.
- Hvorslev MJ. 1951. Time lag and soil permeability in ground water observations. Waterways Experimental Station, Corps of Engineers, US Army, Bulletin no. 36.
- INETER. 1991. Anuarios Meteorológicos (1990, 1991) [meteorological charts] Catastro e Inventario de Recursos Naturales: Nicaragua.
- Jenkins GM, Watts DG. 1968. *Spectral Analysis and its Applications*. Holden-Day series in time series analysis: San Francisco.
- Kim JH, Lee J, Cheong TJ, Kim RH, Koh DC, Ryu JS, Chang HW. 2005. Use of time series analysis for the identification of tidal effect on groundwater in the coastal area of Kimje, Korea. *Journal of Hydrology* **300**(1–4): 188–198.
- Larocque M, Mangin A, Razack M, Banton O. 1998. Contribution of correlation and spectral analyses to the regional study of a large karst aquifer (Charente, France). *Journal of Hydrology* **205**(3–4): 217–231.
- Lee JY, Lee KK. 2000. Use of hydrologic time series data for identification of recharge mechanism in a fractured bedrock aquifer system. *Journal of Hydrology* **229**: 190–201.
- Lerner DN. 1997. Groundwater recharge. In *Geochemical Processes, Weathering and Groundwater Recharge in Catchments*, Saether OM, deCaritat P (eds) AA Balkema: Rotterdam, Holland; 109–150.
- Loke MH, Barker RD. 1996. Rapid least-squares inversion of apparent resistivity pseudosections by a quasi-Newton method. *Geophysical Prospecting*, **44**(1): 131–152.
- Loke MH. 1997. Rapid 2D resistivity inversion using the least squares method, Manual for RES2DINV, Geoelectrical Imaging 2D and 3D.
- Mendoza JA. 2002. *Geophysical and hydrogeological investigations in the Rio Sucio watershed, Nicaragua*. Lic Thesis, ISBN 91-972406-0-X. Lund University, Sweden.
- Mendoza JA, Dahlin T, Barmen G. 2004. Use of resistivity imaging in a surface water—groundwater interactions study, Proc. XXXIII Congress IAH—7° ALHSUD 11–15 October, 2004, Zacatecas City, Mexico.
- Mendoza JA, Dahlin T, Barmen G. 2006. Hydrogeological and hydrochemical features of an area polluted by heavy metals in central Nicaragua. *Hydrogeology Journal* **14**: 777–784.
- Padilla A, Pulido-Bosch A. 1995. Study of hydrographs of karstic aquifers by means of correlation and cross-spectral analysis. *Journal of Hydrology* **168**(1–4): 73–89.
- Romero F. 1996. Contaminación de Hg y Pb en fuentes de agua. area de Santo Domingo, Chontales [Hg and Pb contamination in water wells], Centro de Investigaciones Geocientíficas: Managua, Nicaragua; 21.
- Sheets RA, Darner RA, Whiteberry BL. 2002. Lag times of bank infiltration at a well field, Cincinnati, Ohio, USA. *Journal of Hydrology* **266**: 162–174.
- Silva G. 1994. Diagnóstico da contaminação ambiental gerada pela atividade minerária sobre os rios Súcio, Mico e Sinecapa, Nicaragua [Diagnose of the contamination caused by the mining activity in the rivers Sucio, Mico and Sinecapa, Nicaragua]. Universidade Federal do Pará Centro de Geociências Curso de Pós-graduação, Belem, Brasil.
- Sophocleous M. 2002. Interactions between groundwater and surface water: the state of the science. *Hydrogeology Journal* **10**: 52–67.
- Winter TC. 1999. Relation of streams, lakes, and wetlands to groundwater flow systems. *Hydrogeology Journal* **7**: 28–45.
- Winter TC, Harvey JW, Franke OL, Alley WM. 1998. Ground water and surface water—a single resource. US Geological Survey Circular 1139, Denver, USA.
- Zhang YK, Schilling K. 2004. Temporal scaling of hydraulic head and river base flow and its implication for groundwater recharge. *Water Resources Research* **40**(3): W03504. DOI:10.1029/2003WR002094.

**A methodology for bi-directional measurement of
flux at the Groundwater- river water interface in
turbulent and rocky streams**

Enfield C., Bengtsson G., Picado P. F., and Mendoza A.

A methodology for bi-directional measurement of flux at the groundwater-river water interface in turbulent and rocky streams

Carl Enfield^a, Francisco Picado^{b,c}, Alfredo Mendoza^{d,c} and Göran Bengtsson^b

^aSchool of Civil Engineering, Purdue University, West Lafayette, IN 47907, USA

^bDepartment of Ecology, Lund University, Sölvegatan 37, SE-223 62 Lund, Sweden

^cUniversidad Nacional Autónoma de Nicaragua, Apartado Postal 663, Managua, Nicaragua

^dDepartment of Engineering Geology, Lund University, John Ericsson v1 221 00 Lund, Sweden

Abstract

We developed a methodology for the measurement of bi-directional flow and flux of water across the interface between groundwater and surface water in rivers with turbulent water and rocky sediment. The interfacial seepage meter consists of a flanged cylinder, a flow tube that allows water to flow in or out of the cylinder at a rate equal to the specific discharge across the sediment-water boundary, and a computerized data collection and analysis system. The cylinder was pushed into the sediment, and sandbags were placed on the flange to create a seal. The pressure head difference between inside the cylinder and outside caused by turbulent stream water was measured and the cylinder rotated to remove the potential Venturi/Bernoulli effect. A heat-pulse method was used to measure flow by heating the centre of the flow tube for a brief time period and measuring the temperature profile within the tube over time. The system was calibrated to measure volumetric flux in the range 0.35-8.4 cm d⁻¹, but by using a flow addition method, the measurement of lower velocities was accomplished. The methodology was tested in Sucio river in the central mountain region of Nicaragua. The river is lined with gold mining activities in its upstream parts, and sediment, river water and groundwater is contaminated with mercury from gold amalgamation. The measured groundwater flow rate was ranged from < 1 and 15.1 mL/min. The methodology promises to be useful in describing the distribution of upwelling and downwelling areas of the river, which can be applied to develop a pattern for mercury transport along the river and across the boundary to the groundwater.

Introduction

Understanding and quantifying ground water/surface water interactions is difficult but necessary in e.g. the assessment of treatment wetlands, salt-water intrusion in coastal aquifers, and transport and fate of anthropogenic chemicals discharging into groundwater or surface water from contaminated sediments. Gases and dissolved and suspended material flowing across the

sediment-water boundary affect the distribution and activity of organisms in the hyporheic zone (Williams 1993, Brunke and Gonser 1997), and hydrochemical and metabolic processes within the hyporheic zone have a profound effect on the biogeochemical exchange between surface water and groundwater (Winter 1999, Sophocleous 2002). A key parameter in this exchange is the flow or flux of water, and a variety of techniques and equipment has been

used to estimate its direction and magnitude.

The first field effort to measure the water flux was conducted by Lee (1977) using seepage meters coupled with measurement of the hydraulic gradient through the sediment to determine the flux of nitrogen and phosphate into a lake from groundwater. The equipment consisted of a submerged flat-topped cylinder, connected to a piece of tubing and a thin plastic film collection bag. The water flux is calculated by measuring the change in weight of the bag after some time has elapsed (Lee and Cherry 1978). Water flux measurement made with this method, however, can be highly variable, and concerns have been raised about the transient effects of meter installation on flows through the lakebed (Shaw and Prepas 1989), head loss related to the ratio of meter diameter to tubing diameter (Fellows and Brezonik 1980; Belanger and Montgomery 1992), and errors associated with bag type (Schincariol and McNeil 2002), and deformation of the bag (Landon et al. 2001, Murdoch and Kelly 2003). Nevertheless, numerous field and laboratory studies have demonstrated these devices can yield accurate data provided adequate care is taken in making measurements and proper calibration coefficients are applied.

Several researches have modified the original approach of Lee by replacing the sampling bag with a flow meter, which permits near continuous measurements. The approaches include heat pulse methods (Taniguchi and Fukuo 1993), ultrasonic methods (Paulsen et al. 2001), electromagnetic flow meters (Rosenberry and Morin 2004), and dye dilution approaches (Sholkovitz et al. 2003). The heat pulse methods measures the rate of advective heat transport within a flow tube connected to a chamber. Other techniques use temperature profiles in the

hyporheic zone (Lapham 1989, Constantz and Thomas 1996) and tracer tests (Lee et al. 1980, Cook et al. 2006).

Data from numerous investigations where seepage meters were used indicate that flux through a lakebed commonly varies over three orders of magnitude and can vary by as much as five orders of magnitude. The spatial variability in seepage can be considerable, even on a scale of only a few metres (Shaw and Prepas 1990). A great variability in hydraulic exchange is also observed for streambeds (Keery et al. 2007, Mendoza et al. 2008), and areas of predominantly down-welling and up-welling flow may replace each other within short distances in a river basin. Such a variability will have implications on the transport and fate of contaminants in a river, and down-welling areas may become sources of groundwater contamination, and up-welling areas may represent sources of dilution of bulk river water concentrations or sources of contaminants desorbing from the streambed.

Sucio river is a small river, historically exposed to gold mining activities in the St Domingo district in the central mountain region of Nicaragua. The river basin covers nearly 28 km², and the mean precipitation is about 2400 mm yr⁻¹. The river drains towards the southwest, and its flow increases downstream due to water inflow from several small streams and probably groundwater discharge. Miners still use mercury in the gold enrichment process. The amalgamation sites are located along the river at a distance of some few metres from the shore, because the river water is used to recover the gold. Residues of mercury are discharged into the river and found in the river water, groundwater, and sediment (papers I, II, VI). The fate of mercury in the river would be better understood if the heterogeneity in

seepage flux could be estimated and integrated in a transport model.

Therefore we developed a method of measuring the bi-directional flux of water at the sediment interface and designed a seepage meter that utilize the basic heat-pulse technique which is responsive to low water flows, in the range from less than 1 cm/day to as much as 20 cm/day. In its basic design, the seepage meter was constructed to be pushed into soft sediments, but since the upstream parts of Sucio river have sediments made up mainly from rock, stones and gravels, we made a construction option for such condition. The objectives for the measurements was to test whether this new seepage meter could collect reliable data on the seepage flux in a normally shallow river with hard-bottom sediment, low hydraulic conductivities, and with possibilities for both upwelling and downwelling flows.

Materials and methods

Flow meter design

We designed two different setups of the seepage meter system. The first one was a two-piece chamber, consisting of a dome that attached to an open cylinder allowing intermittent measurements to be made at the same location by leaving the cylinder in the sediment between the measurements, the flow tube and vent, circuit board, and computer (Fig. 1). The sealed dome also eliminates the problem of changing hydraulic head in the water body, e.g. after a storm event, but if there is gas production in the sediment, it would be measured as water flow until sufficient gas accumulates in the dome to cause gas flow through the sensor. A gas vent minimizes the gas problem, which shows up as noise in the data rather than having a consistent pattern. The cylinder was a HDPE-cylindrical tank (55.9 cm outside diameter (OD), and 0.64 cm wall

thickness) from Cole-Parmer (Vernon Hills, IL) cut 25.4 cm below the rim. The rim extends 2.54 cm out and 3.18 cm up, providing a 61.0 cm OD flange with a 2.54 cm rim on which the dome is attached. The dome was stainless steel and has an OD of 57.5 cm, is 19.1 cm high, and a volume of 28.4 L. The gas vent was a 1.27-cm diameter PVC pipe attached to the top of the dome with a bulk-head flange and of sufficient length to extend above the water surface, allowing gas to escape and water to rise within the pipe to the river's water table level. Once the cylinder is pushed into the sediment, four stainless steel cables, connected to the outside of the cylinder, are connected to the pipe at a location above the water surface, holding the dome onto the cylinder. Closed-cell polyurethane foam, attached to the rim of the dome ensures a watertight seal.

Within the dome is a 1.27-cm inside diameter (ID) by 33.0-cm long Teflon made "flow tube" that has a heating element and thermocouple located at its midpoint, and two thermocouples located on each side of the midpoint. One end of the tube is open within the dome and the other end is open to the river through a bulkhead fitting on the dome. This allows water to flow between the river and the inside of the dome at a volumetric rate equal to the rate across the sediment-water interface. In operation, the heating element is activated for 3 s, increasing the temperature measured at the thermocouple next to the heating element by approximately 1 °C, raising the local water temperature within the tube.

The heat flow is controlled by two primary components. At low flow rates, the predominate components is heat conduction through the media. At high flow rates the primary component is advective flow of the water. As water flows through the tube, the four

thermocouples positioned within the tube at different positions sense the temperature change as a function of time. When flow is low, much of the energy is lost to the surrounding environment. For this reason, one of the pairs of thermocouples is placed close to heat sensor and is the detector used under low flow conditions. The volumetric flow rate in the tube is calculated from the temperature-time profile measured by the two thermocouples downstream from the heater, as described later. The differential temperature at each thermocouple is determined via the potential difference with a thermocouple reference junction co-located with a linear temperature measuring integrated circuit used to measure the absolute temperature outside and away from the flow tube. The micro volt-level thermocouple signals are amplified using precision instrumentation amplifiers, housed within a 7.0 cm OD cylinder that surrounds the flow tube and is filled with an epoxy resin that acts as a heat insulator and water barrier. The signals are transmitted through a shielded 12 conductor cable to a PC-interface. The PC-interface includes a PMD-1608FS I/O Module (Measurement Computing Cooperation, Middleboro, MA) to convert the analog data to digital data, protection circuitry, and switching logic used to operate the heater through the PMD-1608FS I/O Module. Data are collected simultaneously from the 6 data channels (5 thermocouples and the reference junction temperature) and

transferred to the computer through a USB port. The heat pulse and data acquisition are controlled by a computer program encoded in SoftWire® (Measuring Computing Cooperation, Middleboro, MA) that allows for data transfer directly into Excel files. Data are displayed and plotted with only a 3 s delay. The flux measurement approach has a set of tradeoffs related to heat losses, noise that is reflected in error of temperature measurement and precision in determining how fast the heat pulse is travelling. Laboratory analysis of the measurement system indicates that the noise on any given data channel is approximately ± 0.02 °C.

The second setup was an open cylinder (Fig. 2) that had one end penetrating the sediment water interface and the other end penetrating the water air interface. The potential shortcoming of this method of measurement is when the water table is changing, as would be the case during heavy rain. To correct for this error, a pressure transducer would be needed to monitor the head within the dome during measurements. The cylinder was made from a commercial water pipe purchased at the local market in Managua. It was made from high-density polyethylene (HDPE), the diameter was 74 cm and the height was 1100 cm. The flow tube was attached to an opening in the cylinder wall by a bulkhead fitting on, and the other end of the tube was kept horizontal within the cylinder by chains attached to hooks in the cylinder wall.

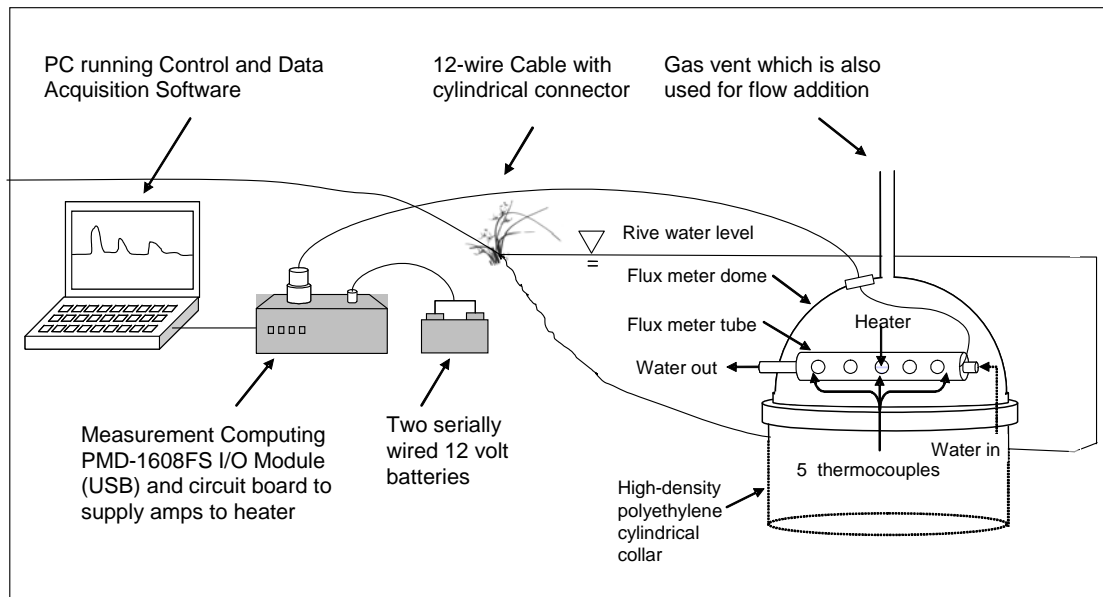


Figure 1. Components of the seepage meter with a dome attached to a cylinder.



Figure 2. Open cylinder used to measure flow across the river sediment. Blocks are placed on top of sandbags resting on a tire inner tube placed around the cylinder to seal it to the bottom. The installation is adjusted to minimize the Venturi/Bernoulli effect anticipated under the turbulent river flow conditions.

Flow calibration

A calibration curve relating the volumetric flow rate (Q) to the time at which the maximum temperature occurs (T_m) at each thermocouple was constructed from measurements in the laboratory at specific flow rates (Table 1, Fig. 4), controlled by a low flow peristaltic pump (REGLO-DIGITAL, ISMATEC 6 channel pump, Switzerland). For each measurement in the lab and in the field, the heater was activated for 3 s with 19 W, recording the temperature change at all five channels at a data acquisition rate of 1000 samples per s per channel. The calibration of the two-parts chamber was made with flows ranging from 1 to 25 mL min⁻¹, and since the volumetric flow rates measured in the field were low, only the data from the thermocouple closest to the heater on the downstream side were used in the calculations (Fig. 4). The specific discharge (q , cm d⁻¹) was calculated by dividing Q by the cross sectional area of the cylinder placed in the sediment, A (cm²). Because the cylinder's area is 4,301 cm², the calibration curve for the

two-parts chamber spans specific discharge values of 0.35 to 8.4 cm d⁻¹.

The equation to calculate the water flow (mL min⁻¹)

$$Q = \frac{C_1 - M \times C_3}{M + C_2}$$

Where:

Q is the water flow through the measurement transducer (ml/min)

M is the measured normalized first moment (seconds)

C₁ is a constant related to the distance from heat source and the cross sectional area of the pipe

C₂ is a constant related to the cross sectional area and the conductive velocity

C₃ is constant related to delay in heat entering the flow path

Table 1. First moment analysis and estimated and measured flows

Flow rate (ml/min)	First moment			Flow (ml/min)				Constants		
	Average	STD	CV	Estimated	Measured	Error	SQE	C ₁	C ₂	C ₃
Channel 0										
1.2	324.8	14.7	0.05	3.9	1.2	-2.75	7.55	1778.612	-59.2314	2.248488
2.6	491.8	13.6	0.03	1.6	2.6	1.04	1.09			
5.4	315.7	2.9	0.01	4.2	5.4	1.23	1.52			
9.1	207.1	3.5	0.02	8.9	9.1	0.22	0.05			
13.3	167.5	6.3	0.04	12.9	13.3	0.35	0.12			
23.6	122.6	4.8	0.04	23.7	23.6	-0.10	0.01			
Channel 1										
	392.7	20.7	0.05	2.1	1.2	-0.95	0.89	1128.846	-68.0335	1.101059
	423.8	24.5	0.06	1.9	2.6	0.74	0.55			
	237.5	2.3	0.01	5.1	5.4	0.28	0.08			
	171.4	1.6	0.01	9.1	9.1	0.00	0.00			
	140.7	6.1	0.04	13.4	13.3	-0.10	0.01			
	110.7	30.0	0.27	23.6	23.6	0.02	0.00			
Channel 3										
-1.2	490.4	31.2	0.06	-1.5	-1.2	0.32	0.10	-3259.85	21.54527	-5.05757
-2.6	430.7	8.8	0.02	-2.4	-2.6	-0.21	0.04			
-5.0	328.9	16.7	0.05	-4.6	-5.0	-0.44	0.20			
-10.0	181.3	6.2	0.03	-11.6	-10.0	1.55	2.41			
-15.0	158.1	9.5	0.06	-13.7	-15.0	-1.30	1.69			
-24.2	93.3	6.5	0.07	-24.3	-24.2	0.08	0.01			
Channel 4										
	419.8	25.8	0.06	-3.1	-1.2	1.86	3.46	-2073.77	-50.0576	-2.24431
	507.9	10.6	0.02	-2.0	-2.6	-0.56	0.31			
	390.8	23.1	0.06	-3.5	-5.0	-1.49	2.22			
	192.5	1.9	0.01	-11.5	-10.0	1.52	2.32			
	174.2	3.4	0.02	-13.6	-15.0	-1.45	2.10			
	123.9	2.4	0.02	-24.3	-24.2	0.11	0.01			

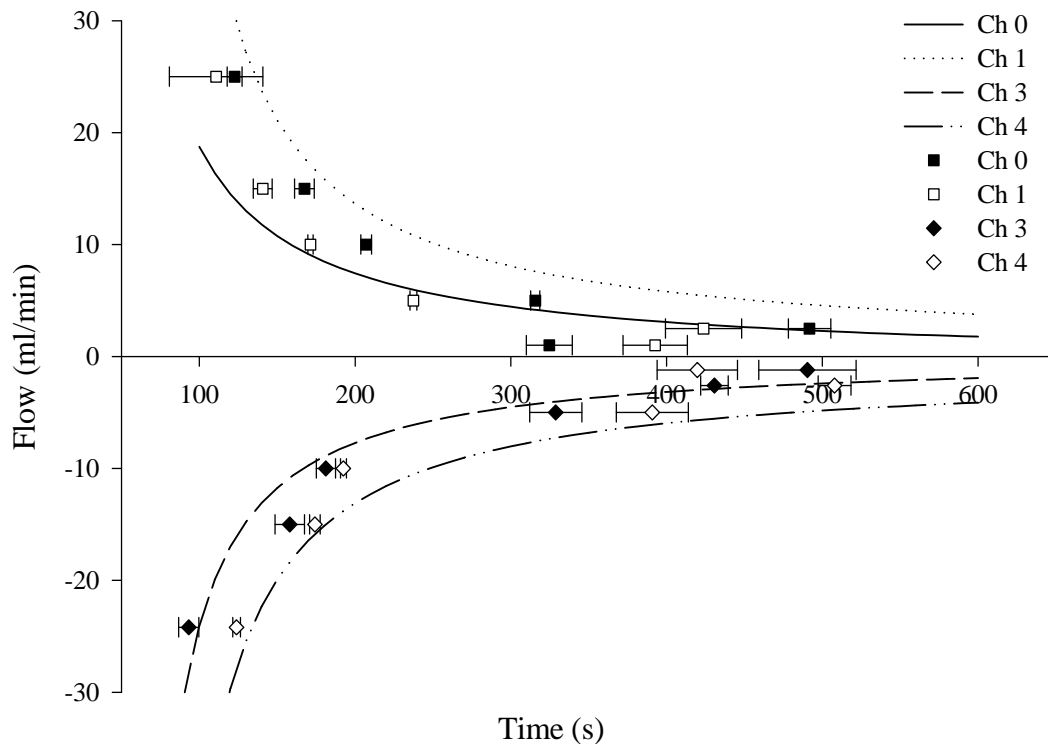


Figure 3. Calibration Curve. Channels 0 and 1 refer to two thermocouples at the left site of the heater (see fig. 1) and channels 3 and 4 refer to the thermocouples at right site of the heater and they receive the heat signal emitted by the heater and transported by the flow toward wire cable end.

Field measurements

The primary sources of environmental measurement error are related to flow bypassing and unstable flow. If the flow enters or exits the cylinder through the sediment interface, there will be an error in the measurement. Therefore, the cylinder was equipped with a tire inner tube glued to the outside of the bottom part of the cylinder as a flange to improve the seal to the formation. The cylinder was pushed into the sediment, and sandbags were placed on the inner tube and then blocks on top of the sandbags to create a seal. A second source of potential error was related to the potential Venturi/Bernoulli effect that may cause the head in the dome to be different than the head outside the dome in a rapidly moving stream. Therefore, a hand vacuum pump was used to measure

the pressure head difference between one water line (water filled Tygon tubing) ending inside the cylinder and the other outside of it, near the discharge from the flow tube (Fig. 2). When a gradient was observed, the cylinder was rotated to remove it. The flow measurements were delayed for about 1 h until the thermocouples approached thermal equilibrium with the surrounding water.

Whatever groundwater discharge into stream or river water infiltrates to the groundwater, the flow rate was measured at two sites along the river.

Since the measured value of T_m exceeded the maximum value on the standard calibration curve, a flow-addition method was employed. Water was pumped into the cylinder with a low-flow peristaltic pump (Masterflex C/L Variable-Speed

Tubing Pump, Cole Palmer) at a constant known flow rate such that the total flow was within the calibration range. The amount of addition was determined by trial and error, and was generally 80 to 300% of the actual flow. This technique is analogous to standard addition methods used in analytical chemistry. The actual flow rate was determined as the difference between the measured Q and the added flow.

Results and discussion

The Venturi/Bernoulli effects in Sucio river caused more than ± 10 cm water differential pressure depending on how the cylinder was oriented in the stream. Just a few degrees of rotation could create a significant gradient.

At one site of the river, the flow rate was measured twice without complications (Table 2). The calculated mean specific discharge was 3.0 m/d. At the other site of the river the water temperature was lightly higher than the calibration temperature (23.5 °C) temperature and water pumping (30 ml/min) into the cylinder was necessary to measure the flow rate. The flow rate at this site was less than 1 ml/min.

Few flow rate data are reported in this study because part of the seepage meter system was stolen after it was installed and left it in the river for a thermal equilibrium. Therefore, more field measurements were not carried out.

We propose to identify all the upwelling and downwelling areas along the river and measure the infiltration of river water to the groundwater or the discharge of groundwater to evaluate the impact of the mercury contamination on groundwater quality and the dilution of the mercury concentration in the river due to groundwater discharge. For instance, in upwelling areas, the measured flow rate can be used with the observed interstitial mercury concentrations to assess the mass of mercury added to the stream due to the resuspension of mercury by the groundwater discharge.

The methodology can be used to map the distribution of upwelling and downwelling areas of the river, which can be useful to develop a pattern for mercury transport along the river and across the boundary to the groundwater.

Table 2. Flow measurements down-welling site at Sucio river. Negative value indicate a flow toward wire cable end (stream water infiltration, see figure 1).

Thermocouples	Peak arrival time (s)	First moment	Flow rate (ml/min)	98% Confident Limits		Darcy Velocity (cm/day)	Specific discharge (m/d)
Measurements in one of the site							
Replicate 1							
Channel 3	79.8	136.1	-13.71	-12.50	-15.19	-8.6	2.9
Channel 4	86.1	188.6	-14.19	-12.55	-16.39	-8.9	3.0
Replicate 2							
Channel 3	67.8	132.7	-14.30	-13.01	-15.86	-9.0	3.01
Channel 4	97.2	180.4	-15.10	-13.31	-17.51	-9.5	3.18

Acknowledgements

The Swedish International Development Agency (SIDA/SAREC) supported this study through the “Environmental Research Multidisciplinary Programme”. It is a cooperative project involving the National Autonomous University of Nicaragua (UNAN-Managua) and Lund University.

References

- Belanger, T. V. and M. T. Montgomery (1992). Seepage meter errors. *Limnology and Oceanography* **37**(8): 1787-1795.
- Brunke M, Gonser T (1997) The ecological significance of exchange processes between rivers and ground-water. *Freshwater Biology* **37**:1–33.
- Constantz, J. and Thomas C.L. (1996). The use of streambed temperature profiles to estimate depth, duration, and rate of percolation beneath arroyos. *Water Resources Research* **32**: 3597-3602.
- Cook, P.G., Lamontagne, S., Berhane, D. and Clark, J.F. (2006). Quantifying groundwater discharge to Cockburn River, southeastern Australia, using dissolved gas tracers ^{222}Rn and SF_6 . *Water Resources Research* **42** doi:10.1029/2006WR004921.
- Fellows, C. r. and P. L. Brezonik (1980). Seepage flow into Florida lakes. *Water Resources Bulletin* **16**: 635-641.
- Keery, J, Binley, A, Crook, N, Smith JWN (2007). Temporal and spatial variability of groundwater-surface water fluxes: Development and application of an analytical method using temperature time series. *Journal of Hydrology* **336**: 1-16.
- Landon, M.K., Rus, D.L., Harvey, F.E. (2001). Comparison of instream methods for measuring hydraulic conductivity in sandy streambeds. *Ground Water* **39**: 870-885.
- Lapham, W.W. (1989). Use of temperature profiles beneath streams to determine rates of vertical ground-water flow and vertical hydraulic conductivity. U.S. Geological Survey Water-Supply Paper 2337.
- Lee, D.R., Cherry, J.A. and Pickens, J.F. (1980). Groundwater transport of a salt tracer through a sandy lakebed. *Limnology and Oceanography* **25**: 45-61.
- Lee, D.R. (1977). A device for measuring seepage flux in lakes and estuaries. *Limnology and Oceanography* **22**; 140-147.
- Lee, D.R., Cherry, J. A. (1978). A field exercise on groundwater flow using seepage meters and mini-piezometers. *Journal of Geological Education* **27**: 6-10.
- Mendoza JA, Ulriksen P, Picado F, Dahlin, T (2008). Aquifer interactions with a polluted mountain river of Nicaragua. *Hydrological Processes* **22**: 2264-2273.
- Murdoch, L.C., Kelly, S.E. (2003). Factors affecting the performance of conventional seepage meters. *Water Resources Research* **39**, doi:10.1029/2002WR001347.
- Paulsen, R. J., C. F. Smith, et al. (2001). Development and evaluation of an ultrasonic ground water seepage meter. *Ground Water* **39**: 904-911.
- Rosenberry, D. O. and R. H. Morin (2004). Use of an electromagnetic seepage meter to investigate temporal variability in lake seepage. *Ground Water* **42**: 68-77.

- Schincariol, R. A. and J. D. McNeil (2002). Errors with small volume elastic seepage meter bags. Ground Water 40(6): 649-651.
- Shaw, R. D. and E. E. Prepas (1989). Anomalous, short-term influx of water into seepage meters. *Limnology and Oceanography* 34: 1343-1351.
- Shaw, R. D. and E. E. Prepas (1990). Groundwater-lake interactions, I: Accuracy of seepage meter estimates of lake seepage. *Journal of Hydrology* 119: 105-120.
- Sholkovitz, E., C. Herbold, et al. (2003). An automated dye-dilution based seepage meter for the time-series measurement of submarine groundwater discharge. *Limnology and Oceanography Methods* 1: 16-28.
- Sophocleous M (2002) Interactions between groundwater and surface water: the state of the science. *Hydrogeology Journal* 10:52–67
- Taniguchi, M. and Y. Fukuo (1993). Continuous measurements of groundwater seepage using an automatic seepage meter. *Ground Water* 31: 465-679.
- Williams DD (1993) Nutrient and flow vector dynamics at the hyporheic/groundwater interface and their effects on the interstitial fauna. *Hydrobiologia* 251:185–198.
- Winter TC (1999) Relation of streams, lakes, and wetlands to groundwater flow systems. *Hydrogeology Journal* 7:28–45

**Ecological, Groundwater, and Human Health Risk
Assessment in a Mining Region of Nicaragua**

Picado., F., Mendoza., A., Cuadra., S., Barmen., G.,
Jakobsson., K., and Bengtsson., G.

Ecological, Groundwater, and Human Health Risk Assessment in a Mining Region of Nicaragua

Francisco Picado^{1,2}, Alfredo Mendoza^{1,3}, Steven Cuadra^{1,4}, Gerhard Barmen³, Kristina Jakobsson⁴, Göran Bengtsson².

¹ Universidad Nacional Autónoma de Nicaragua, Apartado Postal 663, Managua, Nicaragua

² Department of Ecology, Lund University, Sölvegatan 37, SE-223 62 Lund, Sweden

³ Department of Engineering Geology, Lund University, John Ericsson v1 221 00 Lund, Sweden

⁴ Department of Occupational and Environmental Medicine, Lund University, 221 85 Lund, Sweden.

Abstract

The objective of the present study was to integrate the relative risks of damages due to mercury exposure to stream biota, groundwater, and local inhabitants from the Sucio river basin. The mercury pollution in this small gold mining area has been aimed by many studies, but none of them have included the risk associated to mercury exposure. The risks for exceeding protective guidelines for these three compartments were addressed through a probabilistic estimation of hazard quotients by means of Monte Carlo simulations. The risk for groundwater was also estimated by a combination of water demand with vulnerability and index methods. Despite the common sources of exposure, the extent of the risk varies between the assessed compartments. The probability of exceeding guidelines was higher for stream organisms, followed by inhabitants and groundwater. Exposure assessment for several receptors identifies potential receptors most at risk and provides a basis for risk management decisions in developing strategies to human and environmental protection.

Key words: Mercury, River, Hazard quotient, Gold mining

Introduction

Risk assessment is the process by which the probability and magnitude of adverse effects is evaluated as a result of exposure to one or more stress factors. Risk assessment can be used to predict, compare, and manage environmental risk and provide a quantitative basis for preventive or remedial action under uncertainty. One of the objectives of risk assessment is to compare and evaluate the realisation of different sources of hazards, and weigh the benefits of reducing or eliminating the risk versus those of accepting it. For instance,

environmental and human exposure to toxic chemicals can often be characterized by low doses of multiple chemicals, and a major challenge is to assess the potential risk from largely single-chemical databases. Similarly, risk assessment in different disciplines, such as economics, engineering, environmental and human health risk, is practically conducted independently, but some efforts have been made to integrate them (Harvey et al., 1995; Cirone and Duncan, 2000; WHO, 2001; II-Suter, 2004).

One dimension for integration is the spatial scale. Ecological and human health risk assessment can be accommodated on a small, local scale level, e.g. when microbial soil respiration and blood levels of benzene in workers on a gasoline station are used as assessment endpoints, but preferably on a larger, e.g. watershed, level when they are integrated with groundwater vulnerability assessment. A watershed approach unifies the evaluation of the impacts of industrial discharges and agricultural activities on water quality, biota, and human welfare, and may be used to identify habitats, sub-areas, and communities within a region most at risk. Different models have been used to evaluate and compare risk at larger geographical areas, e.g. the Relative Risk Model (Landis and Weigers, 1997), combined with tiered procedures (Moraes and Molander, 2004), and weight-of-evidence approaches (Lowell et al., 2000).

Here we calculate the relative risk of mercury (Hg), released by gold mining in a Nicaraguan watershed, to stream biota, local inhabitants, and groundwater using hazard quotients (HQ) approaches. Those are essentially applicable to large as well as small areas, they assume that toxicity can be assessed relative to a reference chemical, and they allow the comparison of risk from exposure to different stress factors (Zhang et al., 2001). The quotients are useful for screening purposes and can be evaluated as the probability of exceeding 1.0 (which represent exceeding a hazard endpoint, e.g. a reference or guideline value). The values are, however, not measures of risk in a statistical sense, and do not reflect effects on population-based metrics, and are usually non-linear above 1.0 (Eaton and Klaassen, 1996; Kolluru, 1996).

In many developing countries around the world, Hg is used for amalgamation in

mining of gold and other metals. Although gold mining plays an important role in the economic development, rural ecosystems in which mining activity has taken place have undergone dramatic deterioration (Salomons, 1995; Moreira, 1996). Metallic Hg is lost to the atmosphere through evaporation when gold particles in crushed ores are amalgamated with Hg, and when amalgam is burned. Exposure to inorganic Hg represents a potential risk, not only to those persons who are directly handling the Hg and their families, but also to persons living in the surroundings (Malm, 1998; Eisler, 2003b). The population in these areas is also potentially exposed to methyl Hg through the diet, mainly by consumption of local fish. Local cattle milk and meat may represent other sources of methyl Hg (Palheta and Taylor, 1995).

The aims of this work were to a) develop an approach to estimate on a watershed basis the risk to groundwater, stream biota and local inhabitants from exposure to Hg in a mining area in Central Nicaragua, b) calculate the probability by which predicted exposure concentrations or internal concentrations would exceed hazard endpoints. The selection of endpoints was based on the precautionary principle, i.e. reference or guideline values assumed to represent absence of effects, or tolerable levels and c) identify a template by which the risks can be compared.

Area description

The study area is a 28 km² basin located 177 km east of the capital of Nicaragua, Managua (Fig. 1). The Sucio river drains from north to south, meandering along the steep topography of the basin. The altitude ranges from 400 m a.s.l in the south to 800 m a.s.l in the north. The tropical savannah climate meets with a tropical humid climate in the basin. The

rainy season lasts from May to December and the dry season for the rest of the year. The average precipitation is 2400 mm/yr, and the yearly temperature varies from 15°C to 34°C, with humidities up to 80%.

The land use in the basin is primarily for cattle farming and crops for domestic consumption. There are sparse zones with rainforest, mainly along the stream valleys and near the springs. More than half of the population in the basin (ca. 13 000 inhabitants) live in the countryside areas, using spring water or stream water as the most common source of domestic water. For more than one century, the Sucio river has received wastes containing Hg, lead, and cyanide from

the gold mining industry in a small town, Santo Domingo, but also from artisanal activity (Belt, 1874). About 40 tons of Hg and 10 tons of lead have been released into the environment during the past 100 years of mining activity, practiced with amalgamation by single individuals in their homes, and in mills.

Previous investigations have reported Hg concentrations in the Sucio river water almost one order of magnitude higher than the permissible concentrations for human consumption (WHO, 1996), and contaminated sediments as far as 50 km downstream from a mill in Santo Domingo, La Estrella (André et al., 1997).

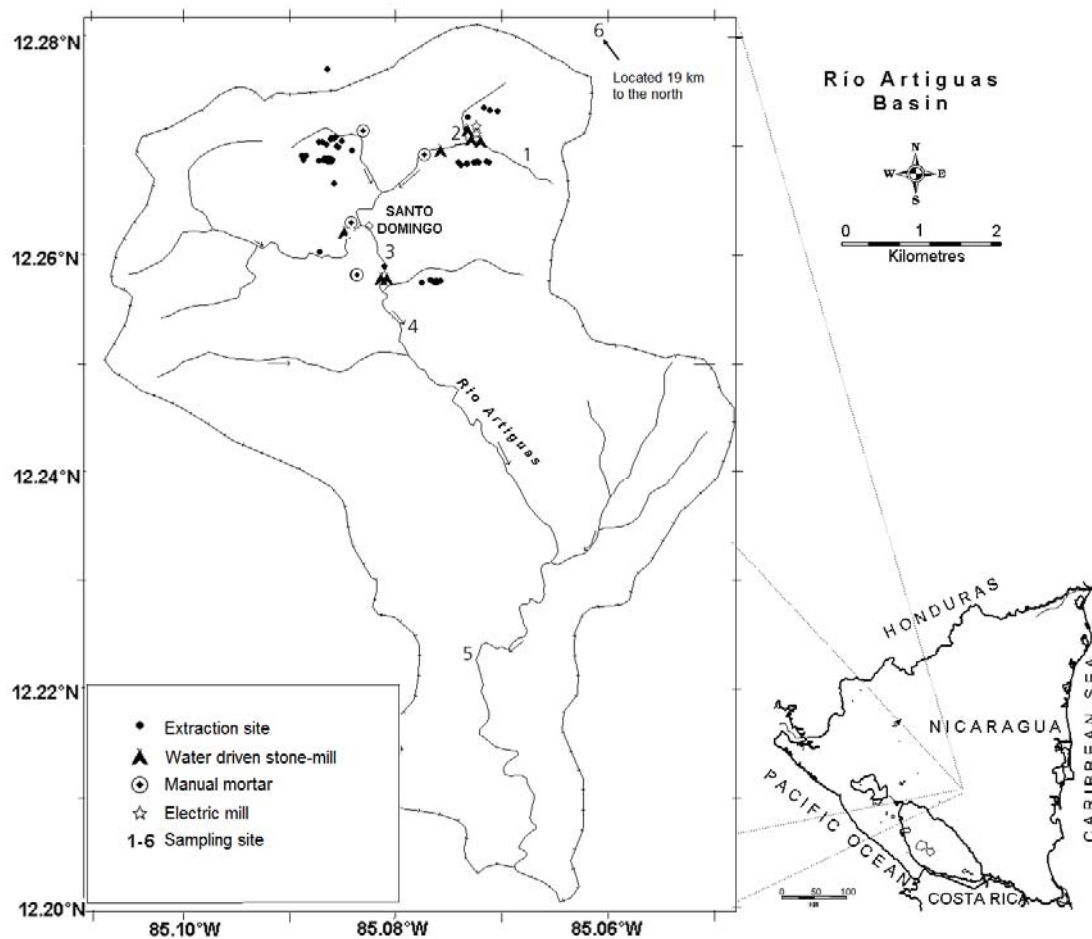


Figure 1. Map of the Sucio river (Río Artiguas) basin with sampling sites and pollution sources indicated.

Methods

Groundwater risk assessment

The groundwater risk is often regarded as a combination of the intrinsic vulnerability, the pollution hazards, and the socioeconomic value that water has for a given population or economic activity. A combination of three maps, the vulnerability map, the hazard map, and the socioeconomic value map, was used to construct a risk map of groundwater pollution. We adopted a combination of the index method (Civita and DeMaio, 1997; Ducci, 1999) and a method based on hazards quotients (Ehteshami et al., 1991; Backman et al., 1998).

The vulnerability assessment method was a modified version (Mendoza and Barmen, 2006) of the DRASTIC method. It used the original seven parameters (Aller et al., 1987) (depth to groundwater (**D**), net recharge (**R**), aquifer media (**A**), soil media (**S**), topography (**T**), influence of the vadose zone (**I**), hydraulic conductivity (**C**)) plus an additional parameter for the degree of fracturing (**M**), which may facilitate the transport of contaminants. Maps connected to each parameter were overlaid to produce a vulnerability map as described by Aller et

al. (1987) and Mendoza and Barmen (2006):

$$5\mathbf{D}_R + 4\mathbf{R}_R + 3\mathbf{A}_R + 2\mathbf{S}_R + \mathbf{T}_R + 5\mathbf{I}_R + 3\mathbf{C}_R + 5\mathbf{M}_R = \text{DRASTIC index}$$

where R is the rating, and the coefficient of each term in the equation is the weight assigned to every parameter. The resulting map with numerical values was normalised and classified as high, moderate (medium) and low vulnerability (Civita and De-Regibus, 1995; Corniello et al., 1997).

The pollution hazard is associated with the mining mills, where Hg is used in the amalgamation process. Different procedures for gold refinement are used in the area and each of them uses different amounts of Hg. Each activity has a different magnitude of hazard since it handles or releases different amounts of Hg. Therefore, each hazard was given different values following a Danger of Contamination Index (*DCI*), modified after Ducci (1999) (Table 1).

The basin has 99 perennial springs and a few dug wells. A socioeconomic value (Ducci 1999), based on the size of the population using the water source and its economic value (Table 2), was assigned to each catchment that supplies water to a

Table 1. Danger of Contamination Index (*DCI*) assigned to different methods for gold refining, adapted from Ducci (1999).

DCI	Pollution source
1	Areas of the basin without mining and polluted sources of water
4	Tailings disposed at areas with groundwater discharge
5	Former mining areas
6	Current mining areas where Hg is occasionally handled
7	Manual mortar, commonly located by a stream
8	Water driven stone mill
9	Electric mill and polluted river water

given well or spring. The groundwater contamination risk was obtained by linking vulnerability, hazards (Table 1) and socio-economic values (Table 2) in 50 × 50 m squares by a cross-table (Table 3) (Civita and DeMaio, 1997).

In a parallel effort to assess the groundwater risk, concentrations of Hg were determined in a group of spring water (hereafter referred to as groundwater) samples (C_{GW}). The samples were filtered through 0.45 µm cellulose acetate filters (Millipore Corp, Bedford, MA) and immediately preserved in 0.1% HNO₃ and kept on ice prior to analyses by inductively coupled plasma mass spectroscopy (ICP-MS) (Perkin Elmer ICP-MS, ELAN-6000). The instrumental detection limit (IDL) was 0.03 ng of total Hg/ml. It was calibrated against a single ²⁰²Hg standard (1 ng/ml). The data were combined with other sources on total Hg concentrations in groundwater in the area (Silva, 1994; Romero, 1996; André et al., 1997; Mendoza and Barmen, 2006; Mendoza et

al., 2006) to expand the pool of exposure data. They were used in three different approaches to calculate the risk, expressed in HQ terms, of exposure from Hg contaminated groundwater. The first approach addressed the spatial distribution of risk to humans from drinking groundwater, by calculating HQ for each individual observation of Hg in groundwater and the guideline of 1 µg/l for drinking water (WHO, 1996). The numerical values of the HQ were transformed into categorical values following the classification suggested in other studies (Reagan et al., 1989; Mosteller and Youtz, 1990). In the second approach, a probability density function (PDF) was calculated by applying BestFit 2.0d (Palisade Inc.) to the same Hg data as in the first approach. The probability that HQ of the ratio between the PDF and the guideline value of 1 µg/l would exceed 1.0 was evaluated by Monte Carlo analysis (see next section for details). The third approach addressed the risk of Hg

Table 2. Characteristics of the two socioeconomic value classes in the Santo Domingo area. The study area has no higher value classes than medium.

Value class	Description of the catchments
Medium	Well or spring supplying 1000 to 10000 inhabitants or an industry with 10 to 99 workers.
Low	Spring supplying less than 1000 inhabitants or an industry with less than 10 workers

Table 3. Cross-table (Civita and DeMaio, 1997) to evaluate the risk of groundwater contamination. V: vulnerability degree; Vr: socioeconomic value; DCI: Danger of contamination index: very low (vl), low (l), medium (m), high (h), very high (vh), and extremely high (eh).*

V→ Vr→ DCI↓	Very low				Low				Medium				High				Very High				Extremely High			
	l	m	h	vh	l	m	h	vh	l	m	h	vh	l	m	h	vh	l	m	h	vh	l	m	h	vh
1																								
2				vl		vl	vl	vl	vl	vl	vl	vl	vl	vl	vl	vl	l	vl	vl	vl	l	m	vl	vl
3	vl	vl	vl	vl	vl	vl	vl	l	vl	vl	l	l	vl	vl	l	l	l	m	vl	l	h	h	l	m
4	vl	vl	vl	vl	vl	vl	l	l	vl	l	l	m	vl	l	m	h	l	m	h	vh	l	m	h	vh
5	vl	vl	l	l	vl	vl	l	m	vl	l	l	m	l	l	m	h	l	m	h	vh	l	h	vh	vh
6	vl	vl	l	m	vl	l	l	m	l	l	m	h	l	m	h	vh	l	h	vh	vh	l	h	vh	vh
7	vl	l	l	m	l	l	m	h	l	m	h	vh	l	m	h	vh	l	h	vh	eh	m	vh	vh	eh
8	l	l	m	h	l	l	h	vh	l	m	h	vh	l	h	vh	eh	m	vh	vh	eh	m	vh	eh	eh
9	l	m	h	vh	l	m	vh	eh	m	h	vh	eh	m	vh	eh	eh	m	eh	eh	eh	h	eh	eh	eh

* In this table all potential categories are included. Cells that correspond to the observed categories given in Table 1 and 2, and the resulting classification of the degree of vulnerability are highlighted.

contamination to groundwater microorganisms. Data on inhibitory Hg concentrations in bacteria (*IC*) were collected from the literature (Vaituzis et al., 1975; Farrell et al., 1993; Frischmuth et al., 1993; Hassen et al., 1998; Ma et al., 1999; Stafford et al., 1999; Golding et al., 2007), a PDF was fitted to the data, divided by an arbitrary uncertainty factor of 100, and then used as the denominator in a Monte Carlo analysis to calculate the probability by which the HQ would exceed 1.0.

Ecological and human health risk assessment

Hazard endpoints

The endpoints for stream organisms were the no-observed-effect concentrations (*NOECs*). For humans, the endpoints were tolerable daily intake (*TDI*) (WHO, 1990; Rice, 2004), and benchmark dose levels with a uncertainty factor of 10 (*BMDL_{0.1}*) (Rice, 2004), being equivalent to the construct of a reference dose. Hazard endpoints were chosen as to relate to the most sensitive endpoint for Hg exposure for the most sensitive species or population segment reported in the scientific literature.

Since few *NOEC* data on Hg were available on freshwater organisms, we used the scaling factor of 100 from comparison of *NOEC* and *LC₅₀* (The lethal concentration that kill the 50% of the exposed organisms) for Hg in embryonic and larval stages of fish (WHO, 1989; Dave and Xiu, 1991) to estimate *NOECs* from lethal concentrations (*LC₅₀*) for Hg in fish and aquatic macroinvertebrates (EPA, 2006).

The *BMDL_{0.1}* account for toxicokinetic and toxicodynamic human variability by applying an uncertainty factor of 10 to the reported benchmark dose level

(*BMDL*) (NRC, 2000; Budtz-Jorgensen et al., 2004; Rice, 2004). The reported *BMDLs* were derived by benchmark doses analysis on standardised neuropsychological endpoints from three longitudinal prospective studies (Rice, 2004). In the analysis a cut-off for abnormal response was set at the 5th percentile of children and a benchmark response 0.05 was chosen doubling the number of individuals with a response at or below the 5th percentile in an unexposed population.

Calculation of predicted environmental concentration (PEC) and predicted body concentration (PBC) for aquatic organisms

The calculation of the ecological risk of Hg contamination was limited to two groups of aquatic organisms, benthic macroinvertebrates and fish. Benthic macroinvertebrates were assumed to become exposed to Hg from two sources, passively via pore water and actively via ingested sediment. Fish were assumed to become exposed via river water and via consumption of benthic macroinvertebrates. The body concentrations of Hg were calculated in the benthic macroinvertebrates and fish to facilitate a comparison of the ecological and health risk, as the latter uses expressions of *PBC*.

The pore water concentrations were calculated from the PDFs of the total Hg concentration (*C_s*) in the top 5 cm of sediment cores (Appendix A) from each of six sampling sites in the river (Fig. 1), and of the sediment partition coefficient, *K_p* (Lyon et al., 1997) (Appendix A). The *PBC* was calculated from the pore water concentrations and bioconcentration factors (*BCFs*) (EPA, 2006), defined as the ratio of Hg concentration in the organism to its concentration in pore water.

The uptake of Hg from ingested sediment was calculated from the PDFs of the total Hg concentrations in the sediments, the estimated fraction of organic Hg to total Hg in a sediment (Muhaya et al., 1997; Ullrich et al., 2001) and the number of times that the concentration of organic Hg in macroinvertebrates, such as the polychaete worm *Nereis diversicolor*, may exceed the concentration in the sediment (Muhaya et al., 1997). The latter two PDFs were taken as uniform (see appendices A and B).

The *PECs* for fish were calculated from the PDFs of the total dissolved concentration of Hg in river water (C_w). They were from hourly measurements for 24 h at the same sites as used for C_s . The *PBC* was based on the *PEC* and *BCFs* (WHO, 1989; EPA, 2006) that were widely ranging from 10 to three orders of magnitude (Appendix B).

The *PBC* in fish was also calculated from uptake via benthic macroinvertebrates as a food source, using the steady state model by (Wang, 2002). The data on ingestion (*IR*) and elimination rate (K_e) were from Trudel and Rasmussen (1997) (Appendix A).

Calculation of personal daily intake (PDI), predicted whole blood concentration (PC_{wb}), and predicted cord blood concentration (PC_{cb}) of Hg in humans

The focus of the human risk assessment was on the general population in Santo Domingo. Even if additional contributions to the intake of Hg can occur through air and water in mining areas (Wickre et al., 2004), we assumed that the total blood Hg concentration was

Fitted observed whole blood concentrations (OC_{wb}) and cord blood concentrations (OC_{cb}) of Hg in humans

solely dependent on the dietary intake of organic forms, particularly methyl Hg (EPA, 2001), by consumption of locally caught fish (Mergler et al., 2007).

The *PDI* was calculated from the PDFs of the estimated total Hg concentration in fish and the daily fish ingestion rate (*FIR*), using consumption data from the literature (USEPA, 2002), and assuming that 70 to 95% of the Hg concentration in fish is organic Hg (Huckabee et al., 1979; Akagi et al., 1994) (Appendix B).

The risk of consuming Hg contaminated fish was assessed from the probability that the *PDI* would exceed the *TDI* as endpoint. For the *TDI*, we used the limits of 0.1 (NCR, 2000) and 0.47 µg methyl Hg/kg body weight per day (WHO, 1990). Even if new analyses in the derivation of the reference dose (RfD) have not been reported, and even though some areas of variability and uncertainties were not addressed in the derivation of the lower oral daily dose for methyl Hg (0.1 µg/kg/day) (Rice, 2004), it is still considered safe for humans. The RfD was derived based on evidence from outcome studies.

The PC_{wb} was calculated from the PDFs of the estimated *PDI* for organic Hg, the absorption and elimination rates (Smith et al., 1994), the total blood volume, and the fraction of Hg in circulating blood (Appendix B).

Furthermore, we calculated expected Hg cord blood concentrations (PC_{cb}) from the PC_{wb} using the PDFs of the reported ratio of total Hg concentration in cord-blood to whole-blood (Q) (WHO, 1990; Stern and Smith, 2003) (Appendix B).

We also had access to observed levels of Hg in whole blood from a sample of 72 adults and children from the general population in Santo Domingo (Table 4)

(Cuadra, 2005). The chemical analysis was performed using cold vapour atomic fluorescence spectrometry. The detection limit was 0.17 $\mu\text{g/l}$ and a Seronorm trace element material human blood, batch OK0336 (Nycomed AS, Oslo, Norway), of $1.8 \pm 0.16 \mu\text{g/l}$ with a certified value of 2 $\mu\text{g/l}$ was measured to give $2.00 \pm 0.27 \mu\text{g/l}$. Observed Hg levels and socio-demographic data are given in Table 4. The observed data were used to generate a probabilistic distribution of OC_{wb} .

We transformed OC_{wb} to OC_{ch} similarly as for PC_{ch} . Even if the OC_{cb} was based on observed concentration in whole blood, is in essence a predicted value, still, we will refer to it as OC_{cb} .

Hazard quotients (HQs) and the probability of exceeding the hazard endpoints

HQs were calculated with PDFs of PBC for macrovertebrates and PC_{cb} for humans as nominators and the corresponding endpoints as denominators. The probability of a HQ exceeding 1 was evaluated by Monte Carlo simulations, using Latin hypercube sampling from PDFs and 10000 iterations with the @RISK 3.5.1 software (Palisade Inc.). The BestFit 2.0d (Palisade Inc.) was used to fit PDFs (Appendix A) to the data. The goodness-of-fit was evaluated by the Chi-square method.

Table 4. Observed Hg concentration and background information of the subjects from Santo Domingo (Cuadra S, personal communication, 2008).

Non-miners' household member	Fathers n=21	Mothers n=22	Children n=25	Other members n=3	Total n= 72
Median (range)					
Age	43 (27-66)	31.5 (22-52)	10 (5-17)	27 (24-61)	27 (5-66)
Weight (kg)	75 (57-111)	65 (51-75)	33 (17-63)	59 (54-73)	60 (17-111)
Residency in community (years)	41 (22-53)	29 (14-52)	8 (5-17)	25 (21-50)	25 (5-53)
Observed Hg in whole blood ($\mu\text{g/l}$)	1.63 (0.21-50.26)	1.52 (0.41-5.54)	1.13 (0.40-4.08)	0.48 (0.39-0.55)	1.36 (0.21-50.26)

Results

Groundwater risk assessment

Areas of medium vulnerability cover most of the stream valleys and lowlands in the basin, with increasing vulnerability southwards (Figure 2a). The variability of the vulnerability in the basin is mostly due to the steep topography and the depth to groundwater, and areas with steep topography are usually less vulnerable to infiltration of contaminants than plain areas. The areas with medium socio-economic values coincide with those with the greatest hazard (largest DCI),

that is, where the mining areas and the mills are located (Figure 2b).

The indexing method approach leads to a pattern of risk on a spatial scale (Figure 2c). The risk of groundwater pollution is higher when higher vulnerabilities coincide with both higher economic values and larger release of Hg. However, the risk in some highly vulnerable areas is lowered by the presence of large areas of low economic value and by the absence of amalgamation sites. In general, areas located downstream of the Hg sources have higher risk than areas upstream. The risk map identifies some spots with a very high risk, such as the gold refining

plants, and larger areas with a very low risk (Figure 2c), e.g. where old mining was operating. Most of the contaminated river channel represents a medium level of risk.

The risk from drinking the water is low for most of the spring areas (Figure 2d), indicating that Hg has not contaminated them or areas far away from the village. The contamination is confined to the vicinity of the gold refining plants and along the river. The concentrations of Hg in the groundwater samples ranged from < IDL to 10 µg/l, and most of them had a concentration below the guideline of 1 µg/l for drinking water (WHO, 1996). The probability of exceeding this concentration in the river basin was 21% (see below, Table 7).

Despite the assumption that Hg is released on the overall ground surface in the indexing method, the overlapping of the indexed parameters (hazards, water demand, and hydrogeological characteristics), yields a similar pattern of risk (Figure 2c) to that from mapping the health based risk by simulating HQs using a probability distribution of the Hg contamination and a guideline value, with most hotspots close to the river in the gold mining areas of the basin (Figure 2d).

The Hg contamination of groundwater was a lower hazard to groundwater bacteria than to humans, and the probability to exceed a HQ of 1.0 was 1% (see below, Table 7).

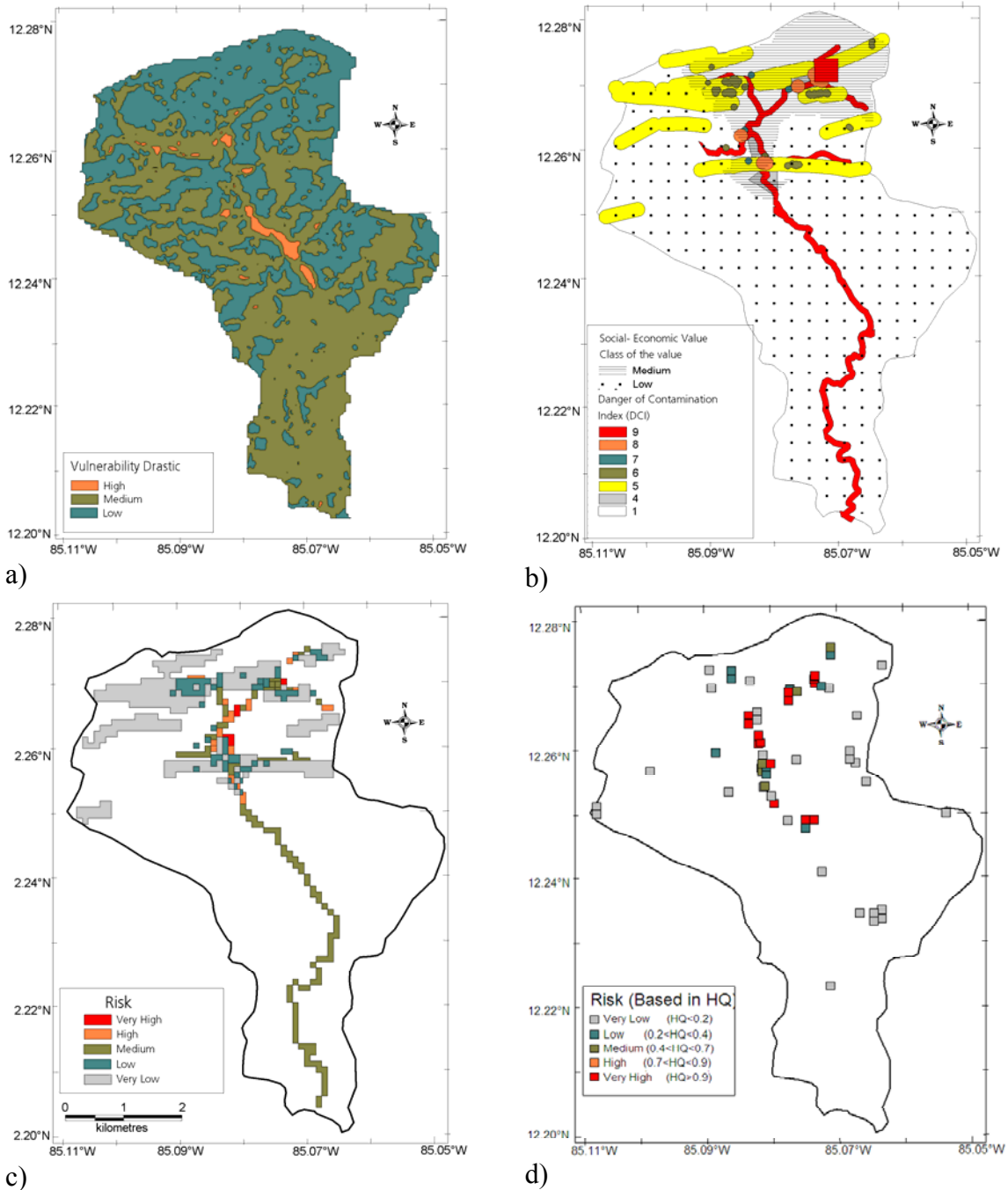


Figure 2. Maps used for characterisation of the risk of exposure to Hg in groundwater. a) vulnerability map, b) the hazard and socioeconomic value map c) the risk map based on the combination of vulnerability, DCI, and socioeconomic value and d) map with risk estimated by categorized HQ.

Ecological and human health risk assessment

The *PBCs* of Hg in the macroinvertebrates and in fish feeding on macroinvertebrates increase downstream from site 2, just downstream of a mining

mill, to site 4, just downstream of another mining mill (Table 5), in a pattern that is similar to the one for the total concentration of Hg in the upper 5 cm of the sediment (Bengtsson and Picado, paper II). The *PBCs* of macroinvertebrates ingesting sediment

are about three times greater than from exposure to Hg in pore water. The *PBCs* of fish from exposure to the river water are only fractions, two to five orders of magnitude, of those from eating macroinvertebrates and, in addition, reasonably independent of the location in the river. The coefficients of variation of the *PBCs* are typically above 1.0, indicating the large uncertainties in data and simulations.

Fish dependent on macroinvertebrates as a food source run the highest risk for exceeding the endpoint (*NOEC/100*), with more than 90 % probability that $HQ \geq 1.0$ in the upper part of the river basin (Table 6). The same risk applies to

the macroinvertebrates ingesting sediment at the sites in conjunction with the mining mills, whereas the probabilities of exceeding an HQ of 1.0 from exposure to water is less than 1.5% for both fish and macroinvertebrates.

In general, the probabilities that the calculated or fitted exposure concentrations would exceed the hazard endpoints varied between 0 and 100 %, depending on the source of exposure and the susceptibility of the endpoint to Hg (Tables 6 and 7). The sediment is the most hazardous source for the macroinvertebrates, and the macroinvertebrates make up the highest

Table 5. Predicted body concentrations (*PBCs*) of mercury in aquatic organisms ($\mu\text{g}/\text{kg}$).

Sites	Mean (Standard Deviation)			
	Macroinvertebrates		Fish	
	<i>Sediment pore water as Hg source ($C_{MI-diff}$)</i>	<i>Ingested sediment as Hg source (C_{MI-s})</i>	<i>Water as Hg source ($C_{F-water}$)</i>	<i>Macroinvertebrates as Hg source (C_{F-food})</i>
Site 1	2.7 (5.2)	7.9 (7.9)	0.01 (0.02)	35.5 (70.1)
Site 2	51.2 (98.4)	148.5 (146.9)	0.03 (0.03)	668.1 (1293.4)
Site 3	57.4 (103.1)	165.5 (146.4)	0.02 (0.02)	740.5 (1336.3)
Site 4	97.8 (176.4)	281.6 (251.3)	0.02 (0.02)	1259.2 (2282.2)
Site 5	9.9 (17.9)	28.4 (25.5)	0.02 (0.02)	127.5 (231.7)
Site 6	0.4 (1.0)	1.2 (1.4)	0.00 (0.00)	5.4 (11.3)

Table 6. Probabilities that the predicted body concentrations (*PBCs*) in aquatic organisms would exceed the hazard endpoints (%).

Sites	Macroinvertebrates		Fish	
	<i>Sediment pore water as Hg source</i>	<i>Ingested sediment as Hg source</i>	<i>Water as Hg source</i>	<i>Macroinvertebrates As Hg source</i>
Site 1	0.0	37.0	0.6	92.3
Site 2	0.0	89.1	1.4	99.8
Site 3	0.2	90.7	0.8	99.8
Site 4	0.4	93.8	1.0	100.0
Site 5	0.0	67.5	1.0	98.7
Site 6	0.0	8.0	0.2	65.0

risk for fish. Humans run much less risk when their predicted daily intake of local fish is compared with the proposed tolerable intake than when their Hg concentrations in cord blood, based on predicted or observational data, are compared with bench mark levels.

Under the assumption that consumption of Hg contaminated fish is the only source of Hg to humans in Santo Domingo, and that the fish consumption data from USEPA are applicable, the probability that humans exceed the *TDI* by fish consumption (*PDI*) is low, 0.3 % (Table 7). The 95th percentile of the calculated personal daily intake of Hg is

below the lower tolerable daily intake of 0.1 $\mu\text{g}/\text{kg}/\text{day}$. The PC_{wb} , calculated with the same local fish consumption assumptions as the *PDI*, is one order of magnitude lower than the OC_{wb} (t-test, $p=0.0001$), based on a frequency distribution of Hg measurements in whole blood of a subpopulation, suggesting that humans are exposed to more Hg sources than local fish or fish consumption is higher. Consequently, the probability that the Hg concentrations calculated for cord blood exceeds the benchmark values ($BMDL_{S_{0.1}}$ Appendix B) was also higher when the observational data were used (30 %) than when estimated from daily intake (10 %).

Table 7. Probability density distributions of the personal daily intake (*PDI*) ($\mu\text{g}/\text{kg}$ day), predicted whole blood (PC_{wb}) and cord blood¹ (PC_{cb}) and fitted observed whole blood (OC_{wb}) and cord blood (OC_{cb}) concentrations of Hg in humans ($\mu\text{g}/\text{l}$), hazard quotients (HQs) for humans and groundwater and the probability of exceeding the hazard endpoints.

	Mean (SD)	Minimum	Maximum	
<i>PDI</i>	0.003 (0.03)	0.00	2.28	
PC_{wb} , based on predicted intake	0.18 (1.79)	0.00	93.1	
PC_{cb} based on predicted intake ¹	0.29 (2.87)	0.00	161	
OC_{wb} , based on observational data	2.41 (2.41)	0.00	22.6	
OC_{cb} , based on observational data ¹	0.24 (0.24)	0.00	2.3	
	Mean (SD)	Minimum	Maximum	Probability that <i>PDI</i> would exceed <i>TDI</i> (%)
HQ of <i>PDI</i>	0.01 (0.22)	0.0	16.6	0.3
				Probability that PC_{cb} and OC_{cb} would exceed $BMDL_{S_{0.1}}$ (%)
HQ of PC_{cb}	1.5 (17.7)	0.0	1209	10.8
HQ OC_{cb} ¹	1.3 (22.9)	0.0	2257	27.9

Table 7 (Continuation)

				Probability that C_{GW} would exceed the WHO's guideline (%)
HQ of observed Hg concentration in groundwater related to the WHO's guideline	0.6 (0.6)	0.0	7.4	21.4
HQ of observed Hg concentration in groundwater related to safety Hg concentration for bacteria	0.1 (1.7)	0.0	165	1.0

¹Transformed from whole blood to cord blood concentrations, according to Stern and Smith 2003.

Discussion

A comparison of multidisciplinary approaches to risk analysis calls for the use of common currency or exchange rates. By letting a hazard quotient represent an exchange rate between the disciplines, we enter into a tradition of quantitative risk assessment that originally took single-value comparisons between measured or estimated environmental concentrations and a reference value for toxicity as a preliminary step in a tiered risk characterization. Although application and interpretation of the quotient should be made with great caution (Tannenbaum et al. 2003), the probabilistic methodology we use in the exposure assessment adds information on the uncertainty in the estimation and the true variability of the environmental concentration, so that risk can be calculated as the probability of exceeding a specified quotient. The nominator of the quotients turn into the same currency by toxicokinetic modelling, by which the external exposure through water and food is transformed into an internal exposure in the blood or whole tissue. The transformation is driven by the tradition in human risk assessment to relate toxicity assessment to blood

concentrations of the contaminant and includes the analogue calculation of the exposure in whole tissue of macroinvertebrates and fish by uncertain steady state constants of uptake and elimination rates of the contaminant. Likewise, the assessment of internal exposure to Hg in groundwater bacteria depends on uncertainties about the speciation rate of Hg from ionic to elemental.

Finding a common currency for the denominator in the quotients was a greater challenge than for the nominator. Even if limitations of the *NOAEL* approach, such as the dose-response dependence on the sample size, are accepted for the purpose of comparing toxicological endpoints in the groundwater and stream environments with a *BMDL*, other translation difficulties remain. One of them is the uncertainty in extrapolations of *LC*₅₀ for macroinvertebrates and fish and *IC* for bacteria to the corresponding *NOAEL* values, and another is the translation between the lethal endpoint available for bacteria, fish, and invertebrates on one hand, and the neuropsychological endpoint used for the *BMDL* for humans. The uncertainty in comparing dose-response values for different endpoints

may be addressed by sampling e.g. their *NOAELs*, finding the most likely probability density distribution representing them, and using that distribution in the denominator when human, stream-water, and groundwater risks are compared. That comparison was not made here because the database was too limited, with only some few samples of *NOAELs* available for the stream-water and groundwater organisms.

The risk might be even higher, because the connections between the heavily polluted river (Figure 2b), and the shallow aquifers nearby (Mendoza, 2006) might facilitate the infiltration of Hg and other pollutants (Mendoza et al., 2008). The temporal changes on the exposure concentration can imply a short term evaluation when the risk is obtained by the HQ approach. This could explain the differences that might exist between the risk expressed by HQ (Figure 2d) and the risk resulting from the indexing method (Figure 2c).

The sensitivity to Hg varies widely among strains of bacteria, as demonstrated by the range of inhibitory concentrations from 0.2 to up 25000 µg/l and even larger. The variation is to some extent due to well-characterized systems of Hg resistance in many strains (Ji and Silver, 1995; Barkay et al., 2003), but Hg is also toxic at low doses to some strains, partly depending on its chemical speciation (Farrell et al., 1993). The mean of the probability distribution of the HQ is six times lower than the mean of the HQ for health effects of groundwater consumption (Table 7), mainly related to differences in the expressions of the denominator. We also notice that the PDF of the HQ of inhibition is orders of magnitude wider than the PDF of the HQ for health effects, reflecting the wide range of *ICs* found in the literature.

The microorganisms share the same low risk, between 0 and 1.4 %, for toxic effects of Hg as the macroinvertebrates and fish exposed to Hg via river water (Table 6). The risk becomes much higher when sediment and food is considered as exposure sources, in agreement with the observation that the uptake of metals from dissolved sources is lower than that from ingested food (Luoma and Rainbow, 2005). The uptake of Hg from ingested sediment or food and the diffusive uptake from water are all important pathways for risk assessment in stream organisms (Bryan and Langston, 1992; Muhaya et al., 1997). Here we separate the risk assessment for macroinvertebrates and fish depending on the exposure source, but realize the difficulties in separating or merging exposures from the different sources under field conditions, even with quantitative data available on daily intake of food.

Risk varies with the susceptibility of organisms, and freshwater insects and macroinvertebrates are sensitive to Hg, but with great species-to-species variations (WHO, 1989; EPA, 2006). Lethal concentrations of inorganic Hg species to tolerant fish or macroinvertebrates are in the order of 10^5 µg/l (EPA, 2006), whereas lethal concentration of total Hg to sensitive aquatic organisms varies from 0.1 to 2.0 µg/l (Eisler, 2003a), and the lethal concentrations of organic Hg are even lower (EPA, 2006). Notwithstanding the risk assessment included the chronic toxicity values to the most tolerant organisms, which are four orders of magnitude higher than the values for sensitive organisms, the risk for the stream biota is high. In addition, since the risk depends also on the exposure concentration, it will vary spatially in response to it (Table 6).

Several sources of uncertainties were accepted for the risk assessment of stream biota: total Hg was used rather than individual species of it, a steady state assumption was used to calculate Hg uptake rather than a kinetic approach, 100 % of the dissolved Hg was assumed to be bioavailable, no individual-to-individual variation in susceptibility to Hg was addressed but a single LC_{50} value taken to represent the entire group of organisms, and an uncertainty factor of 100 was used to scale down the toxicity from LC_{50} to the $NOEC$ level. Nevertheless, the predicted body concentrations ($PBCs$) of Hg in the stream biota (Table 5) are comparable with Hg concentrations observed in stream organisms from similar contaminated environments (Lacerda, 1997; Tarras-Wahlberg et al., 2001), and the $PBCs$ for fish are in the same order of magnitude as the concentrations observed by André et al. (1997) in fish from Sucio river (30 - 420 $\mu\text{g}/\text{kg ww}$).

Human health risk assessments have established permissible exposure levels e.g. TDI , RfD . A common procedure is to apply a uncertainty factor to $NOAEL$ (Filipsson et al., 2003). However, BMD approach offers significant advantages over the $NOAEL$ approach. This discussion is presented by Filipsson et al. (2003). For instance, the occurrence of adverse effects at $NOAEL$ can not be ruled out due to statistical and analytical limitations. In addition, since the $NOAEL$ depends on the selected dose, the $NOAEL$ -generated permissible exposure levels are dictated by the experimental dose, not by biological relevance. The BMD represents the dose corresponding to the benchmark response (BMR), and a lower confidence limit on the BMD accounts for the $BMDL$ (Crump, 1984). The BMD approach incorporate more biological information and it has been recommended over the traditional $NOEL$ approach for a more accurate risk

assessment (Filipsson et al., 2003). A hazard endpoint ($BMDL_{s0.1}$), which accounts for neuropsychological consequence of *in utero* exposure to methyl Hg (Budtz-Jorgensen et al., 2000) and for an uncertainty factor of 10, was used to assess the risk due to internal exposure of Hg in the Santo Domingo inhabitants. Another endpoint source in our calculation was a BMD analysis by The US National Research Council on the same data (NRC, 2000). The uncertainty factor is thought to account for individual differences related with the uptake and transfer of Hg in the body and for interindividual differences in the response, in relation to the same concentration at the target compartment (Budtz-Jorgensen et al., 2004).

Humans in gold mining areas are exposed to Hg via several routes. However, fish are considered the primary source of Hg in the human diet (Clarkson, 1992) and most of the Hg in fish is methyl Hg (Huckabee et al., 1979; Akagi et al., 1994), the most toxic species of Hg. Therefore, the consumption of Hg contaminated fish becomes the focus of most human health risk assessments. There are different estimates of tolerable daily intake, a lower (NRC, 2000) and a higher (WHO, 1990). The higher value correspond to a no-observed-adverse-effect level ($NOAEL$) divided by an uncertainty factor that account for variations to a given level of exposure and for variability in Hg toxicokinetics due to population heterogeneity, (Clewell et al., 2000; Sanga et al., 2001; Filipsson et al., 2003), whereas the lower value correspond to a reference dose based on benchmark dose analysis (NCR 2000, Rice 2004). As detailed data on fish consumption in the region was not available. we have used a surrogate probabilistic distribution of low fish ingestion rate based on published data from the US (USEPA, 2002) was used to

estimate the *PDI*. This surrogate variable, which clearly is lower than ingestion data from high fish consumption populations (Sanga et al., 2001), yields a low daily intake, such that, the probability that the estimated daily Hg intake would exceed the tolerable daily intake is very low (Table 7). It suggests a low risk even if the reported (André et al., 1997) and predicted Hg concentrations in fish (Table 5) are sufficiently high to make concern about human health.

However, the higher probability to exceed the hazard endpoint when using the PDF of OC_{cb} than the PDF of PC_{cb} (Table 7), suggests that the daily Hg intake of the Santo Domingo inhabitants may be underestimated. This assumption is supported by recent data on fish consumption from the Santo Domingo community, indicating higher fish consumption than the USEPA estimates (Cuadra et al., 2008). Also, more than one source of exposure, e. g. drinking water, may contribute to the levels of Hg in the Santo Domingo inhabitants.

The probability of exceeding a *TDI* based on estimated daily intake was significantly lower than the probability of exceeding *BMDLs* based on predictive or observational data. These two estimates cannot be directly compared, due to the differences on the nature of the two hazard endpoints (for details, see Appendix A, B) and the availability of data on the variation for both the *TDI* and *BMDLs*. A large amount of data is available for *BMDLs* (Rice 2004, NRC 2000), whereas reported data on the variation of *TDI* for Hg was very limited, only two values were included in the analysis (see Appendix A) with a considerable gap in between.

We don't know of any site-specific applications of integrated human, ecological, and groundwater risk assessments, but several attempts have

been made to define frameworks for integrated human and ecological risk assessments (Cirone and Duncan 2000, Suter II et al. 2003, Pereira et al. 2004). Here, the risk due to Hg exposure was estimated to stream organisms, humans, and groundwater in a watershed, by means of the probability that the internal Hg exposure in those three systems would exceed the hazard endpoints (Table 6 and 7). Even though the effects of Hg are not directly comparable between the assessed endpoints because they have different Hg susceptibilities, the use of probabilistic predictions of toxicological endpoints such as the *NOEC*, a *BMDL* lowered by a factor of 10, and the *IC* lowered by a factor of 100, as denominator of the hazard quotient is at least a transparent exposure of the quality of the currencies, although exchanges between them are impaired by ambiguities.

Conclusions

The approach of an exposure assessment integrates the risk to several potential receptors with different susceptibilities to Hg. Although the risk differs for the assessed endpoints, the risks are comparable each other in the sense that the used hazard endpoints represent similar levels of protection. When the risks are compared, stream organisms are faced with higher risk than human health and groundwater.

Acknowledgements

The Swedish International Development Agency (SIDA/SAREC) supported this study through the "Environmental Research Multidisciplinary Programme". It is a cooperative project involving the National Autonomous University of Nicaragua (UNAN-Managua) and Lund University.

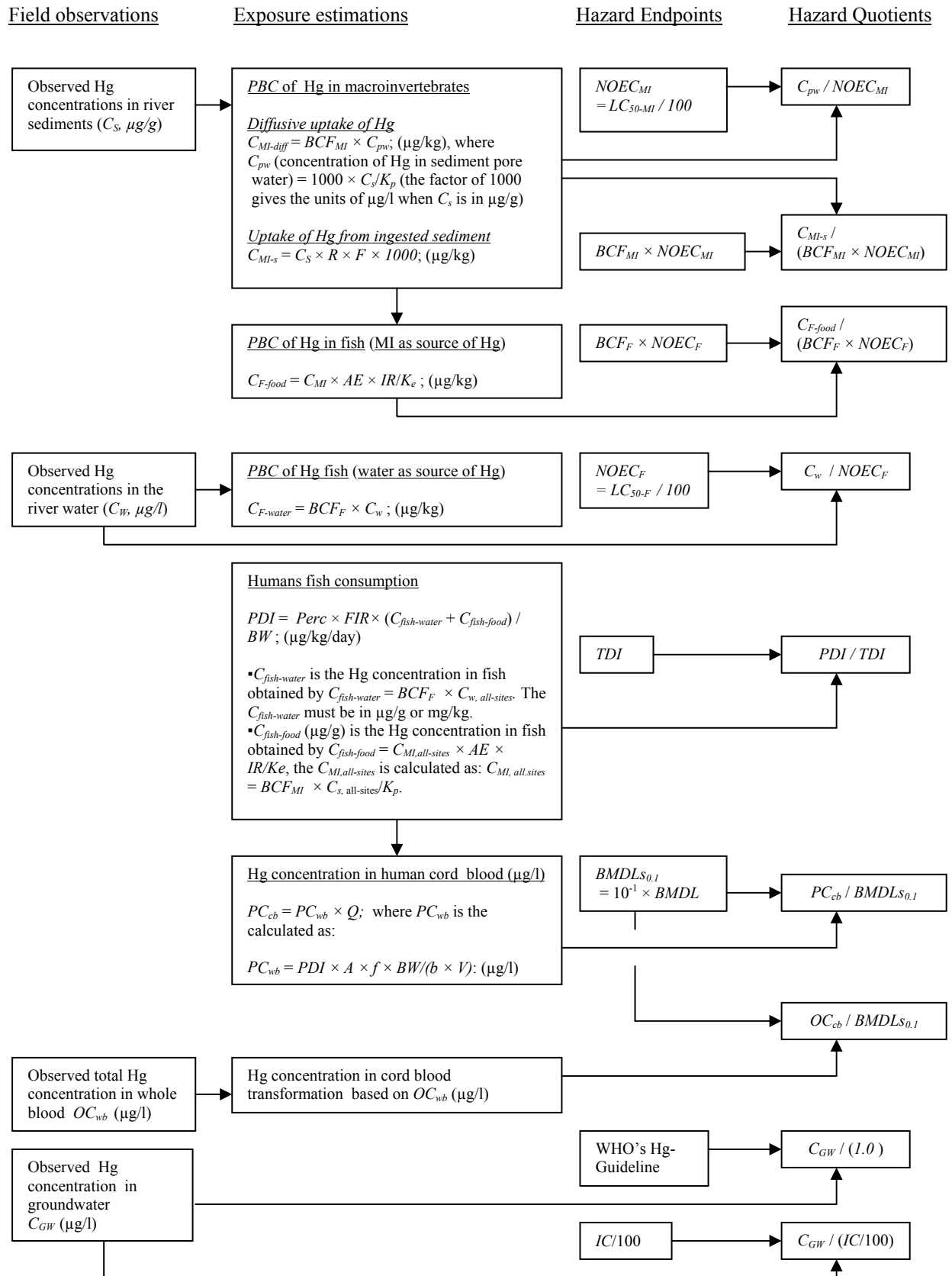
Appendix A: Probability distribution function (PDF) for parameters used to calculate the Hazard Quotients (HQs).

Input variables	Symbol	PDF ^(b) <i>n</i>	PDF parameters		
			Mean (SD)	Lower bound	Upper bound
^a Water Hg concentration (µg/l)	C_w				
Site 1		Uniform (2)		0.03	0.28
Site 2		Normal truncated (24)	0.32 (0.15)	0.34	0.63
Site 3		Normal truncated (24)	0.18 (0.09)	0.04	0.42
Site 4		Normal truncated (24)	0.22 (0.12)	0.01	0.52
Site 5		Normal truncated (24)	0.21 (0.12)	0.04	0.57
Site 6		Uniform (2)		0.03	0.06
Water Hg concentration at all sites (µg/l)	$C_{w, all-sites}$	Exponential truncated (100)	β Value = 0.22	0.01	0.63
^a Sediment Hg concentration (µg/g dw)	C_s				
Site 1		Uniform (3)		0.10	0.43
Site 2		Uniform (3)		2.04	7.88
Site 3		Uniform (3)		4.86	6.17
Site 4		Uniform (3)		7.71	11.07
Site 5		Uniform (3)		0.75	1.14
Site 6		Uniform (3)		0.07	0.08
Sediment Hg concentration at all sites (µg/g dw)	$C_{s, all-sites}$	Uniform (18)		0.07	11.07
<u>Macroinvertebrates</u>					
Benthic sediment partition coefficient for Hg (l/kg)	K_p	Triangle	83 000	5 700	990000
Bioconcentration factor of freshwater macroinvertebrates	BCF_{MI}	Exponential truncated (42)	β Value = 2084.78	11	19 600
Hg lethal concentration to macroinvertebrates (µg/l)	LC_{50-MI}	Exponential truncated (99)	β Value = 2143.7	7.0	35000
Fraction of organic Hg to total Hg in sediment	R	Uniform		0.0	0.0
<u>n-fold concentration of organic Hg in macroinvertebrates to the concentration in sediments</u>	F	Uniform		0.0	17.0
<u>Fish</u>					
Bioconcentration factor of freshwater fish	BCF_F	Exponential truncated (40)	β Value = 0.09	0.0005	1.68
Hg lethal concentration to freshwater fish (µg/l)	LC_{50-F}	Exponential truncated (154)	β Value = 2265.98	0.10	30 000
Hg assimilation efficiency in fish (%)	AE	Uniform		0.8	1.0
Hg ingestion rate in fish (g/g/day)	IR	Uniform		0.007	0.087
Elimination rate of Hg in fish (day ⁻¹)	K_e	Exponential truncated (95)	β Value = 0.009	0.000	0.500
<u>Humans</u>					
Tolerable Daily Intake (µg/kg/day)	TDI	Uniform		0.10	0.47
Percentage of organic Hg to total Hg in fish	$Perc$	Uniform		0.70	0.95
Fish ingestion rate (g/day)	FIR	Exponential truncated (57)	β Value = 0.087	0.0000	0.723
^a Human body weight (kg)	BW	Normal truncated (334)	55.2 (19.5)	17.0	111.0
Fraction of absorbed Hg	A	Uniform		0.94	1.00
Fraction of Hg intake (from the body to blood)	f	Uniform		0.051	0.095
Ratio of Hg-cord blood to Hg-total blood	Q	Normal truncate	1.63(0.95)	0.00	100
Hg elimination constant (day ⁻¹)	b	Uniform		0.013	0.02
Volume of blood in the body (l)	V	Uniform		1.0	8.0
^a Observed total Hg in whole blood (µg/l)	OC_{wb}	Exponential truncate (72)	β Value = 2.41	0.00	300
Benchmark dose levels with a safety factor of 10 (µg/l)	$BMDL_{S0.1}$	Normal truncate	5.6 (2.3)	0.0	50.0
<u>Groundwater</u>					
Total Hg in groundwater (µg/l)	C_{GW}	Exponential Truncate (54)	β Value = 0.65	0.0	50.0
<u>Inhibitory total Hg concentration for bacteria (µg/l)</u>	IC	Exponential Truncate (72)	β Value = 7449.4	0.2	30000

^aMeasured concentrations; ^bNumber of measurements or number of data available in the literature.

PDFs of Hg aqueous concentration were limited at the lower and upper bound values of 0 and 10 respectively; Both the BCF_{MI} and LC_{50-MI} probability density functions were truncated at the lower bound value of 0 and at upper bound values of 25000 and 9000 respectively; the PDF of BCF_F , LC_{50-F} , FIR and BW were truncated at a lower bound value of 0 or 1 and at upper limits of 5, 30000, 5 and 150 respectively; the PDF of Q , K_e and $BMDL_{0.1nj5}$ were truncated at their lower and upper bound values. Data of FIR are the per capita fish consumption in the United States and data of BW are from Santo Domingo population.

Appendix B : Calculation of hazard quotients (most of the variables are defined in appendix A)



References

- Akagi, H., Kinjo, Y., Branches, F., Malm, O., Harada, M., Pfeiffer, W.C., Kato, H., 1994. Methylmercury in the Tapajós River Basin, Amazon. *Environmental Science*. 3, 25-32.
- Aller, L., Bennet, T., Hehr, J.H., Petty, R.J., Hackett, G., 1987. DRASTIC: A standardized system for evaluation groundwater pollution potential using hydrogeologic settings. U S Environmental Protection Agency, Ada Ok, EPA/600/2-87-036, 455 p.
- André, L., Rosén, K., Torstendahl, J., 1997. Minor field study of mercury and lead from gold refining in Central Nicaragua. Luleå tekniska universitet.
- Backman, B., Bodis, D., Lahermo, P., 1998. Application of a groundwater contamination index in Finland and Slovakia. *Environmental Geology*. 36(1-2).
- Barkay, T., Miller, S.M., Summers, A.O., 2003. Bacterial mercury resistance from atoms to ecosystems. *FEMS Microbiology Reviews*. 27, 355-384.
- Belt, T., 1874. *The Naturalist in Nicaragua; A Narrative of Residence at the Gold Mines of Chontales; Journeys in the Savannahs and Forest*. J. S. Dent and Sons, London.
- Bryan, G.W., Langston, W.J., 1992. Bioavailability, accumulation and effects of heavy metals in sediments with special reference to United Kingdom estuaries: A review. *Environmental Pollution*. 76, 89-131.
- Budtz-Jorgensen, E., Grandjean, P., Keiding, N., White, R.F., Weihe, P., 2000. Benchmark dose calculations of methylmercury-associated neurobehavioural deficits. *Toxicology Letters*(112-113), 193-199.
- Budtz-Jorgensen, E., Keiding, N., Grandjean, P., 2004. Effects of exposure imprecision on estimation of the benchmark dose. *Risk Analysis*. 24(6), 1689-1696.
- Cirone, P.A., Duncan, B., 2000. Integrating human health and ecological concerns in risk assessments. *Journal of Hazardous Materials*. 78, 1-17.
- Civita, M., De-Regibus, C., 1995. Sperimentazione di alcune metodologie per della valutazione della vulnerabilità degli acquiferi (in Italian). In: Pitagora (Editor), *Quad Geology Applied*, Bologna, pp. 63-71.
- Civita, M., DeMaio, M., 1997. Assessing groundwater contamination risk using ARC/INFO via GRID function, ESRI Conference 1997, San Diego, USA.
- Clarkson, T.W., 1992. Mercury: Major issues in environmental health. *Environmental Health Perspectives*. 100, 31-38.
- Clewell, H.J., Crump, K.S., Gentry, P.R., Shipp, A.M., 2000. Site-specific reference dose for methylmercury for fish-eating populations. *Fuel Processing Technology*. 65-66, 43-54.
- Corniello, A., Ducci, D., Napolitano, P., 1997. Comparison between parametric methods to evaluate aquifer pollution vulnerability using GIS: an example in the "Piana Campana", southern Italy. In: P.G. Marinos, G.C. Koukis, G.C. Tsiambaos, G.C. Stournaras (Editors), *Engineering geology and the environment*. Balkema, Rotterdam, pp. 1721-1726.
- Crump, K., 1984. A new method for determining allowable daily

- intakes. *Fundamental and Applied Toxicology*. 4, 854-871.
- Cuadra, S., 2005. Child labour and health hazards: Chemical exposures and occupational injuries in Nicaraguan children working in a waste disposal site. Licentiate thesis Faculty of Medicine, Lund University.
- Dave, G., Xiu, R., 1991. Toxicity of mercury, copper, nickel, lead, and cobalt to embryos and larvae of zebrafish, *Brachydanio rerio*. *Archives of Environmental Contamination and Toxicology*. 21, 126-134.
- Ducci, D., 1999. GIS Techniques for mapping groundwater contamination risk. *Natural Hazards*. 20(2-3), 279-294.
- Eaton, D.L., Klaassen, C.D., 1996. Principles of Toxicology. In: C.D. Klaassen (Editor), Casarett & Doull's Toxicology 5th ed. McGraw-Hill, New York, USA, pp. 13-33.
- Ehteshami, M., Richard, R.C., Eisele, H., Deer, H., Tindall, T., 1991. Assessing pesticide contamination to ground water: A rapid approach. *Ground Water*. 29(6), 862-868.
- Eisler, E., 2003a. Mercury, *Handbook of Chemical Risk Assessment: Health Hazard to Humans, Plants and Animals*. Lewis Publisher, Boca Raton, London New York Washington DC.
- Eisler, R., 2003b. Health risk of gold miners: A synoptic review. *Environmental Geochemistry and Health*. 25, 325-345.
- EPA, 2001. Methylmercury (MeHg) (CASRN 22967-92-6). Integrated Risk Information System, U.S. Environmental Protection Agency (U.S. EPA), Washington, DC.
- EPA, U.S., 2006. ECOTOX Database. <http://cfpub.epa.gov/ecotox/>.
- Farrell, R.E., Germida, J.J., Huang, P.M., 1993. Effects of chemical speciation in growth media on the toxicity of mercury(II). *Applied and Environmental Microbiology*. 59(5), 1507-1514.
- Filipsson, A.F., Sand, S., Nilsson, J., Victorin, K., 2003. The benchmark dose method-Review of available models, and recommendations for application in human health risk assessment. *Critical Reviews in Toxicology*. 33(5), 505-542.
- Frischmuth, A., Weppen, P., Deckwer, W.-D., 1993. Microbial transformation of mercury(II). I. Isolation of microbes and characterization of their transformation capabilities. *Journal of Biotechnology*. 29, 39-55.
- Golding, G.R., Kelly, C.A., Sparling, R., Loewen, P.C., Barkay, T., 2007. Evaluation of mercury toxicity as a predictor of mercury bioavailability. *Environmental Science and Technology*. 41, 5685-5692.
- Harvey, T., Mahaffey, K.R., Vasquez, S., Dourson, M., 1995. Holistic risk assessment: An emerging process for environmental decisions. *Regulatory Toxicology and Pharmacology*. 22, 110-117.
- Hassen, A., Saidi, N., Cherif, M., Boudabous, A., 1998. Resistance of environmental bacteria to heavy metals. *Bioresource Technology*. 64, 7-15.
- Huckabee, J.W., Elwood, J.W., Hildebrand, S.G., 1979. Accumulation of mercury in freshwater biota. In: J.O.N. (ed) (Editor), *The Biogeochemistry of Mercury in the Environment*. Elsevier/North-Holland Biomedical Press, New York.
- II-Suter, G.W., 2004. Bottom-up and top-down integration of human and

- ecological risk assessment. *Journal of Toxicology and Environmental Health. Part A* 67, 779-790.
- Ji, G., Silver, S., 1995. Bacterial resistance mechanisms for heavy metals of environmental concern. *Journal of Industrial Microbiology*. 14, 61-75.
- Kolluru, R., 1996. Health risk assessment: principles and practices. In: B.S. Kolluru R., Pitblado R., et al. (Editor), *Risk Assessment and Management Handbook*. McGraw-Hill, New York, USA, pp. 10.3-10.59.
- Lacerda, L.D., 1997. Atmospheric mercury and fish contamination in the Amazon. *Environmental Impact*. 49(1/2), 54-57.
- Landis, W.G., Weigers, J.A., 1997. Design considerations and a suggested approach for regional and comparative ecological risk assessment. *Human and Ecological Risk Assessment*. 3, 287-297.
- Lowell, R.B., Culp, J.M., Dubé, M.G., 2000. A weight-of-evidence approach for northern river risk assessment: integrating the effects of multiple stressors. *Environmental Toxicology and Chemistry*. 19, 1182-1190.
- Luoma, S.N., Rainbow, P.S., 2005. Why is metal bioaccumulation so variable? Biodynamics as a unifying concept. *Environmental Science and Technology*. 39(7), 1921-1931.
- Lyon, B.F., Ambrose, R., Rice, G., Maxwell, C.J., 1997. Calculation of soil-water and benthic sediment partition coefficients for mercury. *Chemosphere*. 35(4), 791-808.
- Ma, M., Tong, Z., Zhu, W.W., 1999. Acute toxicity bioassay using the freshwater luminescent bacterium *Vibrio-qinghaiensis* sp. Nov.-Q67. *Bulletin of Environmental Contamination and Toxicology*. 62, 247-253.
- Malm, O., 1998. Gold mining as a source of mercury exposure in the Brazil Amazon. *Environmental Research*. 77, 73-78.
- Mendoza, J.A., Barmen, G., 2006. Assessment of groundwater vulnerability in the Río Artiguas basin, Nicaragua. *Environmental Geology*. 50, 569-580.
- Mendoza, J.A., Dahlin, T., Barmen, G., 2006. Hydrogeological and hydrochemical features of an area polluted by heavy metals in central Nicaragua. *Hydrogeology Journal*. 14(1052-1059).
- Mendoza, J.A., Ulriksen, P., Picado, F., Dahlin, T., 2008. Aquifer interactions with a polluted mountain river of Nicaragua. *Hydrological Processes*. 22, 2264-2273.
- Mergler, D., Anderson, H.A., Chan, L.H.M., Mahaffey, K.R., Murray, M., Sakamoto, M., Stern, A.H., 2007. Methylmercury exposure and health effects in humans: A worldwide concern. *Ambio*. 36(1), 3-11.
- Moraes, R., Molander, S., 2004. A procedure for ecological tiered assessment of risks (PETAR). *Human and Ecological Risk Assessment*. 10, 349-371.
- Moreira, J.C., 1996. Threats by heavy metals: Human and environmental contamination in Brazil. *The Science of the Total Environment*. 188 Suppl.(1), S61-S71.
- Mosteller, F., Youtz, C., 1990. Quantifying probabilistic expressions. *Statistical Science*. 5(1), 2-12.
- Muhaya, B.B.M., Leermakers, M., Baeyens, W., 1997. Total mercury and methylmercury in sediments and in the Polychaete

- Nereis diversicolor* at Groot Buitenschoor (Scheldt estuary, Belgium). Water, Air, and Soil Pollution. 94, 109-123.
- NRC, 2000. Toxicological effects of methylmercury. Committee on the Toxicological Effects of Methylmercury, Board on Environmental Studies and Toxicology, Commission of Life Sciences, National Research Council. National Academic Press, Washington, DC.
- Palheta, D., Taylor, A., 1995. Mercury in environmental and biological samples from a gold mining area in the Amazon region of Brazil. The Science of the Total Environment. 168, 63-69.
- Reagan, R.T., Mosteller, F., Youtz, C., 1989. The quantitative meanings of verbal probability expressions. Journal of Applied Psychology. 74, 433-442.
- Rice, D.C., 2004. The US EPA reference dose for methylmercury: sources of uncertainty. Environmental Research. 95, 406-413.
- Romero, F., 1996. Contaminación de Hg y Pb en fuentes de agua del area de Santo Domingo, Chontales [Hg and Pb contamination in water wells]. Centro de Investigaciones Geo-científicas, Managua [in Spanish], 21p.
- Salomons, W., 1995. Environmental impact of metals derived from mining activities: Processes, predictions, prevention. Journal of Geochemical Exploration. 52, 5-23.
- Sanga, R.N., Bartell, S.M., Ponce, R.A., Boischio, A.A.P., Joiris, C.R., Pierce, C.H., Faustman, E.M., 2001. Effects of uncertainties on exposure estimates to methylmercury: A Monte Carlo analysis of exposure biomarkers versus dietary recall estimation. Risk Analysis. 21(5), 859-868.
- Silva, G., 1994. Diagnóstico de la contaminación ambiental generada por la actividad minera sobre los ríos Sucio, Mico y Sinecapa Nicaragua. Universidad Federal de Pará /Centro de Geociencias.
- Smith, J., Allen, P., Turner, M., 1994. The kinetics of intravenously administered methyl mercury in man. Toxicology and Applied Pharmacology. 128, 251-256.
- Stafford, S.J., Humphreys, D.P., Lund, P.A., 1999. Mutation in *dsbA* and *dsbB*, but not *dsbC*, lead to an enhanced sensitivity of *Escherichia coli* to Hg²⁺ and Cd²⁺. FEMS Microbiology Letters. 174, 179-184.
- Stern, A.H., Smith, A.E., 2003. An assessment of the cord blood-maternal blood methylmercury ratio: implications for risk assessment. Environmental Health Perspective. 111, 1465-1470.
- Tarras-Wahlberg, N.H., Flachier, A., Lane, S.N., Sangfors, O., 2001. Environmental impacts and metal exposure of aquatic ecosystems in rivers contaminated by small scale gold mining: the Puyango River Basin, Southern Ecuador. The Science of the Total Environment. 278, 239-261.
- Ullrich, S.M., Tanton, T.W., Abdrashitova, S.A., 2001. Mercury in the aquatic environment: A review of factors affecting methylation. Critical Reviews in Environmental Science and Technology. 31(3), 241-293.
- USEPA, 2002. Estimate Per Capita Fish Consumption in the United States. U.S. Environmental Protection Agency.
- Vaituzis, Z., Nelson-Jr, J.D., Wan, L.W., Colwell, R.R., 1975. Effects of mercury chloride on growth and

- morphology of selected strains of mercury-resistant bacteria. *Applied Microbiology*. 29(2), 275-286.
- Wang, W.-X., 2002. Interactions of trace metals and different marine food chains. *Marine Ecology Progress Series*. 243, 295-309.
- WHO, 1989. Mercury Environment Aspect, Geneva- Environmental Health Criteria 86.
- WHO, 1990. Methyl mercury, International Program on Chemical Safety, Geneva: Environmental Health Criteria 101.
- WHO, 1996. Guidelines for Drinking Water Quality, 2nd ed., VOL. 2., Geneva.
- WHO, 2001. Report on integrated risk assessment. WHO/IPCS/IRA/01/1
- 2 Geneva, Switzerland, World Health Organization.
- Wickre, J.B., Folt, C.L., Sturup, S., Karagas, M.R., 2004. Environmental exposure and fingernail analysis of arsenic and mercury in children and adults in a Nicaragua gold mining community. *Archives of Environmental Health: An International Journal*. 59(8), 400-409.
- Zhang, Q., Crittenden, J.C., Mihelcic, J.R., 2001. Does simplifying transport and exposure yield reliable results? An analysis of four risk assessment methods. *Environmental Science and Technology*. 35, 1282-1288.

The following is a list of Doctoral theses from the Section of Chemical Ecology and Ecotoxicology, Department of Ecology, University of Lund, Sweden

1. ANDERS TUNLID, Chemical signatures in studies of bacterial communities. Highly sensitive analyses by gas chromatography and mass spectrometry. October 3, 1986
2. ANDERS THURÉN, Phthalate esters in the environment: analytical methods, occurrence, distribution and biological effects. November 4, 1988.
3. PETER SUNDIN, Plant root exudates in interactions between plants and soil microorganisms. A gnotobiotic approach. March 16, 1990.
4. ANDERS VALEUR, Utilization of chromatography and mass spectrometry for the estimation of microbial dynamics. October 16, 1992.
5. HANS EK, Nitrogen acquisition, transport and metabolisation in intact ectomycorrhizal associations studied by ¹⁵N stable isotope techniques. May 14, 1993
6. ROLAND LINDQUIST, Dispersal of bacteria in ground water-mechanism, kinetics and consequences for facilitated transport. December 3, 1993.
7. ALMUT GERHARDT, Effect of metals on stream invertebrates. February 17, 1995.
8. OLOF REGNELL, Methyl mercury in lakes: factors affecting its production and partitioning between water and sediment. April 21, 1995.
9. PER WOIN, Xenobiotics in aquatic ecosystems: effects at different levels of organization. December 15, 1995.
10. GÖRAN EWALD, Role of lipids in the fate of organochlorine compounds in aquatic ecosystems. October 18, 1996.
11. JOHAN KNULST, Interfaces in aquatic ecosystems: Implications for transport and impact of anthropogenic compounds. December 13, 1996
12. GUDRUN BREMLE, Polychlorinated biphenyls (PCB) in a river ecosystem. April 25, 1997.
13. CHRISTER BERGWALL, Denitrification as an adaptive trait in soil and groundwater bacteria. November 14, 1997
14. ANNA WALLSTEDT, Temporal variation and phytotoxicity of Batatasin-III produced by *Empetrum hermaphroditum*. November 27, 1998

15. DARIUS SABALIUNAS, Semipermeable membrane devices in monitoring of organic pollutants in the aquatic environment. April 28, 1999.
16. CECILIA AGRELL, Atmospheric transport of persistent organic pollutants to aquatic ecosystems. May 21, 1999
17. OLOF BERGLUND, The influence of ecological processes on the accumulation of persistent organochlorines in aquatic ecosystems. September 17, 1999
18. HELENA BJÖRN, Uptake, turn-over and distribution of chlorinated fatty acids in aquatic biota. October 1, 1999
19. RUEY-JANE FAN, Learning and memory in moths Plasticity in behaviour and neurophysiology. December 1, 2000.
20. FREDRIK ÖSTRAND, Behaviour of pine sawflies in relation to pheromone-based pest management. January 19, 2001.
21. MATTIAS LARSSON, Neural interfaces to the odour world of scarab beetles. March 2, 2001
22. CECILIA BACKE, Persistent organic pollutants in the atmosphere- spatial and temporal variations. May 4, 2001.
23. RICKARD IGNELL, Olfaction in desert locusts — Anatomy, function and plasticity of the central olfactory system. May 11, 2001.
24. CAMILLA RYNE, Pyralid moth reproduction: Communication, constraints & control. November 2, 2001.
25. DAINIUS PLEPYS, Odour-mediated nectar foraging in the silver Y moth, *Autographa gamma*. November 30, 2001.
26. DAVID ABRAHAM, Molecular aspects of pheromone evolution in moths. May 7, 2002.
27. GLENN SVENSSON, Disruption of moth mating behaviour by olfactory and acoustic cues. October 25, 2002.
28. LINA WENDT-RASCH, Ecological effects of pesticides in freshwater model ecosystems. February 28, 2003.
29. ARNOUT TER SCHURE, Polybrominated diphenylethers in the environment. October 3, 2003.

30. ELNA NILSSON, Movement patterns and displacement of a soil insect. May 28, 2004.
31. PER BENGTSON, Microbial mobilization and immobilization of soil nitrogen. June 4, 2004.
32. BETINA KOZLOWSKY SUZUKI, Effects of toxin-producing phytoplankton on copepods: feeding, reproduction and implications to the fate of toxins. June 7, 2004, Campus Helsingborg.
33. NIKLAS TÖRNEMAN, Spatial variability linking carbon resource heterogeneity and microorganisms; causes and consequences. May 13, 2005.
34. NIKLAS HOLMQVIST, Persistent organic pollutants in benthic foodwebs. June 10, 2005.
35. P.-O. CHRISTIAN OLSSON, Semiochemical-mediated attraction and oviposition in pyralid moths. November 11, 2005.
36. PARDIS PIRZADEH, Ecotoxicological assessment by microcosm tests on plankton communities. April 7, 2006.
37. CHRISTEL CARLSSON, Limitations and possibilities for microbial degradation of organic contaminants in aquifers. April 21, 2006.
38. MARIA PERSSON, The threat to the Baltic Salmon: a combination of persistent pollutants, parasites and oxidative stress. Nov 17, 2006.
39. GERMUND VON WOWERN, Circadian rhythms in moth sex pheromone communication. November 24, 2006.
40. LINA KRISTOFFERSEN, Getting to know *Trioza apicalis* (Homoptera: Psylloidea) – a specialist host-alternating insect with a tiny olfactory system December 1, 2006.
41. SÉVERINE JANSEN, Structure and function of odorant binding proteins and chemosensory proteins in moths. March 6, 2007.
42. MARIA STRANDH, Pheromones, genes & transcriptomes – a molecular analysis of moth sex pheromone production. November 30, 2007.
43. KATIA MONTENEGRO, Hierarchical responses to organic contaminants in aquatic ecotoxicological bioassays: from microcystins to biodegradation. September 23, 2008.

44. FRANCISCO J. PICADO PAVÒN, Fluvial transport and risk of mercury in a gold mining area. September 30, 2008.